Higgs Boson Production via Gluon Fusion at Hadron Colliders: Soft Gluon Resummation with Mass Effects

---

Dissertation

zur Erlangung der naturwissenschaftlichen Doktorwürde (Dr.sc.nat)

vorgelegt der Mathematisch-naturwissenschaftlichen Fakultät
der
Universität Zürich
von

Timo Schmidt

aus
Deutschland

Promotionskomitee:
PD Dr. Michael Spira (Leiter der Dissertation)
Prof. Dr. Thomas Gehrmann (Vorsitz)
Prof. Dr. Stefano Pozzorini

für meine Mutter Gabriele

Contents

Abstract

After the discovery of a scalar Higgs boson by the ATLAS and CMS experiments at the LHC precise theoretical calculations of all production and decay channels are needed to determine the Higgs properties, including its coupling to SM fermions. The gluon fusion is the dominant source of Higgs bosons over the entire mass range at the LHC. Apart from fixed-order calculations this thesis deals with the resummation of large logarithms near the partonic threshold. Based on previous work in the gluon fusion process we extend the soft gluon resummation to the highest known accuracy. We also consistenly treat collinear and top quark mass effects within the resummation method by providing an alternative approach to literature. In addition we apply the same resummation procedure to a pseudoscalar Higgs, as it is proposed by the MSSM. At the end of this thesis we discuss the numerical implementation and analysis of the threshold resummation in the gluon fusion process.

Zusammenfassung

Nach der Entdeckung eines skalaren Higgs-Bosons durch die ATLAS und CMS Experimente am LHC sind präzise theoretische Berechnungen aller Produktions- and Zerfallskanäle von Nöten um die Eigenschaften des Higgs-Bosons, inklusive deren Kopplung an die Fermionen des Standardmodels, zu bestimmen. Die Gluonfusion ist der dominante Produktionsmechanismus der Higgs Bosonen über den gesamten Energiebereich am LHC. Neben festen Ordnungsrechungen behandelt diese Arbeit die Resummation grosser Logarithmen nahe der partonischen Schwelle. Basierend auf früheren Arbeiten in der Gluonfusion erweitern wir die weiche Gluonresummation bis zur höchsten Genauigkeit. Wir behandeln ebenfalls kollineare und Top-Quark-Masseneffekte innerhalb der Resummationsmethodik und bieten dabei einen alternativen Zugang zur Literatur. Darüber hinaus wenden wir die gleiche Resummationsprozedur auf das pseudoskalare MSSM Higgs an. Am Ende dieser Arbeit diskutieren wir die numerische Implementierung und Analyse der Schwellenresummation im Gluonfusionsprozess.

Chapter 1

Prologue

The fundamental model of theoretical particle physics, the Standard Model (SM), provides a very successful description and prediction of physical observables in all experimental measurements. It comprises two different kinds of elementary matter particles, the quarks and the leptons, as well as the three fundamental forces, the strong, the weak and the electromagnetic interactions, mediated by gauge bosons. Additionally the SM predicts the existence of a scalar particle the Higgs boson which has been detected by the ATLAS and CMS experiments at the Large Hadron Collider (LHC) in Geneva. The Higgs particle is a consequence of the electroweak symmetry breaking by means of the Higgs mechanism and thus a cornerstone of the SM model. Its coupling to matter generates the particle masses. Moreover, the theory of electroweak interactions based on the Higgs mechanism permits very precise theoretical predictions due to renormalizability which are in striking agreement with experimental measurements at LEP and SLC.

The experimental analysis for the Higgs boson is one of the most important endeavors at the Tevatron and the LHC colliders. Experimental difficulties arise from the huge number of background processes induced by strong interactions that come along with Higgs signal events. Therefore precise theoretical predictions of all Higgs boson production and decay rates are needed.

The dominant Higgs production mechanism at the LHC is the gluon fusion process, an essentially strong interacting process, which has attracted a lot of theoretical interest in the last decades. The coupling of the gluons to the Higgs is mediated by top and bottom quark loops. To next-to-leading order QCD quantum corrections with the full dependence on the quark masses have been calculated. They increase the total cross section by a huge amount of 50–100%. Recent works at NNLO (next-to-next-to-leading order) in the limit of a large top-quark mass showed that the NNLO corrections are moderate in size which signalizes perturbative convergence.

In order to receive a better understanding about the residual higher orders in perturbation theory factorization theorems in particular kinematical regions allow to to improve the theoretical predictions by exploiting renormalization group methods. The resummation of kinematically enhanced terms near the partonic threshold and the matching to fixed-order calculations precise the theoretical predictions to the highest accuracy.

Quite recently, N^3LO calculations in the threshold region have been published which allows us to extend the the resummation techniques up to NNNLL (next-to-next-to-next-leading logarithmical) level. In this thesis we systematically include previously neglected mass effects into the resummation procedure and provide a method to incorporate collinear effects in a consistent way. Furthermore, we also consider the numerical impact to the total hadronic cross section of the gluon fusion process for a SM Higgs and a pseudoscalar Higgs, as it is proposed by the Minimal Supersymmetric extension of the Standard Model (MSSM)

This thesis is organized as follows: In Chapter 2 we review the main theoretical concepts of electroweak symmetry breaking in the SM and MSSM and also recapitulate the relevant processes for the production of a scalar and pseudoscalar Higgs. Within Chapter 3 we treat the theoretical methods of resummation by attaching importance to the fundamental basis of the theory of strong interaction, Quantum Chromodynamics. Fixed-order calculations to the gluon fusion process, both in QCD and electroweak theory, are summarized in Chapter 4. The second last Chapter 5 shall serve as a detailed description of the extension of the known resummation procedure, including theoretical developments and numerical analysis. We conclude this work in Chapter 6.

Chapter 2

Introduction

1 Standard Model of Particle Physics

The Standard Model of particle physics (SM) is nowadays the widely accepted theory describing the interactions and matter of the universe. In contrast to Quantum Mechanics (QM), Quantum field theories (QFT) provide an elegant treatment of particles as fields. The advantage compared to QM is that not only it solves the causality problem but moreover handles multiparticle states as well as transitions between states of different particle numbers. Particles, formally pointlike fermionic excitations of the vacuum, are the fundamental constituents of the matter. The interactions among the particles are generated due to the exchange of spin 1 vector bosons of the strong, weak and electromagnetic sector. The class of particles is subdivided into quarks and leptons. The latter can only interact via electroweak interactions mediated by photons γ, Z-bosons or $W^{\pm}$-bosons while the former participate also in the strong interactions via the 8 gluons. The dynamics of the SM are contained in a $SU(3)_C \otimes SU(2)_L \otimes U(1)_Y$ local gauge invariant Lagrangian of the form [1, 2, 3]

$$\begin{aligned}\mathcal{L}_{SM} = &-\frac{1}{4}\sum_a \left(G^a_{\mu\nu}\right)^2 + i\sum_f \bar{\psi}_f \not{D}\psi_f + |D\phi|^2 + \mu^2|\phi|^2 - \frac{\lambda}{4}|\phi|^4 \\ &- (\sum_{ij} y_{ij}\bar{\psi}_{i,L}(\phi + \phi^c)\psi_{j,R} + h.c)\end{aligned} \tag{2.1}$$

where the subscripts C, L, Y refer to color, left isospin and weak hypercharge. The first term in Eq. (2.1) contains a sum over all the 12 generators of the gauge group of the SM and depicts the kinematical terms the repective gauge bosons G^{α}_{μ}, W^j_{μ} and B_{μ} which transform according to the adjoint representations of $SU(3)_C \otimes SU(2)_L \otimes U(1)_Y$. The gluons are always massless and the $SU(2)_L$ gauge bosons $W^{0,1,2}$ and

the $U(1)_Y$ gauge boson B are introduced without explicit mass terms in the exact electroweak theory. The fermion fields ψ belong to different representations of the gauge group. Leptons and quarks come in three different generations and can be ordered by left-handed isospin doublets and right handed isospin singlets. The hypercharge Y is related to the electromagnetic charge Q_f and the third component of the left chiral weak isopsin T_{3L} via

$$Q = T_{3L} + \frac{Y}{2} \tag{2.2}$$

The fields of the three generations of leptons and quarks with the respective quantum numbers $(\mathbf{I}, Y)$ of the electroweak sector can be depicted as

$$\begin{pmatrix} \nu_e \\ e^- \end{pmatrix}_L, \quad \begin{pmatrix} \nu_\mu \\ \mu^- \end{pmatrix}_L, \quad \begin{pmatrix} \nu_\tau \\ \tau^- \end{pmatrix}_L : (\mathbf{2}, -1) \tag{2.3}$$

$$e_R^-, \quad \mu_R^-, \quad \tau_R^- : (\mathbf{1}, -2) \tag{2.4}$$

$$\begin{pmatrix} u \\ d \end{pmatrix}_L, \quad \begin{pmatrix} c \\ s \end{pmatrix}_L, \quad \begin{pmatrix} t \\ b \end{pmatrix}_L : (\mathbf{2}, \frac{1}{3}) \tag{2.5}$$

$$u_R, \quad c_R \quad t_R : (\mathbf{1}, \frac{4}{3}) \tag{2.6}$$

$$d_R, \quad s_R, \quad b_R : (\mathbf{1}, -\frac{2}{3}) \tag{2.7}$$

Moreover, the quark fields are color triplets $(\mathbf{3})$ while lepton fields are color singlets $(\mathbf{1})$ of $SU(3)_C$. Due to the requirement of local gauge invariance the usual derivative of the fields must be replaced by a covariant one

$$D_\mu = \partial_\mu + ig_s \sum_{a=1}^{8} T^a G_\mu^a + ig \sum_{j=1}^{3} W_\mu^j T_W^j + ig' B_\mu \frac{Y}{2} \tag{2.8}$$

where T^a and T_W^j are the generators of $SU(3)$ and $SU(2)$ and Y is the hypercharge of $U(1)$. The remaining terms in (2.1) contain an additional $SU(2)_L$ doublet of scalar Higgs fields $\phi = \binom{\phi^+}{\phi^0}$ with hypercharge $Y = 1$.

1.1 Electroweak theory and the Higgs mechanism

The electroweak subgroup $SU(2)_L \otimes U(1)_Y$ remains intact above the weak scale at about $v \sim 246$ GeV but at energies below that scale the original symmetry is hidden or "spontanously broken" by virtue of the scalar Higgs field which acquires a real non-zero expectation value in the isospin $I_3 = -\frac{1}{2}$ component about the ground

state [4, 5, 6, 7, 8]. Vacuum fluctuations of the isodoublet ϕ value are usually known as the Higgs particle denoted by h. In unitary gauge the isospin doublet is given by

$$\phi = \frac{1}{\sqrt{2}} \begin{pmatrix} 0 \\ v + h \end{pmatrix}. \tag{2.9}$$

Due to the presence of the VEV v the weak bosons $W^{\pm}$ and Z acquire masses while the photon remains massless

$$M_W = \frac{1}{2} g v, \quad M_Z = \frac{1}{2} \sqrt{g'^2 + g^2}\, v, \quad v = \left(\frac{1}{\sqrt{2} G_F} \right)^{1/2} \tag{2.10}$$

The relation between the vector fields $W_{\mu}^{1,2,3}$, B_{μ} and the mass eigenstates $W_{\mu}^{\pm}$, Z_{μ} are

$$W^{\mu,\pm} = \frac{1}{\sqrt{2}} (W_1^{\mu} \mp i W_2^{\mu}) \tag{2.11}$$

$$Z^{\mu} = \frac{g}{\sqrt{g'^2 + g^2}} W_3^{\mu} - \frac{g'}{\sqrt{g'^2 + g^2}} B^{\mu}, \tag{2.12}$$

$$= -\sin\theta_w B^{\mu} + \cos\theta_w W_3^{\mu}, \tag{2.13}$$

$$A^{\mu} = \cos\theta_w B^{\mu} + \sin\theta_w W_3^{\mu}, \tag{2.14}$$

$$\tag{2.15}$$

where θ_w is the Weinberg angle. In unitary gauge the additional degrees of freedom in the Higgs potential, the Nambu-Goldstone bosons, are absorbed as longitudinal degrees of freedom of the massive vector bosons. The Higgs isopsin doublet ϕ also generates masses of the up-type fermions with isospin $I_3 = +\frac{1}{2}$ while the charge conjugated isospin doublet ϕ^c generates the masses of down-type fermions with isospin I_3. The resulting mass terms can conveniently be written as the Lagrange density

$$\mathcal{L}_m = -(\bar{\psi}_{Li} m_{ij} \psi_{Rj} + h.c.) \tag{2.16}$$

where m_{ij} is the respective mass matrix of the leptons and quarks. Moreover, the vacuum fluctuations h around the minimum of the Higgs potential lead to a Higgs mass term and Higgs self interactions of the form

$$\mathcal{L}_h = -\mu^2 h^2 - \lambda v h^3 - \frac{1}{4} \lambda h^4 \tag{2.17}$$

$$= -\frac{1}{2} m_h^2 h^2 - \sqrt{\frac{\lambda}{2}} m_h h^3 - \frac{1}{4} \lambda h^4 \tag{2.18}$$

Since the Fermi coupling G_F is fixed due to the μ-decay the determination of the Higgs mass by ATLAS ans CMS [9, 10] completed the set of the 19 free input parameters of the SM. From Eq. (2.1) one can also derive interaction terms between the Higgs particle and the vector bosons

$$\mathcal{L}_{hVV} = \left(m_W^2 W^{\mu+} W_\mu^- + \frac{1}{2} m_Z^2 Z^\mu Z_\mu \right) \frac{2h}{v} \tag{2.19}$$

as well as with the SM fermions of the kind

$$\mathcal{L}_{hff} = -(\bar{\psi}_{Li} m_{ij} \psi_{Rj} + h.c.) \frac{h}{v} \tag{2.20}$$

which allows to derive Feynman rules of the interaction vertices, see Fig. 2.1

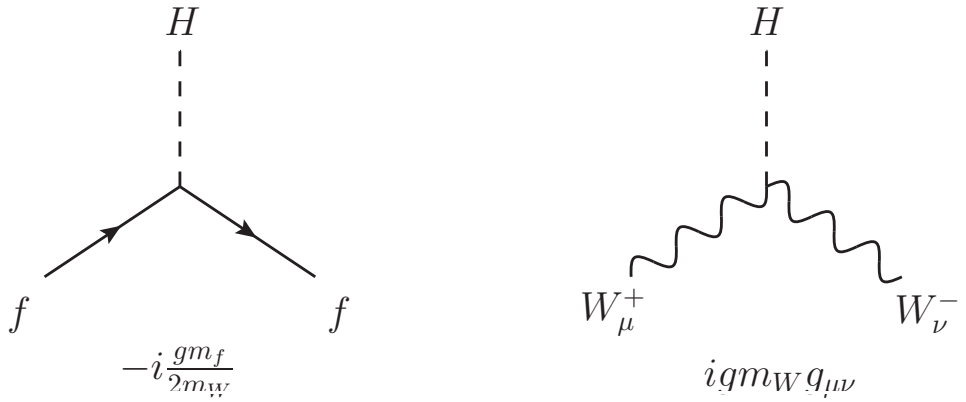

Figure 2.1: Feynman rules for the Higgs couplings to fermions and W-bosons

1.2 Unitarity argument and theoretical bounds on the Higgs mass

Perturbative unitarity arguments also show [11] that a theory with massive vector bosons and massive fermions which are coupled weakly up to an asymptotic scale Λ requires the inclusion of a scalar 0^+ Higgs boson with a coupling proportionaly to the masses of the particles. Without a scalar particle in the electroweak sector the S-wave amplitude of the longitudinal $W_L W_L \to W_L W_L$ scattering would diverge quadratically in energy. Amplitudes with a Higgs boson exchange not only exactly cancel the quadratic rise of the pure gauge boson amplitudes but also render finite amplitudes $A_0(f\bar{f} \to W_L W_L)$. If one also includes channels $W_L W_L \to W_L W_L$, $Z_L Z_L \to Z_L Z_L$, etc. the requirement that the largest eigenvalues of the S-wave

amplitude respects the unitarity constraint yields an upper bound on the Higgs mass [12, 13]

$$M_H \lesssim 710 \text{ GeV} \tag{2.21}$$

Moreover, upper and lower limits on the Higgs mass can be derived by the triviality and stability bound of the Higgs quartic coupling. At one loop the RGE of the coupling λ can be expressed as [14, 15, 16, 17, 18, 19, 20]

$$\frac{\mathrm{d}\lambda}{\mathrm{d}\ln\mu^2} \sim \frac{1}{16\pi^2}\left[12\lambda^2 + 6\lambda y_t^2 - 3y_t^4 - \frac{3}{2}\lambda(3g'^2 + g^2) + \frac{3}{16}\left(2g'^4 + (g'^2 + g_1^2)^2\right)\right] \tag{2.22}$$

where the top Yukawa coupling is $y_t = \sqrt{2}m_t/v$. The RGE covers all one loop contributions including fermions and vector bosons of the electroweak theory. For large Higgs masses the Higgs self coupling becomes the dominant effect. The solution of the RGE in this limits yields an upper bound on the Higgs mass dependent on the energy scale Λ where new strong interactions emerge. i.e. the coupling λ diverges. For smaller values of the quartic coupling the heavy quark mass loops can drive the coupling even to negative values leading to a lower limit on the mass of the scalar boson. Including also two loop effects in the RGE of λ and assuming that the SM is valid up to the Planck scale $\Lambda \approx 10^{19}$ GeV restricts the Higgs mass in the range $130 - 190$ GeV. If new physics appear near 1 TeV the Higgs mass has to lie between $60 - 800$ GeV.

1.3 SM Higgs boson production and decays at the LHC

The discovery of a scalar CP even Higgs boson by the ATLAS and CMS experiments [9, 10] completed the long search for the missing cornerstone of SM. Besides an heroic effort on the experimental side, precise theoretical calculations both for the production and the decay channels are of high importance. The SM Higgs can decay at tree level into a fermion-antifermion and vector boson pair. Due to the linear rise of the Yukawa coupling with the fermion mass the Higgs tends to decay into the heaviest fermions and gauge bosons allowed by phasespace. On the other side a direct coupling to two photons, to a photon-Z pair or to two gluons is prohibited at tree level. These decay channels can only arise due to loop-induced processes. In the low mass range 110 GeV, $\lesssim M_h \lesssim$ 130 GeV the Higgs decays mainly into a $b\bar{b}$ pair with a branching ratio of $\sim 75 - 50\%$ while other decay modes $H \to c\bar{c}, \tau^+\tau^-, gg$ develop branching ratios at the per-cent level. $H \to \gamma\gamma, Z\gamma$ decays are very rare and occur only at the per-mille level. In the intermediate mass range 120 GeV $\lesssim M_h \lesssim$ 180 GeV the WW and ZZ channels open up dominating the branching

ratios with a ratio 2:1 in the high mass range 180 GeV $\lesssim m_h \lesssim$ 1 TeV. The $t\bar{t}$ decay mode only leads to a slight modification ot these branching ratios above the $t\bar{t}$-threshold. Although the Higgs to bottom anti-bottom decay channel is the dominant to detect the Higgs in the low mass region the $b\bar{b}$ final state is disfavored due to huge QCD jet backgrounds in hadron hadron collisions highly complicate the experimental detection. Nevertheless, the observed excess was most significantly observed in the decay of a Higgs into two photons combined with the vector boson channels further decaying into 2 charged lepton anti-lepton pairs.

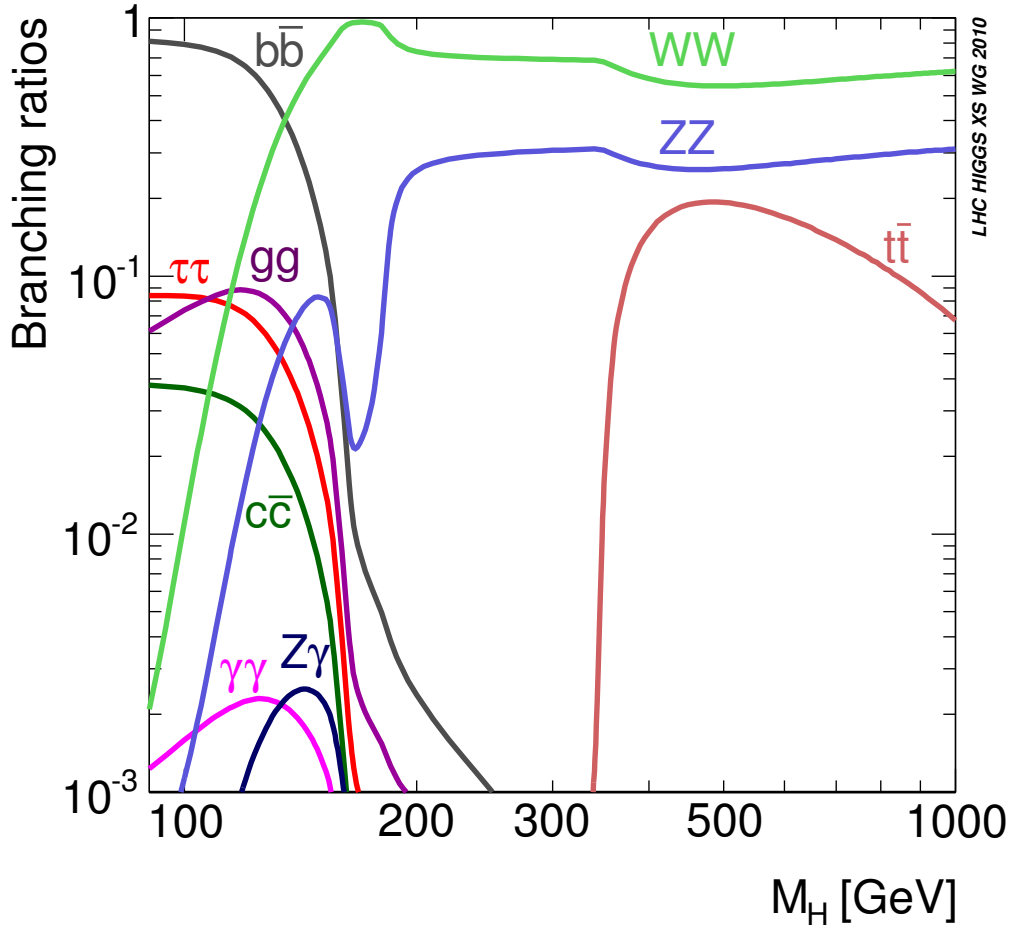

Figure 2.2: SM Higgs branching ratios as a function of the Higgs mass M_H [21]

Although the total estimated cross section of all visible processes at the LHC is about $\sim$ 100 mb for a center of mass energy $\sqrt{s} = 14$ TeV the ratio of the signal of the production of a single Higgs over the background is about $\sim 10^{-10}$ which makes experimental searches for the Higgs boson very challenging. Mainly due to its large

Yukawa coupling to heavy quarks and massive vector bosons the main production processes in hadron colliders are:

gluon fusion	:	$gg \to H$
vector boson fusion	:	$W^+W^-, ZZ \to H$
Higgs-strahlung off W, Z	:	$q\bar{q} \to W^*/Z^* \to W/Z + H$
Higgs bremsstrahlung off top	:	$q\bar{q}, gg \to t\bar{t} + H$

Although loop-suppressed the gluon fusion, mediated by a heavy quark triangle, is the dominant production process over the entire mass range of the Higgs at the LHC. The domincance of $gg \to H$ stems from the fact that the loop suppression is balanced out by the size of the heavy quark Yukawa coupling and the sensitivity of the partonic cross section to the gluon parton distributions at small Bjorken-x. Higher-order perturbative QCD corrections turn out to be large [22, 23, 24] by virtue of the large color charges in gluon induced processes, thus questioning the reliability of the perturbative approach. This thesis addresses this issue to a large extent. A detailed description of the gluon fusion mechanism at fixed orders can be found in chapter 4 while the soft and collinear gluon resummation is explained in chapter 5.

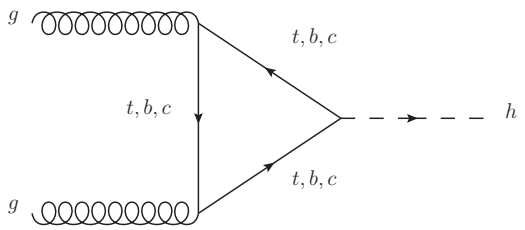

Figure 2.3: Loop induced diagram to the leading order partonic cross section of the gluon fusion

The vector-boson-fusion process is subdominant for small Higgs masses but becomes competitive to the gluon fusion in the large Higgs mass range. The production of the Higgs in association with two hard jets in the forward and backward direction also plays an important role in the determination of the Higgs coupling to vector bosons. The LO electroweak cross section consists of s, t and u-channel diagrams with a quark anti-quark pair in the initial state. The quarks emit two off-shell vector bosons which fuse into the Higgs boson as depicted in Figure 2.4.

NLO QCD corrections are small in size [25, 26, 27, 28, 29] since no color charge is exchanged between the quarks lines at LO, hence the corrections arise merely from

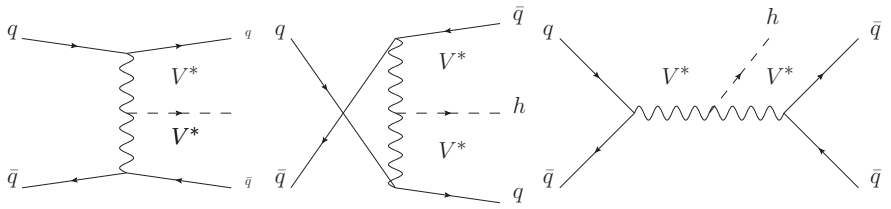

Figure 2.4: Leading order t-,u- and s-channel diagrams to the vector boson fusion process

vertex contributions to the quark anti-quark vector boson vertex and from gluon radiation up to NLO. Mainly by virtue of including real photon corrections in the initial state the theoretical uncertainties of electroweak corrections combined with the NLO QCD contributions, estimated by the scale variation, are reduced to the per-cent level [26, 30].

In the intermediate mass range $M_H \lesssim 2M_Z$ Higgs-strahlung off vector bosons plays a significant role. The LO cross section described by the first two diagrams in Figure 2.5 can be factorized into a Drell-Yan like part $\bar{q}q \to V^*$ and into a part which only contains the radiation of a Higgs off a virtual gauge boson. Higher-order QCD corrections can be inferred from the Drell–Yan process and increase the cross section by about (30%) [31, 32, 33]. The relative NNLO corrections are only small [34]. NLO electroweak corections to this process lead to a decrease of the total cross section by $5-10\%$ [35]. Additional contributions to HZ-production at NNLO come from the gluon-gluon initiated diagram, the third in Figure 2.5. The residual theoretical uncertainty in Higgs-strahlung is estimated at around $\mathcal{O}(5\%)$ [34]

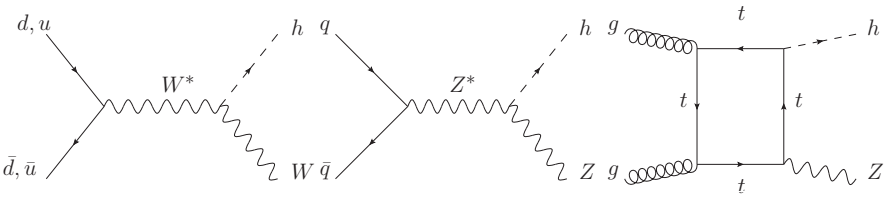

Figure 2.5: Diagrams contributing to the LO cross section in associated Higgs production with W/Z-bosons

For Higgs masses below $M_H \sim 150$ GeV Higgs radiation off top quarks is a relevant production process. Although the LO calculation already is quite involved the process plays an essential role in the determination of the fundamental top-Yukawa coupling since the cross section is directly proportional to this coupling. Full NLO calculations increase the total hadronic cross section at most by $\sim 20\%$ [36, 37, 38] whereas the scale dependence decreases from $\mathcal{O}(50\%)$ to $\mathcal{O}(10\%)$. The production

process is plagued by large background processes as $t\bar{t}b\bar{b}, t\bar{t}jj, t\bar{t}\gamma\gamma, t\bar{t}Z$ and $t\bar{t}W^+W^-$ production which experimentally increases the difficulties to separate the signal from the background.

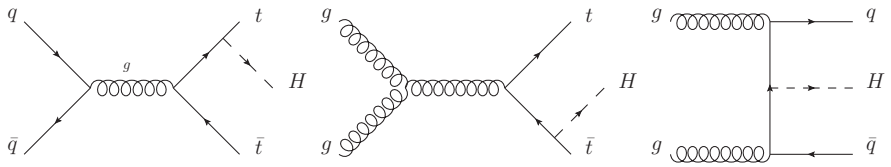

Figure 2.6: Generic diagrams contributing at LO to the Higgs production in association with a $t\bar{t}$-pair

All four relevant production cross sections at the LHC are depicted in Fig. 2.7. The blue line represents the gluon fusion cross section which is the dominant production mechanism at the LHC over the entire mass range. Vector-boson-fusion, the red band, becomes competitive to the gluon fusion for large Higgs masses. Higgs radiation off electroweak vector bosons as well as Higgs bremsstrahlung are subdominantly contributing.

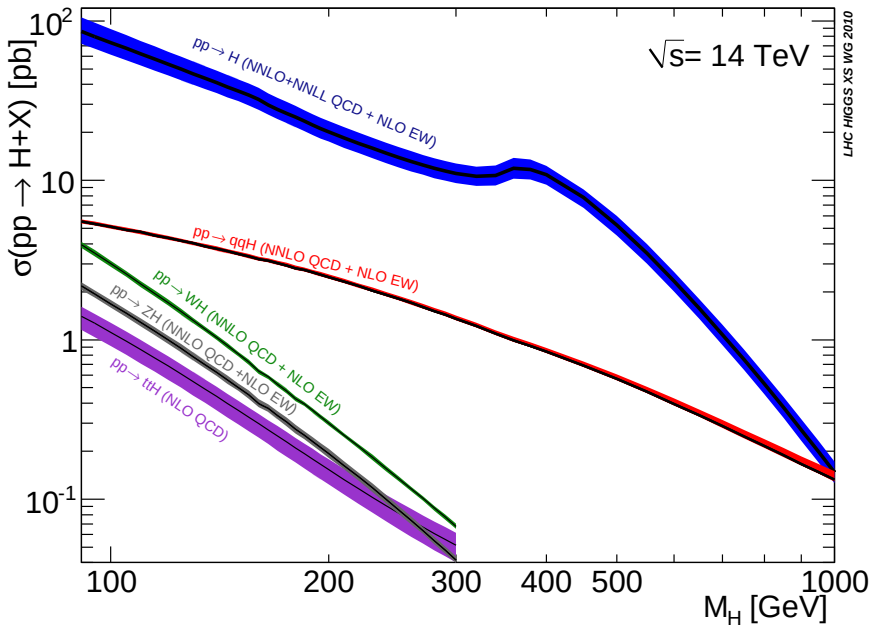

Figure 2.7: Total hadronic cross section of all relevant Higgs production processes at the LHC including their theoretical uncertainties [21].

2 Minimal Supersymmetric Standard Model

Although the Standard Model of Particle Physics provides an excellent description of the matter building blocks of the universe it can only partly solve the puzzles towards a 'theory of everything': Gravity, the fourth known force, cannot be consistently included into the quantum field theoretical framework due to its non-renormalizability. The origin of electroweak symmetry breaking, introduced ad-hoc in the SM by the Higgs–Kibble mechanism, calls for a thorough explanation. Moreover, equal amounts of baryonic matter and anti-matter should be present in the universe. However, cosmological observations indicate a baryonic asymmetry that cannot be explained within the SM. Besides the 'visible' matter, dark matter was hypothesized in order to explain the discrepancies between the predicted and observed value of the mass of large astronomical objects. Dark matter constituents are believed to only weakly interact with the baryonic matter and do not absorb or emit photons at a significant level. Dark energy, hypothesized to explain the accelerating expansion of the universe, is not consistent with the quantum vaccum of the SM. If one assumes that the SM is valid up to the Planck scale the mass of the Higgs is unprotected against quantum corrections thus requiring an unnatural fine tuning. Within the SM baryon number is conserved, thus the proton cannot decay at the classical level. At the quantum level the baryonic current is not conserved due to the $\mathrm{U}(1)_B$ Adler-Bell-Jackiw anomaly. The proton decay rate due to this CP-violating terms has to be unnaturally fine-tuned in order to match the experimental data. As we have seen in section 1 the SM contains three kinds of families of leptons and quarks and it needs 19 input parameters to make physical predictions. The excistence of 3 baryonic families and the input parameters are yet unexplained.

One possibility to answer some of the open questions is provided by supersymmetric extensions of the Standard Model. As the name reveals, supersymmetric theories (SUSY's) can be constructed by the assumption of a space-time symmetry which relates the known particle spectrum to their supersymmetric partners. The Coleman-Mandula theorem, however, states that there cannot exist further bosonic symmetries than the Poincare and the Lie-algebras of internal gauge symmetries. The only way to to circumvent this no-go theorem is to impose fermionic operators in order to transform bosonic into fermionic states and vice versa,

$$Q|\mathrm{Boson}\rangle = |\mathrm{Fermion}\rangle, \quad \mathrm{Q}|\mathrm{Fermion}\rangle = |\mathrm{Boson}\rangle. \tag{2.23}$$

Referring to [39] these operators can be included into a Z_2-graded Lie algebra where the odd (fermionic) operators belong to the representation $(\frac{1}{2}, 0)$ and $(0, \frac{1}{2})$ of the homogeneous Lorentz group and the even generators are a direct sum of the Poincare algebra and other internal symmetries In the following we concentrate on $N = 1$ SUSY's with N referring to the number of supersymmetries, e.g. the number of

distinct copies of $Q, Q^\dagger$. The graded Lie-algebra is defined by (anti-) commutation rules

$$[P_\mu, P_\nu] = 0, \tag{2.24}$$
$$[M_{\mu\nu}, P_\rho] = i(\eta_{\nu\rho}P_\mu - \eta_{\mu\rho}P_\nu), \tag{2.25}$$
$$[M_{\mu\nu}, M_{\rho\sigma}] = -i(\eta_{\mu\rho}M_{\nu\sigma} - \eta_{\mu\sigma}M_{\nu\rho} - \eta_{\nu\rho}M_{\mu\sigma} + \eta_{\mu\sigma}M_{\mu\rho}), \tag{2.26}$$
$$\{Q_a, Q_b^\dagger\} = 2(\sigma^\mu)_{ab}P_\mu, \tag{2.27}$$
$$[Q_a, P_\mu] = 0, \tag{2.28}$$
$$[M_{\mu\nu}, Q_a] = -i(\sigma_{\mu\nu})_{ab}Q_b, \tag{2.29}$$
$$[Q_a, R] = (\gamma_5)_{ab}Q_b. \tag{2.30}$$

where P_μ and $M_{\mu\nu}$ are the generators of the Poincare group representing space-time translations and homogeneous Lorentz transformations while the Q_a are two component Weyl spinor and R is an axial $U(1)$ generator.

The particle spectrum of SUSY is then described by supermultiplets which contain the SM particles and their superpartners. Moreover, each supermultiplet contains an equal number of fermionic and bosonic degrees of freedom. In a particular case one multiplet consists of a two component Weyl spinor and two real scalars and is called chiral supermultiplet. Another possibility is provided by a vector multiplet where a massless spin-1 gauge boson with two helicity states is accompanied by a massless Weyl fermion, the gaugino. The latter vector multiplet can be imbedded in renormalizable theory whereas a supermultiplet with a spin-$\frac{3}{2}$ fermion cannot. Gravity can be included via a spin-2 graviton in combination with its superpartner, the spin-$\frac{3}{2}$ gravitino.

In the minimal supersymmetric extension of the SM the known particles have to be incorporated in either a chiral or vector multiplet. Quarks and leptons live in chiral multiplets with their superpartners, the squarks and sleptons. The vector bosons of the Standard model, including gluons, W- and B-bosons occur together with their spin 1/2-partners, the winos and binos as members of vector supermultiplets. After the electroweak symmetry breaking the corresponding gauginos $\tilde{W}^0$ and $\tilde{B}$ mix to zinos and photinos.

In order to render the MSSM anomaly-free the Higgs boson must reside in two chiral supermultiplets H_u and H_d with hypercharge $Y = 1/2$ and $Y = -1/2$ respectively. The corresponding superpartners are the Higgsinos. Apart from the anomaly freedom and due to the analyticity of the MSSM the two doublets are needed to give different Yukawa couplings to the up and down type quarks. The overall particle spectrum of the MSSM is depicted in Tab. 1.

One can define an R-parity by

$$P_R = (-1)^{3B-L+2s}.$$

Names		spin 0	spin 1/2	$SU(3)_C$, $SU(2)_L$, $U(1)_Y$
squarks, quarks	Q	$(\tilde{u}_L \;\; \tilde{d}_L)$	$(u_L \;\; d_L)$	$(\mathbf{3}, \mathbf{2}, \frac{1}{6})$
($\times$3 families)	$\bar{u}$	$\tilde{u}_R^*$	$u_R^\dagger$	$(\overline{\mathbf{3}}, \mathbf{1}, -\frac{2}{3})$
	$\bar{d}$	$\tilde{d}_R^*$	$d_R^\dagger$	$(\overline{\mathbf{3}}, \mathbf{1}, \frac{1}{3})$
sleptons, leptons	L	$(\tilde{\nu} \;\; \tilde{e}_L)$	$(\nu \;\; e_L)$	$(\mathbf{1}, \mathbf{2}, -\frac{1}{2})$
($\times$3 families)	$\bar{e}$	$\tilde{e}_R^*$	$e_R^\dagger$	$(\mathbf{1}, \mathbf{1}, 1)$
Higgs, higgsinos	H_u	$(H_u^+ \;\; H_u^0)$	$(\tilde{H}_u^+ \;\; \tilde{H}_u^0)$	$(\mathbf{1}, \mathbf{2}, +\frac{1}{2})$
	H_d	$(H_d^0 \;\; H_d^-)$	$(\tilde{H}_d^0 \;\; \tilde{H}_d^-)$	$(\mathbf{1}, \mathbf{2}, -\frac{1}{2})$

Table 1: Scalar supermultiplets in the MSSM.

Names	spin 1/2	spin 1	$SU(3)_C$, $SU(2)_L$, $U(1)_Y$
gluino, gluon	$\tilde{g}$	g	$(\mathbf{8}, \mathbf{1}, 0)$
winos, W bosons	$\tilde{W}^\pm \;\; \tilde{W}^0$	$W^\pm \;\; W^0$	$(\mathbf{1}, \mathbf{3}, 0)$
bino, B boson	$\tilde{B}^0$	B^0	$(\mathbf{1}, \mathbf{1}, 0)$

Table 2: Vector supermultiplets in the MSSM.

where s is the spin and B, L the baryon number and the lepton number of the corresponding particle. While SM particles possess an even R-parity ($P_R = +1$) squarks, sleptons, gauginos and higgsinos have odd R-parity ($P_R = -1$). Assuming the global U(1)-symmetry being preserved the lightest $P_R = -1$ sparticle (LSP) must be stable. Additionally, if the LSP is electrically neutral, thus only weakly interacting with ordinary matter, it is an attractive candidate for non-baryonic dark matter.

Furthermore, Grand unified theories (GUT's) not only unify the strong and the electroweak theory but also provide a theory describing the decay of the proton. However, the proton lifetime is larger than 10^{+32} years contrary to the theoretical predictions of at least 10^{+31} years. Supersymmteric GUT's suppress the decay rate and lead to a prediction of the electroweak mixing angle in agreement with measurements. Moreover, the Higgs mechanism can be explained by SUSY-GUT's due to radiative corrections to the Higgs mass which alter the effective Higgs potential to negative values of the squared of the Higgs mass.

2.1 The MSSM Higgs sector

Due to a lack of symmetry the SM Higgs mass receives huge radiative corrections due to fermion, vector boson and self-coupling contributions. Neglecting the vector boson and self energy contributions and assuming the fermion mass is heavy compared to the Higgs mass, the loop momenta of the scalar can be neglected leading to the correction

$$\Delta M_H^2 = \sum_f \frac{y_f^2}{8\pi^2}\left[-\Lambda^2 + 6m_f^2 \ln\frac{\Lambda}{m_f} - 2m_f^2\right] + \mathcal{O}(1/\Lambda^2) \tag{2.31}$$

where $y_f = \sqrt{2}m_f/v$ is the corresponding Yukawa coupling, m_f the fermion mass and Λ the UV-cutoff. If new physics would be present at the GUT-scale, $M_{\text{GUT}} \sim 10^{16}$ GeV, or the Planck-scale, $M_{\text{P}} \sim 10^{18}$ GeV one must add a counterterm that requires an unnatural fine tuning of $28-32$ digits. Supersymmetric theories as the MSSM contain $N_S = 2N_F$ scalars corresponding to the heavy fermions in the same multiplet. In our toy model the Higgs mass thus obtains additional corrections due to scalar one-loop diagrams of the kind

$$\Delta M_H^2 = -\frac{y_s}{16\pi^2}\left[-\Lambda^2 + 2m_s^2 \ln\frac{\Lambda}{m_s}\right] - \frac{\lambda_s^2}{16\pi^2}v^2\left[-1 + 2\ln\frac{\Lambda}{m_s}\right] + \mathcal{O}\left(\frac{1}{\Lambda^2}\right) \tag{2.32}$$

If one assumes that the Higgs coupling to the scalars fulfills $y_s = y_f^2$ the quadratic divergences cancel leaving a total correction

$$\Delta M_H^2 = \sum_f \frac{y_f^2}{4\pi^2}\left[(m_f^2 - m_s^2)\ln\frac{\Lambda}{m_s} + 3m_f^2 \ln\frac{m_s}{m_f}\right] + \mathcal{O}\left(\frac{1}{\Lambda^2}\right). \tag{2.33}$$

The logarithmic divergence also cancels if $m_s = m_f$. This would require an exact supersymmetry which is not the case in the MSSM where a non-degeneracy of the SM particles and the sparticles is assumed. However, this non-degeneracy of the masses, imposed by soft symmetry breaking terms, is expected to be small in order not to violate fine-tuning bounds on the Higgs mass.

As mentioned earlier, the Higgs field can be parametrized by two doublets

$$H_1 = \begin{pmatrix} H_1^0 \\ H_1^- \end{pmatrix}, \quad H_2 = \begin{pmatrix} H_2^+ \\ H_2^0 \end{pmatrix} \tag{2.34}$$

where the $+, -$ and 0 superscripts indicate the electric charge. The Higgs potential can be derived via the superfield and superspace formalism as

$$V_H = \bar{m}_1^2(|H_1^0|^2 + |H_1^-|^2) + \bar{m}_2^2(|H_2|^0 + |H_2^+|^2) - \bar{m}_3^2(H_1^- H_2^+ - H_1^0 H_2^0 + h.c.)$$

$$+\frac{g^2+g'^2}{8}(|H_1^0|^2+|H_1^-|^2-|H_2^0|^2-|H_2^+|^2)^2$$
$$+\frac{g'^2}{2}|(H_1^-)^*H_1^0+(H_2^0)^*H_2^+|^2 \tag{2.35}$$

where we defined the mass squared terms as

$$\bar{m}_1^2=|\mu|^2+m_{H_1}^2,\quad \bar{m}_2^2=|\mu|^2+m_{H_2}^2,\quad \bar{m}_3^2=B\mu \tag{2.36}$$

The parameter μ originates from the F-term of the superpotential while the parameters B, $m_{H_1}^2$ and $m_{H_2}^2$ can be attributed to the soft SUSY-breaking scalar Higgs mass terms. The electroweak symmetry is hidden in a similar fashion as in the SM. In the MSSM, however, the two neutral components aquire two different vacuum expectation values

$$\langle H_1^0\rangle=\frac{v_1}{\sqrt{2}},\quad \langle H_2^0\rangle=\frac{v_2}{\sqrt{2}}. \tag{2.37}$$

Minimizing the scalar potential at the electroweak minimum, $\partial V_H/\partial H_1^0=\partial V_H/\partial H_2^0=0$, using the relation

$$(v_1^2+v_2^2)^2=v^2=\frac{4M_Z^2}{g_2^2+g_1^2} \tag{2.38}$$

and defining the parameter

$$\tan\beta=\frac{v_2}{v_1} \tag{2.39}$$

one obtains two minimizing conditions

$$B\mu=\frac{(m_{H_1}^2-m_{H_2}^2)\tan 2\beta+M_Z^2\sin 2\beta}{2} \tag{2.40}$$
$$\mu^2=\frac{m_{H_2}^2\sin^2\beta-m_{H_1}^2\cos^2\beta}{\cos 2\beta}-\frac{M_Z^2}{2} \tag{2.41}$$

The physical quantum fluctuations of the Higgs field around the vacuum expectation values can be split into real and imaginary parts. The real parts then correspond to the neutral CP-even Higg bosons whereas the imaginary parts represent the CP-odd Higgs and the Goldstone bosons. In order to obtain the tree level masses of the 5 physical Higgs particles one has to diagonalize the mass matrix

$$M^{ij}=\left.\frac{\partial^2 V_H}{\partial H_i\partial H_j}\right|_{\langle H_1^0\rangle=\frac{v_1}{\sqrt{2}},\langle H_2^0\rangle=\frac{v_2}{\sqrt{2}},\langle H_{1,2}^{\pm}\rangle=0} \tag{2.42}$$

The eigenvalues of the diagonalized mass matrix then lead to the physical Higgs masses of the neutral CP-even, CP-odd, charged Higgs and Goldstone bosons at tree level.

$$m_{H,h}^2 = \frac{1}{2}\left[m_A^2 + m_Z^2 \pm \sqrt{(M_A^2 + m_Z^2)^2 - 4m_A^2 m_Z^2 \cos^2(2\beta)}\right], \tag{2.43}$$

$$m_A^2 = \frac{2m_3^2}{\sin 2\beta}, \tag{2.44}$$

$$m_G^2 = 0, \tag{2.45}$$

$$m_{H^\pm} = m_A^2 + m_W^2, \tag{2.46}$$

$$m_{G^\pm} = 0. \tag{2.47}$$

The Yukawa coupling of the fermions to the Higgs field is given by the following Lagrangian

$$\mathcal{L}_{\text{y,MSSM}} = \sum_u y_u u\bar{u}H_2^0 + \sum_d y_d d\bar{d}H_1^0 \tag{2.48}$$

where $y_{u,d}$ are the Yukawa couplings of the up and down type quarks. In case of the pseudoscalar Higgs the couplings read

$$y_{Auu} = \frac{m_u}{v}\cot\beta\gamma_5, \quad y_{Add} = \frac{m_d}{v}\tan\beta\gamma_5 \tag{2.49}$$

2.2 Pseudoscalar Higgs boson production and decay at the LHC

For small and moderate values of $\tan\beta$ the gluon fusion process $gg \to A$ via a top or bottom triangle is the dominant production mechanism. While for $\tan\beta \lesssim 5$ the top-quark contributions are dominating bottom loops become relevant for larger values of $\tan\beta$. NLO corrections have been calculated in the limit of a heavy top quarks in Ref. [40, 41] as well as by including the full mass dependence in Refs. [24]. For smaller values of $\tan\beta$ they lead to an increase of the cross section by $\mathcal{O}(100\%)$ whereas for large $\tan\beta$ the increase amounts to about $\mathcal{O}(40\%)$. NNLO calculations are only available in the heavy top-quark limit, first published in Refs. [42, 43, 44]. Due to the similarities to the SM Higgs production resummation of large logarithms at NNLL has been performed in the limit of a heavy top-quark [45]. In this thesis we will review the fixed order calculations and improve the resummation in case of a pseudoscalar Higgs by including mass effects of the top-quark.

Subdominantly contributing for small values of $\tan\beta$ Higgs-bremsstrahlung off a $b\bar{b}$-pair plays a significant role at large $\tan\beta$ while Higgs radiation of top quarks is

smaller by one order of magnitude. For large values of $\tan\beta$ the process $gg/gg \to b\bar{b} + A$ forms the dominant production process. NLO QCD corrections again turn out to be large due to large logarithms which appear by virtue of the integration over the transverse momenta of the final state bottom quarks [46, 47]. In order to rescale these large logarithms one has to introduce bottom-quark densities inside the proton and exploit their DGLAP evolution equations. Within this five flavor scheme approach, starting with the LO process $b\bar{b} \to A$, NLO [48, 49] and NNLO [50] contributions are moderate in size if the running scale of the bottom mass is chosen of the order of the Higgs mass M_A. Both results in the 4FS and the 5FS will converge against the same value at higher perturbative orders.

The overall situation in case of the pseudoscalar Higgs production is depicted in Fig. 2.8 in the $m_h^{\max}$ benchmark scenario [51]. The grey solid line represents the gluon fusion process at a c.m. energy $s = 7$ TeV and $\tan\beta = 5$ in (a) and $\tan\beta = 30$ in (b) while the solid black line constitutes the pseudoscalar Higgs production in association with a bottom pair in the combination of 4FS+5FS.

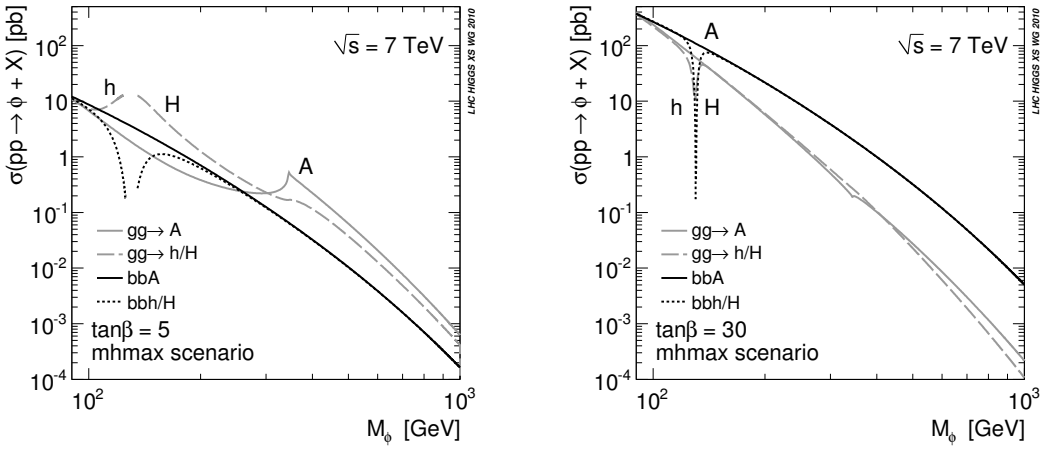

(a) (b)

Figure 2.8: Total hadronic cross section of the MSSM neutral Higgs boson production via gluon fusion and Higgs radiation off bottom quarks for a c.m. energy $\sqrt{s} = 7$ TeV for $\tan\beta = 5$ (a) and $\tan\beta = 30$ (b)

Chapter 3

Resummation

1 Quantum Chromodynamics

The aim of this section is to give a short introduction to Quantum Chromodynamics (QCD) as a basis of the main subject of this thesis, namely resummation. Starting from the basic Lagrangian, the theory of QCD suffers from infrared and ultraviolet divergences since certain statistical and quantum mechanical constructions are ill-defined. This 'illness' can be cured by the renormalization of quantum field operators. The effect of this redefinition of the Quantum field theory results in the appearance of large logarithms of unphysical scales. These contributions turn out to be universal, thus their structure can be predicted up to all orders. Nonetheless, in this context fixed order calculations of physical observables help to estimate and to improve the theoretical predictions. We have selected three kinds of processes to review the origin of the mentioned divergences in QCD and how to treat them in order to render QCD finite. Nevertheless, kinematical artifacts remain divergent in particular regions of the phase-space. At the end of this section we will discuss to the origin and basis for a resummation of large logarithms present in fixed higher order calculations.

1.1 Basics of QCD

Historically the theory of Quantum Chromodynamics was born due to the interplay of theoretical developments and experiments, such as the quark model of hadron states, the current algebra by virtue of analysis of flavor symmetries of strong interactions, the development of non-abelian gauge theories, asymotic freedom and the oberservation of the weakness of the strong force in Deep Inelastic Scattering (DIS).

The kinematics to describe the interactions of the quarks as a Dirac field ψ and the gluons as gauge fields G_μ can be extracted from an SU(3) Yang-Mills Lagrangian in Lorenz gauge.

$$\mathcal{L} = \mathcal{L}_{GI} + \mathcal{L}_{GF} + \mathcal{L}_{GC} \tag{3.1}$$

with

$$\mathcal{L}_{GI} = \bar{\psi}_0(i\not{D} - m_0)\psi_0 - \frac{1}{4}(G^a_{(0)\mu\nu})^2 \tag{3.2}$$

$$\mathcal{L}_{GF} = -\frac{1}{2\zeta_0}(\partial \cdot G_{(0)a})^2 \tag{3.3}$$

$$\mathcal{L}_{GC} = \partial_\mu \bar{\eta}_{0a}\partial^\mu \eta_{0a} + g_0 \partial^\mu \bar{\eta}_{0c} f_{abc} G^b_{(0)\mu}\eta_{0a}. \tag{3.4}$$

The covariant derivative is given by

$$D_\mu \psi_0 = (\partial_\mu + i g_{s(0)} t^a G^a_{(0)\mu})\psi_0 \tag{3.5}$$

where t^a are the generators of the SU(3) group. The gluon field strength tensor is

$$G^a_{(0)\mu\nu} = \partial_\mu G^a_{(0)\nu} - \partial_\nu G^a_{(0)\mu} - g_0 f_{abc} G^b_{(0)\mu} G^c_{(0)\nu} \tag{3.6}$$

where f_{abc} are the fully antisymmetric structure constants of the gauge group, defined by $[t_a, t_b] = i f_{abc} t_c$. Imposing local gauge transformations

$$\psi_0(x) \to \left[e^{-ig_o \alpha_a(x) t^a}\right] \psi_0(x) \tag{3.7}$$

$$G^a_{(0)\mu}(x) t^a \to \frac{-i}{g_0} e^{-ig_0 \alpha_a(x) t^a} D_\mu e^{ig_0 \alpha_a(x) t^a} \tag{3.8}$$

the Lagrangian in Eq. (3.1) is manifestly invariant under SU(3) gauge transformation. The gauge fixing term Eq. (3.3) is needed to define the gluon field propagator. A common choice for this kind of covariant gauges is the Feynman ($\zeta_{(0)} = 1$) or Landau ($\zeta_{(0)} = 0$) gauge. In the path integral formalism the Fadeev-Popov method then requires, dependent on the gauge fixing condition, the introduction of anticommuting scalars, the Fadeev-Popov ghosts. These fields obey the wrong spin statistics but ensure the cancellation of unphysical gauge boson polarizations. In axial gauges $\mathcal{L}_{GF} = -\frac{1}{2\zeta_0}(n \cdot G_{(0)a})^2$, with n beeing another vector, no ghost fields are needed but the form of the gluon field propagator become more complicated. We used the subscript 0 or (0) for the bare quantities. Quantum field theories as QCD suffer from UV divergences when the continuum limit is taken. Diagrammatically these divergences appear due to large loop momenta which can be regularized, e.g. in dimensional regularization. The renormalization procedure comprises the redefinition of the bare parameters of the Lagrangian in terms of physical parameters. The

aim is to obtain finite Greens functions which can be realized due to the change of normalization of the field wave function

$$G_{(0)\mu} = Z_3^{1/2} G_\mu, \quad \psi_0 = Z_2^{1/2}\psi \quad \text{and} \quad \eta_0 = \tilde{Z}_2^{1/2}\eta. \tag{3.9}$$

The counterterm approach then organizes the QCD-Lagrangian into three parts

$$\mathcal{L} = \mathcal{L}_{\text{free}} + \mathcal{L}_{\text{int}} + \mathcal{L}_{\text{c.t.}}. \tag{3.10}$$

with

$$\mathcal{L}_{\text{free}} = \bar{\psi}(i\not{D} - m)\psi - \frac{1}{4}(G^a_{\mu\nu})^2 - \frac{1}{2\zeta}(\partial \cdot G_a)^2 + \partial_\mu \bar{\eta}_a \partial^\mu \eta_a \tag{3.11}$$

$$\mathcal{L}_{\text{int}} = -g\mu^\epsilon \bar{\psi} t^a \not{G}^a \psi + g\mu^\epsilon f_{abc} G^{b\mu} G^{c\nu} \partial_\mu G^a_\nu - \frac{g^2\mu^{2\epsilon}}{4}(f_{abc} G^b_\mu G^c_\nu)^2 \tag{3.12}$$

$$+ g\mu^\epsilon f_{abc} \partial^\nu \bar{\eta}^c G^b_\mu \eta^a \tag{3.13}$$

$$\mathcal{L}_{\text{c.t.}} = (Z_2 - 1)\bar{\psi} i\not{\partial}\psi - \left(g_0 Z_2 Z_3^{1/2} - g\mu^\epsilon\right)\bar{\psi}\not{G}^a t^a \psi + \dots \tag{3.14}$$

The free Lagrangian $\mathcal{L}_{\text{free}}$ contains all the free propagators while the Lagrangian $\mathcal{L}_{\text{int}}$ includes the interation terms with the renormalized couplings. The third term in Eq. (3.10) depicts the counterterm Lagrangian which is needed to cancel the UV divergences from the basic interaction vertices. Feynman rules can be derived, e.g. by the path integral formalism, see Figure 3.1. Independent of the renormalization prescription the counterterm propagators and vertices shall only cancel the UV divergences. In dimensional regularization additional ϵ-dependent factors appear due to angular phase space integrations. The commonly used subtraction formalism in QCD is the $\overline{\text{MS}}$-scheme [52] which cancels not only the UV divergences but also subtracts universal constant terms. To be precise, the relations between the bare parameters and the renormalized quantities in the $\overline{\text{MS}}$-scheme for each loop are

$$g_{d(0)} = g_s \mu^\epsilon \left[1 + g_s^2 S_\epsilon \frac{B_{11}}{\epsilon} + g_s^4 S_\epsilon^2 \left(\frac{B_{22}}{\epsilon^2} + \frac{B_{21}}{\epsilon}\right) + \dots\right] \tag{3.15}$$

$$Z_2 = 1 + g^2 S_\epsilon \frac{Z_{2,11}}{\epsilon} + g^4 S_\epsilon^2 \left(\frac{Z_{2,22}}{\epsilon^2} + \frac{Z_{2,21}}{\epsilon}\right) + \dots.$$

where we define

$$S_\epsilon = \frac{(4\pi)^\epsilon}{\Gamma(1-\epsilon)} \tag{3.16}$$

The bare strong coupling does not depend on the introduced renormalized scale μ

$$\frac{\mathrm{d}}{\mathrm{d}\mu^2} g_0(\mu, g(\mu), \epsilon) = 0 \tag{3.17}$$

m,μ ∿∿∿ n,ν	$-i\frac{\delta^{mn}}{k^2}\left[g_{\mu\nu}-(1-\xi)\frac{k_\mu k_\nu}{k^2}\right]$	$i\Delta^{mn}_{\mu\nu}(k)$
m ⋯⋯→⋯⋯ n	$i\frac{\delta^{mn}}{k^2}$	$iD^{mn}(k)$
i,f ——→—— j,f'	$i\frac{\delta^{ij}\delta^{\mathrm{ff}'}}{k^\mu\gamma_\mu-m_\mathrm{f}}$	$iS^{\mathrm{ff}'}_{ij}(k)$
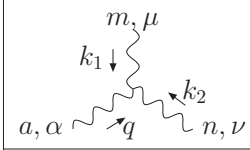	$gf^{amn}\left[g_{\mu\nu}(k_1-k_2)_\alpha+g_{\alpha\nu}(k_2-q)_\mu+g_{\alpha\mu}(q-k_1)_\nu\right]$	$i\Gamma_{A^a_\alpha A^m_\mu A^n_\nu}(k_1,k_2)$
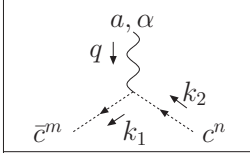	$gf^{amn}k_{1\alpha}$	$i\Gamma_{c^n A^a_\alpha \bar{c}^m}(q,-k_1)$
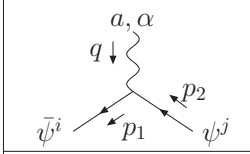	$ig\gamma^\alpha(t^a)_{ij}$	$i\Gamma_{\psi^j A^a_\alpha \bar{\psi}^i}(q,-p_1)$
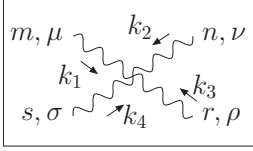	$-ig^2\left[f^{mse}f^{ern}(g_{\mu\rho}g_{\nu\sigma}-g_{\mu\nu}g_{\rho\sigma})+f^{mne}f^{esr}(g_{\mu\sigma}g_{\nu\rho}-g_{\mu\rho}g_{\nu\sigma})+f^{mre}f^{esn}(g_{\mu\sigma}g_{\nu\rho}-g_{\mu\nu}g_{\rho\sigma})\right]$	$\Gamma_{A^m_\mu A^n_\nu A^r_\rho A^s_\sigma}(k_2,k_3,k_4)$

Figure 3.1: Feynman Rules in QCD in covariant gauge

Using Eq. (3.15) this leads to the running coupling equation

$$\frac{\mathrm{d}}{\mathrm{d}\ln\mu^2}\alpha_s = \beta(\alpha_s), \quad \beta = \sum_{n=1}^{\infty} \frac{g^{2n+2}}{8\pi^2} n B_{n1} \tag{3.18}$$

The coefficients β can be found in Appendix A. This invariance is a general feature of renormalized Quantum Field Theories, i.e. in the full theory physical quantities are renormalization-group invariant. Assuming that these observables R only depend on the energy scale Q and neglecting all quark masses R depends on the ratio Q^2/μ^2 and the renormalized coupling α_s. Applying the RG-equation to R leads to

$$\left[\mu^2\frac{\partial}{\partial\mu^2} + \mu^2\frac{\partial\alpha_s}{\partial\mu^2}\frac{\partial}{\partial\alpha_s}\right] R\left(Q^2/\mu^2, \alpha_s(\mu^2)\right) = 0 \tag{3.19}$$

as well as to the running coupling equation. The solution of the running coupling equation as well as the initial condition of the solution to Eq. (3.19), $R(1, \alpha_s(Q^2))$, resum correctly logarithms of the kind $\alpha_s^m \ln^n(Q^2/\mu^2)$ with m being the respective loop order. The solution to the running coupling equation is explained in A and the restauration of the scale dependence of cross sections can be found in C. The crucial difference to QED is that the running coupling becomes small for large values of μ. This property is called asymptotic freedom and is related to the negative sign of the beta function (see Appendix A). Diagrammatically the inclusion of the triple gluon vertex contribution causes this behavior contrary to QED. Physical quantities, e.g. cross sections, can be calculated order by order of the strong coupling α_s as we will see in the next sections.

1.2 Electron-positron annihilation

As a starting point to perturbative QCD calculations we will contemplate the process $e^+e^- \to$ hadrons for many reasons. Not just the process serves as an excellent test of the color hypothesis of QCD and gave rise to the parton model, but also the cancellation of soft an collinear singularities is a nice example of the infrared safety. In the inclusive process the electron-positron initial state annihilate via a neutral vector boson into a quark-antiquark pair. By confinement the quarks and gluons subsequently form themselves into hadrons at timescales larger than the invariant hard scattering process. Hereafter we only consider the annihilation process via a photon at leading (LO) and next-to-leading order (NLO) in massless QCD. It can easily be shown that the leptonic part factorizes from the hadronic one

$$\sigma = \frac{e^4}{2Q^6} L_{\mu\nu} W^{\mu\nu} = \sigma_0^{\epsilon}\left[1 + \frac{\alpha_s}{\pi}(C_{\mathrm{vc}} + C_{\mathrm{rc}})\right] + \mathcal{O}(\alpha_s^2) \tag{3.20}$$

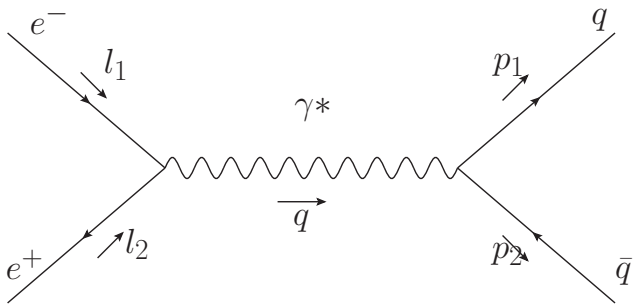

Figure 3.2: Lowest order cross section for the annihilation of an electron-positron initial state to a quark anti-quark pair

where $Q^2 = q^2$ is the invariant mass of the lepton pair, σ_0^ϵ the $(4-2\epsilon)$-dimensional Born term,

$$L^{\mu\nu} = tr[\not{l}_2\gamma^\mu\not{l}_1\gamma^\nu] = l_1^\mu l_2^\nu + l_2^\mu l_1^\nu - g^{\mu\nu} l_1 \cdot l_2 \tag{3.21}$$

and

$$W^{\mu\nu}(q) = \int \mathrm{d}^4x \mathrm{e}^{iq\cdot x}\langle 0|j^\mu(x)j^\nu(0)|0\rangle. \tag{3.22}$$

Due to the conservation of the electromagnetic current j^μ the hadronic tensor can further be decomposed into

$$W^{\mu\nu} = (-g^{\mu\nu}q^2 + q^\mu q^\nu)\frac{1}{6\pi}R(Q^2)\theta(q^0). \tag{3.23}$$

Hence by contraction with the leptonic part the cross section can be written as

$$\sigma = \sigma_0 R(Q^2) \tag{3.24}$$

with $\sigma_0 = \frac{4\pi\alpha^2}{3Q^2}$. R is defined in such a way that it reflects the ratio of $q\bar{q}$ and $\mu^+\mu^-$ production in electron positron annihilation

$$R = \frac{\sigma(e^+e^- \to hadrons)}{\sigma(e^+e^- \to \mu^+\mu-, \mathrm{LO}, \mathrm{em})}. \tag{3.25}$$

At lowest order a straightforward calculation yields

$$R^{(0)} = 3\sum_q Q_q^2. \tag{3.26}$$

The factor 3 originates from the sum over all quark colors and the sum is over all accessible quark flavors of the corresponding charges Q_f of the quarks. Only those quarks which are above the threshold of the production a $q\bar{q}$-pair are included in the sum. Yet at lowest order and far below the Z-resonance experimental data

[53] on the ratio R are in reasonable agreement with theoretical predictions which besides the π^0-decay into two photons provides another verification of the three color hypothesis. The main difference originates from the fact that one has to calculate higher-order QCD corrections. At NLO corrections both from virtual and real gluon emission diagrams have to be taken into account. The self energy contribution to

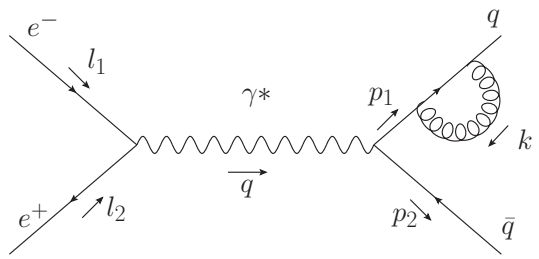

(a) External self-energies

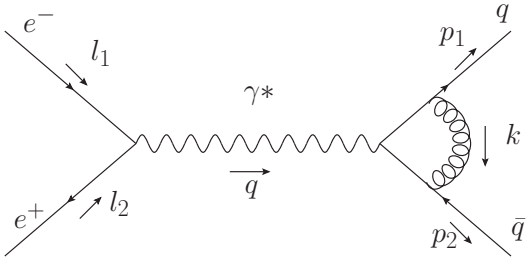

(b) Vertex corrections

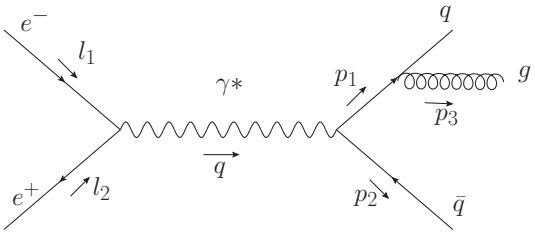

(c) Real gluon emission

Figure 3.3: Virtual and real contributions to $e^+e^- \to q\bar{q}$

the external quark propagator in Feynman gauge can be written in the following form

$$\Sigma(p_i) = -\mathrm{i}g_s^2\mu^{2\epsilon}C_F \int \frac{\mathrm{d}^{4-2\epsilon}k}{(2\pi)^{4-2\epsilon}}\gamma^\sigma \frac{\not{p}_i - \not{k}}{[(p_i-k)^2+\mathrm{i}0]}\gamma^\delta \left(\frac{g_{\sigma\delta}}{k^2+\mathrm{i}0}\right). \tag{3.27}$$

Since $\Sigma(p_i) = -i\not{p}_i\bar{\Sigma}(p_i)$ and using dimensional regularization for the integration over the loop momenta we get

$$\bar{\Sigma}(p_i) = \frac{g_s^2 C_F}{16\pi^2}\left(\frac{4\pi\mu^2}{-p_i^2}\right)^\epsilon \frac{1}{\epsilon}\frac{\Gamma(1+\epsilon)\Gamma(1-\epsilon)^2}{\Gamma(1-2\epsilon)}\frac{(1-\epsilon)}{(1-2\epsilon)}. \tag{3.28}$$

By taking ϵ to negative values and letting $p_i \to 0$ we can deduce that the two external leg diagrams do not contribute to the total cross section. The vertex graph can be calculated in a similar way giving a correction

$$\delta\Gamma^\mu(q^2) = -g_s^2\mu^{2\epsilon}C_F \int \frac{\mathrm{d}^{4-2\epsilon}k}{(2\pi)^{4-2\epsilon}} \frac{\mathrm{Tr}\{\gamma^\sigma(\not{k}+\not{p}_1)\gamma^\mu(\not{k}-\not{k}_2)\gamma_\sigma\}}{(k^2+\mathrm{i}0)[(k+p_1)^2)+\mathrm{i}0][(p_2+k)^2+\mathrm{i}0]} \tag{3.29}$$

Due to the Ward identity and exploiting the Dirac equation for massless quarks the vertex correction takes the form $\delta\Gamma^\mu(q^2) = \bar{\Gamma}(q^2)\gamma^\mu$ with

$$\bar{\Gamma}(q^2) = \mathrm{i}g_s^2 C_F[2q^2 C_0(p_1, p_2, 0, 0, 0) + (3+2\epsilon)B_0(q^2, 0, 0)] \tag{3.30}$$

where the scalar integrals of the three-point and the two-point functions can be derived as

$$B_0(q^2, 0, 0) = \frac{\Gamma(1-\epsilon)}{\Gamma(1-2\epsilon)} \frac{\left(\frac{1}{\epsilon}+2\right)}{16\pi^4} \tag{3.31}$$

$$C_0(p_1, p_2, 0, 0, 0) = \frac{\Gamma(1-\epsilon)}{\Gamma(1-2\epsilon)} \frac{\left(\frac{1}{\epsilon^2}+\frac{\pi^2}{6}\right)\left(1-\frac{\pi^2\epsilon^2}{2}\right)}{16\pi^4 s}. \tag{3.32}$$

Since the virtual corrections contribute to the same final state as the Born term the amplitudes must be added and squared as follows

$$|A_0 + 2A_1^{(a)} + A_1^{(b)}|^2 = |A_0| + 2\mathrm{Re}(A_0 A_1^{(b)*}) + \mathcal{O}(\alpha_s^2) \tag{3.33}$$

Performing the phase-space integral over the two particle final state and factorizing off the d-dimensional Born term leads to the final expression for the virtual corrections

$$C_{\mathrm{vc}} = \left(\frac{4\pi\mu^2}{q^2}\right)^\epsilon \frac{\Gamma(1-\epsilon)}{\Gamma(1-2\epsilon)} C_F \left(-\frac{1}{\epsilon^2} - \frac{3}{2\epsilon} + \frac{\pi^2}{3} - 4\right) \tag{3.34}$$

The computation of the real gluon emission graph contains the evaluation of the three particle phase space resulting in the $\mathcal{O}(\alpha_s)$-real corrections

$$C_{\mathrm{rc}} = \left(\frac{4\pi\mu^2}{q^2}\right)^\epsilon \frac{\Gamma(1-\epsilon)}{\Gamma(1-2\epsilon)} C_F \left(\frac{1}{\epsilon^2} + \frac{3}{2\epsilon} - \frac{\pi^2}{3} + \frac{19}{4}\right) \tag{3.35}$$

The real and virtual corrections contain both IR-divergences containing soft-collinear $1/\epsilon^2$- and collinear $1/\epsilon$-poles. As mentioned above the final result

$$R = R^0 \left(1 + \frac{3}{4} C_F \alpha_s(\mu_R^2) + \mathcal{O}(\alpha_s^2)\right) \tag{3.36}$$

is IR-safe due to the Kinoshita-Lee-Nauenberg theorem [54, 55] and does not contain any logarithms $\ln\left(\frac{Q^2}{\mu_R}\right)$ at this perturbative order due to the RG-invariance of the ratio. At NNLO and higher orders UV-divergences appear which have to be renormalized leading to results depending on the renormalization scale. Next we want to review these kind of processes with hadrons in the initial state, discuss the incomplete cancellation of infrared divergences in Deep Inelastic Scattering and review the main concepts of the Parton Model.

1.3 Deep Inelastic Scattering and Parton Model

In this section we will give an heuristic derivation of the Parton Model in QCD. Deep Inelastic Scattering (DIS) processes generally stand for all the processes where a lepton scatters off a hadron, e.g. a proton or a neutron. In case of a large momentum transfer between the lepton and the hadron DIS serves as an excellent test of probing the substructure of the hadron as well as the properties of its constituents, called partons. Due to asymptotic freedom at short distances the hadron itself can phenomenologically be described as a loosely bound state of quarks that are moving with large longitudinal momentum along the direction of the hadron. Furthermore, the partons itself cannot achieve a large transverse momentum. Thus, the only possibility of energy transfer with a large invariant mass $Q^2 = -q^2$ is due to the exchange of a vector boson of the electroweak sector, i.e. a photon or Z-boson. In this case the quark is pulled out of the hadron which cannot be balanced out by subsequent soft processes. The situation is depicted in figure 3.4. In the following we restrict

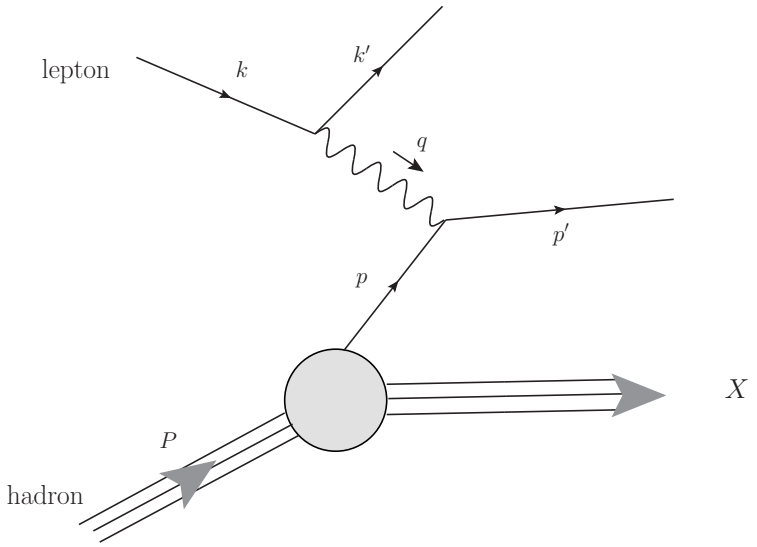

Figure 3.4: Diagramatic Picture of the DIS

ourselves to the case of electron-proton scattering. Similar to e^+e--annihilation into hadrons it is convenient to decompose the cross section into a leptonic and into a hadronic part. Starting from the generalized structure of the S-matrix element for this process the cross section can be written as

$$\mathrm{d}\sigma = \frac{2\alpha^2}{Q^4 s}\frac{\mathrm{d}^3 k'}{|k'_0|} L_{\mu\nu}\mathrm{d}W^{\mu\nu}. \tag{3.37}$$

The leptonic tensor can be determined as

$$L^{\mu\nu} = \frac{1}{2}\mathrm{Tr}\left[\not{k}'\gamma^{\mu}\not{k}\gamma^{\nu}\right]. \tag{3.38}$$

while the hadronic tensor takes the form

$$W^{\mu,\nu}(q,P) = \frac{1}{8\pi}\sum_{\sigma}\int \mathrm{d}^4x e^{iq\cdot x}\langle P,S|j^{\mu}(x)j^{\nu}(0)|P,S\rangle \tag{3.39}$$

$$= -(g^{\mu\nu} - \frac{q^{\mu}q^{\nu}}{q^2})W_1(x,q^2) + (P_{\mu} - q_{\mu}\frac{P\cdot q}{q^2})(P_{\nu} - q_{\nu}\frac{P\cdot q}{q^2})W_2(x,q^2) \tag{3.40}$$

α is the fine structure constant, P and S the momentum and the spin of the incoming hadron and j^{μ} the electromagnetic current. The notation $\langle P,S|\cdots|P,S\rangle$ is a shorthand notation for a trace with a spin density matrix. We also introduce the Bjorken$-x$ variable

$$x = \frac{Q^2}{2P\cdot q} \tag{3.41}$$

and for further issues we redefine the scalar functions F_1 and F_2 as

$$F_1(x,Q^2) = 2W_1(x,Q^2) \quad F_2(x,Q^2) = \frac{P\cdot q}{x}W_2(x,Q^2) \tag{3.42}$$

As explained above, due to the absence of interactions of the partons among each other during the electron-parton scattering the cross section for the hard scattering may be computed by combining probabilities incoherently rather than amplitudes. The naive parton model assumes that the constituents only carry a longitudinal fraction ξ of the momentum of the proton.

$$p = \xi P \tag{3.43}$$

where $0 \leq \xi \leq 1$. Furthermore, the probability of finding a parton a inside a proton is called the parton distribution function (PDF) or parton density $f_a(\xi)$. Governed by this factorization theorem the total hadronic cross section in DIS can be written as

$$\sigma_{DIS}(x,Q^2) = \sum_a \int_x^1 f_{a,h}(\xi)\hat{\sigma}_{DIS}(\frac{x}{\xi},Q^2) \tag{3.44}$$

where $\hat{\sigma}_{DIS}$ is the partonic cross section of electron-parton scattering and the sum is over all possible types of a parton a. The theorem itself can also be applied to the measurable structure functions

$$F_1(x,Q^2) = \sum_a \int_x^1 \frac{\mathrm{d}\xi}{\xi}C_1^a\left(\frac{x}{\xi},\frac{Q^2}{\mu^2},\alpha_s(\mu^2)\right)f_{a,h}(\xi,\epsilon,\alpha_s(\mu^2)) + \mathcal{O}\left(\frac{1}{Q^2}\right) \tag{3.45}$$

$$F_2(x,Q^2) = \sum_a \int_x^1 \mathrm{d}\xi C_2^a\left(\frac{x}{\xi},\frac{Q^2}{\mu^2},\alpha_s(\mu^2)\right) f_{a,h}(\xi,\epsilon,\alpha_s(\mu^2)) + \mathcal{O}\left(\frac{1}{Q^2}\right) \tag{3.46}$$

where C_i^a are the partonic coefficient functions that are calculable in perturbation theory and higher-twist contributions of order $\mathcal{O}(1/Q^2)$ are neglected. The fundamental content of the factorization theorem is the separation of short distance effects, such as Q-dependence in the structure functions $\mathcal{F}_i$, and long distance effects contained in the parton distributions. The scale μ is usually chosen to be equal to the renormalization scale μ_R. The hadronic tensor $W_{\mu\nu}$ as well as its partonic equivalent $H_{\mu\nu}$ can thus be expanded in a series of the strong coupling

$$\mathcal{W}_{\mu\nu}(q,p) = \sum_{n=0}\left(\frac{\alpha_s}{\pi}\right)^n \mathcal{W}_{\mu\nu}^{(n)}(q,p) \tag{3.47}$$

At the Born level the contribution to the partonic tensor can simply be determined as

$$\mathcal{W}_{\mu\nu}^{(0)}(q,p) = \frac{1}{8\pi}\int \frac{\mathrm{d}^{n-1}|\mathbf{p}'|}{(2\pi)^{n-1}2p_0'} Q_q^2 \mathrm{Tr}\left[\not{p}'\gamma_\mu \not{p}\gamma_\nu\right](2\pi)^n\,\delta^{(n)}\left(p'-p-q\right) \tag{3.48}$$

Contracting this tensor with $-g_{\mu\nu}$ and with $p_\mu p_\nu$ leads to

$$\begin{aligned} -g^{\mu\nu}\mathcal{W}_{\mu\nu}^{(0)} &= Q_q^2(1-\epsilon)\delta(1-z) = (1-\epsilon)\frac{\mathcal{F}_2^{(0)}}{z} - (3-2\epsilon)\left[\frac{\mathcal{F}_2^{(0)}}{2z} - \mathcal{F}_1^{(0)}\right] \\ p^\mu p^\nu \mathcal{W}_{\mu\nu}^{(0)} &= \frac{Q^2}{4z^2}\left[\frac{\mathcal{F}_2^{(0)}}{2z} - \mathcal{F}_1^{(0)}\right] \end{aligned} \tag{3.49}$$

The final result at the partonic level reads

$$\mathcal{F}_1^{q,(0)}(z,Q^2) = \frac{1}{2}Q_q^2\delta(1-z) \tag{3.50}$$

$$\mathcal{F}_2^{q,(0)}(z,Q^2) = Q_q^2\delta(1-z) \tag{3.51}$$

where

$$z = \frac{Q^2}{2p\cdot q} \tag{3.52}$$

We observe that the structure functions are independent of the momentum Q which is called Bjorken scaling. Another interesting property of the parton model can be deduced from Eq. (3.49), Eqs. (3.45) and (3.46), namely

$$2zF_1^{q,(0)} = F_2^{q,(0)} \tag{3.53}$$

which is the Callan-Gross relation. In accordance with experiments this relation manifests the spin-$\frac{1}{2}$ property of the parton constituents, the quarks, since otherwise for spin-0 partons the structure functions would be $F_1^{(0)} = 0$ and $F_2^{(0)} \neq 0$ As we approach higher-order corrections the Bjorken scaling and the Callan–Cross relation is violated logarithmically. The NLO calculation of the hadronic tensor involves the computation of virtual and real corrections as illustrated in Figure 3.5.

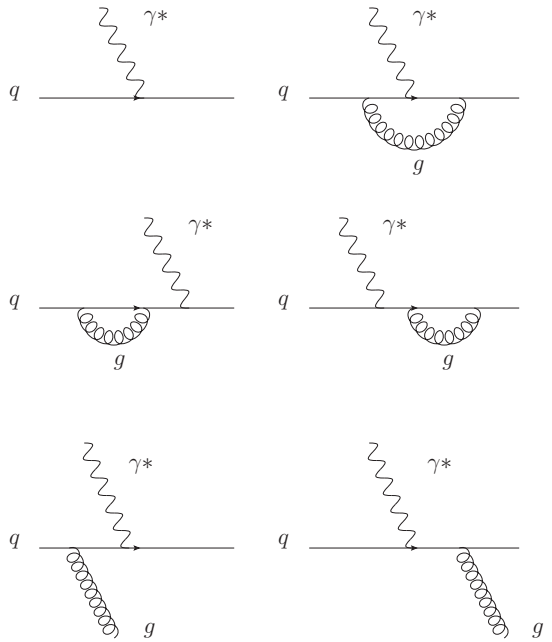

Figure 3.5: Born level contribution and NLO corrections to the partonic tensor $H_{\mu\nu}$

Again external leg corrections do not contribute as explained in section 1.2. Hence we dedicade ourselves to the vertex correction which develops a similar form as the final state corrections in the previous section. The one loop virtual corrections can be calculated as

$$\mathcal{W}_{\mu\nu}^{(1,v)}(q,p) = \frac{1}{8\pi}\int \frac{\mathrm{d}^{n-1}|\mathbf{p}'|}{(2\pi)^{n-1}2p_0'} Q_q^2 \mathrm{Tr}\left[\not{p}'\Gamma_\mu \not{p}\Gamma_\nu\right](2\pi)^n \delta^{(n)}(p'-p-q) \tag{3.54}$$

$$= \mathcal{W}_{\mu\nu}^{(0)}(q,p) 2\bar{\Gamma}(Q^2) + \mathcal{O}(\alpha_\int^\in) \tag{3.55}$$

where we adopted $\bar{\Gamma}$ from Eq. (3.29). The real corrections of the single gluon emission diagrams call for the evaluation of the two particle phase space in n-dimensions

$$H_{\mu\nu}^{(1,r)}(q,p) = -\frac{1}{8\pi}\int \frac{\mathrm{d}^{n-1}|\mathbf{p}'|}{(2\pi)^{n-1}2p_0'}\int \frac{\mathrm{d}^{n-1}|\mathbf{l}'|}{(2\pi)^{n-1}2l_0'} Q_q^2 \mathrm{Tr}\left[\not{p}' S^{\mu\sigma} \not{p} S_\sigma^\nu\right](2\pi)^n \delta^{(n)}(p'+l-p-q). \tag{3.56}$$

where

$$S^{\mu\sigma} = -i\bar{g}_s T_a \left[\gamma^\mu \frac{(\not{p} - \not{l})}{(p-l)^2} \gamma^\sigma + \gamma^\sigma \frac{(\not{p}' + \not{l})}{(p'+l)^2} \gamma^\mu \right]. \tag{3.57}$$

After combining the results of the real and virtual contributions we arrive at the final result for the structure functions at one-loop level [56]

$$\mathcal{F}_2^{q,(1)}(z,Q^2) = \frac{1}{2} Q_q^2 z \left[-\left(\frac{4\pi\mu^2}{Q^2}\right)^\epsilon \frac{\Gamma(1-\epsilon)}{\Gamma(1-2\epsilon)} \frac{1}{\epsilon} P_{qq}^{(0)}(z) \right. \tag{3.58}$$

$$+ C_F \left((1+z)^2 \left[\frac{\ln(1-z)}{(1-z)} \right]_+ - \frac{3}{2} \left[\frac{1}{(1-z)} \right]_+ \right. \tag{3.59}$$

$$\left. \left. - \frac{(1+z^2)}{(1-z)} \ln(z) + 3 + 2z - \left(\frac{9}{2} + \frac{1}{3}\pi^2 \right) \delta(1-z) \right) \right] \tag{3.60}$$

$$\mathcal{F}_1^{q,(1)}(z,Q^2) = \mathcal{F}_2^{q,(1)}(z,Q^2) - Q_q^2 C_F z, \tag{3.61}$$

where $C_F = 4/3$. The plus distributions are defined as

$$\int_y^1 \left[\frac{\ln^m(1-z)}{1-z} \right]_+ g(z) = \int_y^1 \left[\frac{\ln^m(1-z)}{1-z} \right] (g(z) - g(1)) - g(1) \int_0^y \mathrm{d}z \left[\frac{\ln^m(1-z)}{1-z} \right]. \tag{3.62}$$

Since the crossed channel $\gamma^* g \to q\bar{q}$ is not distinguishable from $\gamma^* q \to qg$ and of the same order in the strong coupling the diagrams of figure 3.6 have also to be added. Here we only want to give the final result

$$\mathcal{F}_2^{g,(1)}(z,Q^2) = -Q_q^2 \frac{1}{\epsilon} P_{qg}^{(0)}(z) \left(\frac{4\pi\mu^2}{Q^2} \right)^\epsilon \frac{\Gamma(1-\epsilon)}{\Gamma(1-2\epsilon)} \tag{3.63}$$

$$+ \frac{1}{2} \left[(z^2 + (1-z)^2) \ln\left(\frac{(1-z)}{z} \right) + 6z(1-z) \right] \tag{3.64}$$

$$\mathcal{F}_1^{g,(1)}(z,Q^2) = \mathcal{F}_2^{g,(1)}(z,Q^2) + Q_q^2 T_R 2z(1-z) \tag{3.65}$$

where $T_R = 1/2$.

We first notice that the difference

$$\mathcal{F}_{2,L}^{a,(1)}(z,Q^2) = \mathcal{F}_2^{a,(1)}(z,Q^2) \frac{1}{2z} - \mathcal{F}_1^{a,(1)}(z,Q^2) \quad a = q, g \tag{3.66}$$

is finite at NLO as $\epsilon \to 0$. However both $\mathcal{F}_1^{a,(1)}$ and $\mathcal{F}_2^{a,(1)}$ individually are not finite although the infrared divergences cancelled completely. This can be related to the configuration that the gluon is emitted collinear to the direction of the quark.

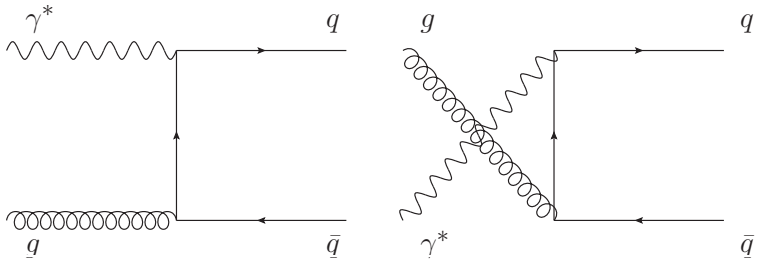

Figure 3.6: NLO contribution to $\mathcal{F}_i^{g,(1)}$.

However, these infrared singularities can be absorbed in a redefinition of the parton densities. Now we can determine the hard part of the coefficient functions

$$C_i^a = C_i^{a,(0)} + \frac{\alpha_s}{\pi} C_i^{a,(1)} + \mathcal{O}\left(\alpha_s^2\right), \tag{3.67}$$

i.e. the part of the cross section which is finite for $\epsilon \to 0$. Although the PDF's are not calculable in perturbation theory parton densities can be defined as matrix elements in a hadronic state of fermion operators that count the number of partons, quarks or gluons, which carry a momentum fraction ξ. The densities for quarks and gluons are defined as [57, 58, 59]

$$f_{q/h}(\xi) = \frac{1}{4\pi} \int \mathrm{d}x^- e^{-i\xi P^+ x^-} \langle P, S | \bar{\psi}(0, x^-, 0_\perp) \gamma^+ \mathcal{G} \psi(0, 0, 0_\perp) | P, S \rangle \tag{3.68}$$

$$f_{g/h}(\xi) = \frac{1}{2\pi \xi P^+} \int \mathrm{d}x^- e^{-i\xi P^+ x^-} \langle P, S | G_a(0, x^-, 0_\perp)^{+\nu} \mathcal{G}_{ab} G_b(0, 0, 0_\perp)^+_\nu | P, S \rangle \tag{3.69}$$

where $P^\pm = (P^0 \pm P^3)/\sqrt{2}$, $x^+ = 0$, $x^- = (x^0 - x^3)/2$, $\gamma^\pm = \gamma^0 \pm \gamma^3$, G_a the field strength tensor and

$$\mathcal{G} = \mathcal{P} \exp\left\{ ig \int_0^{x^-} \mathrm{d}y^- G_c^+(0, y^-, 0_\perp) T_c \right\} \tag{3.70}$$

is a non-local operator that ensures the gauge invariance of the expressions above. $\mathcal{P}$ indicates the path-ordering of the gluon fields $G^+(0, y^-, 0_\perp)$ in the $G^+ = 0$ gauge. At one loop the parton-in-parton densities read [60]

$$f_{a/b}(\xi, \epsilon) = \delta_{ab}\delta(1-\xi) - \frac{\alpha_s}{2\pi} \frac{1}{\epsilon} \left(\frac{4\pi\mu^2}{\mu_F^2} \right)^\epsilon \frac{\Gamma(1-\epsilon)}{\Gamma(1-2\epsilon)} P_{ab}^{(0)}(\xi) \tag{3.71}$$

Finally, in order to determine the hard coefficients we simply expand the partonic equivalent of Eq. (3.46) arriving at

$$\mathcal{F}_2^{q,(1)}(z, Q^2) = Q_q^2 \delta(1-z) + \left(\frac{\alpha_s}{\pi}\right) \left[Q_q^2 f_{a/a}^{(1)}(z, \epsilon) + C_2^{a,(1)}\left(z, \frac{Q^2}{\mu^2}\right) \right] + \mathcal{O}\left(\alpha_s^2\right) \tag{3.72}$$

repectively,

$$\mathcal{F}_2^{g,(1)}(z,Q^2) = + \left(\frac{\alpha_s}{\pi}\right) \left[Q_q^2 f_{q/g}^{(1)}(z,\epsilon) + C_2^{g,(1)}\left(z, \frac{Q^2}{\mu^2}\right)\right] + \mathcal{O}\left(\alpha_s^2\right) \tag{3.73}$$

We want to note that the coefficients $C_2^{a,(1)}$ and $C_2^{g,(1)}$ are finite in ϵ and furthermore contain logarithms of the kind $\ln\left(\frac{Q^2}{\mu_F^2}\right)$ due to the renormalization of the bare parton densities. Taking the derivative on Eq. (3.46) with respect to $\partial/\partial \ln \mu^2$ we arrive at the DGLAP evolution equations [61, 62, 63]

$$\frac{\partial}{\partial \ln \mu} f_{i/h}(x,\mu^2) = \sum_b P_{ij}(x,\mu^2) \otimes f_{j/h}(x,\mu^2) \tag{3.74}$$

where $\otimes$ denotes the Mellin convolution

$$(f \otimes g)(x) = \int_x^1 \frac{\mathrm{d}\xi}{\xi} f\left(\frac{x}{\xi}\right) g(\xi) \tag{3.75}$$

and the Altarelli–Parisi splitting functions obey the perturbative expansion

$$P_{ij}(x,\mu^2) = \sum_k \left(\frac{\alpha_s}{\pi}\right)^{k+1} P_{ij}^{(k)}(x) \tag{3.76}$$

The splitting functions can be found in Appendix A. The DGLAP equation (3.74) is formally a $(2N_f+1)$-dimensional intro-differential matrix equation of a vector of quarks, anti-quarks and gluons.

$$\frac{\partial}{\partial \ln \mu} \begin{pmatrix} q_i \\ g \end{pmatrix} (x,\mu^2) = \sum_{q_j,\bar{q}_k} \left[\begin{pmatrix} P_{q_i q_j} & P_{q_i g} \\ P_{g q_j} & P_{gg} \end{pmatrix} \otimes \begin{pmatrix} q_j \\ g \end{pmatrix} \right] (x,\mu^2) \tag{3.77}$$

This system of equations is most conveniently decoupled by using charge conjugation and flavor symmetries. Due to the flavor independence of the gluon-quark and quark-gluon splitting

$$P_{gq} = P_{gq_i} = P_{g\bar{q}_i}, \quad P_{qg} = 2N_f P_{q_i g} = 2N_f P_{\bar{q}_i g} \tag{3.78}$$

any difference $q_i - q_j$ and $q_i - \bar{q}_j$ decouples from the gluon. The singlet quark distributions

$$q_s = \sum_{r=1}^{N_f} (q_r + \bar{q}_r) \tag{3.79}$$

couple maximally to the gluon distribution via

$$\frac{\partial}{\partial \ln \mu} \begin{pmatrix} q_s \\ g \end{pmatrix} (x, \mu^2) = \left[\begin{pmatrix} P_{qq} & P_{qg} \\ P_{gq} & P_{gg} \end{pmatrix} \otimes \begin{pmatrix} q_s \\ g \end{pmatrix} \right] (x, \mu^2) \tag{3.80}$$

The non-singlet quark distributions can further be decomposed into a flavor asymmetrical part $q_{ns}^{\pm}$ and a valence part q_{ns}^{v} via the combinations

$$q_{NS,ik}^{\pm} = (q_i \pm \bar{q}_i) - (q_k \pm \bar{q}_k), \quad q_{ns}^{v} = \sum_{r=1}^{N_f} (q_r - \bar{q}_r) \tag{3.81}$$

and due to the general structure of the (anti-)quark (anti-)quark splitting functions

$$P_{q_i q_k} = P_{\bar{q}_i \bar{q}_k} = \delta_{ik} P_{qq}^{v} + P_{qq}^{s}, \quad P_{q_i \bar{q}_k} = P_{\bar{q}_i q_k} = \delta_{ik} P_{q\bar{q}}^{v} + P_{q\bar{q}}^{s} \tag{3.82}$$

This leads to two additional independent differential equations

$$\frac{\partial}{\partial \ln \mu} q_{ns}^{\pm}(x, \mu^2) = P_{ns}^{\pm} \otimes q_{ns}^{\pm}(x, \mu^2) \tag{3.83}$$

and

$$\frac{\partial}{\partial \ln \mu} q_{ns}^{v}(x, \mu^2) = P_{ns}^{v} \otimes q_{v}^{\pm}(x, \mu^2) \tag{3.84}$$

where the non-singlet parton splitting functions are defined as

$$\begin{aligned} P_{\rm ns}^{\pm} &= P_{\rm qq}^{\rm v} \pm P_{\rm q\bar{q}}^{\rm v} \ , \\ P_{\rm ns}^{\rm v} &= P_{\rm qq}^{\rm v} - P_{\rm q\bar{q}}^{\rm v} + N_F (P_{\rm qq}^{\rm s} - P_{\rm q\bar{q}}^{\rm s}) \ \equiv \ P_{\rm ns}^{-} + P_{\rm ns}^{\rm s} \ . \end{aligned} \tag{3.85}$$

The solutions of Eqs. (3.80), (3.83) and (3.84) can be derived analytically in Mellin space since the integro-differential equations then become usual differential equations as we will describe in Sec. 4.1.

1.4 Drell–Yan

Drell–Yan (DY) processes, first calculated at LO in [64], include the production of a pair of leptons $l^+ l^-$ due to the collision of two hadrons of type A and type B.

$$h_A(P_1) + h_B(P_2) \to l^+(k_1) l^-(k_2) + X \tag{3.86}$$

The production itself is mediated by an electroweak vector boson exchange of invariant mass $Q^2 = q^\mu q_\mu$, e.g. an off-shell photon γ^* or Z-boson in case of the production

of a $\mu^+\mu^-$ pair. Another possibility includes the mediation by a W-boson into a lepton-neutrino pair. However, for illustration issues we will not consider the latter kind of processes as well as the case of the Z-boson exchange into leptons. We frequently will use the ratio of the invariant mass Q^2 over the center of mass energy s. From the theoretical point of view this kind of processes provide two mainly important subjects which are contents of this thesis. The factorization theorem, successfully confirmed by experiments in the case of DIS, can be extended to hadron-hadron collision processes [65, 66, 67, 68, 69, 70]. In particular, the total hadronic cross section in the naive parton model can be written as a weighting of the partonic cross section by LO parton densities $f_{a/h_i}(x_i)$ which do not yet depend on the unphysical factorization scale μ_F. Quarks and gluons which contribute to the partonics sub-crossection are assumed to carry a fraction $p_i = x_i P_i$ of the momentum of the respective hadron h_i similar to DIS. Higher-order corrections in DY again develop ultraviolet and infrared divergences which can be cured by renormalization of the strong coupling α_s and the bare parton densities in order to determine the finite coefficient functions ω_{ab} contained in the mass factorization formula of the hadronic cross section

$$
\begin{aligned}
Q^2 \frac{\mathrm{d}\sigma_{DY}}{\mathrm{d}Q^2} &= \sigma_0(\tau_h, Q^2) W(\tau_h, \alpha_s(\mu_R^2), \frac{Q^2}{\mu_R^2}, \frac{Q^2}{\mu_F^2}) + \mathcal{O}\left(\frac{1}{Q^2}\right), \\
W(\tau_h, \alpha_s(\mu_R^2), \frac{Q^2}{\mu_R^2}, \frac{Q^2}{\mu_F^2}) &= \sum_{a,\bar{b}} Q_q^2 \int_0^1 \frac{\mathrm{d}x_1}{x_1} \frac{\mathrm{d}x_2}{x_2} \\
&\quad \times f_{1,a/h}(x_1, \mu_F^2) \omega_{a\bar{b}}(z, \alpha_s(\mu_R^2), \frac{Q^2}{\mu_R^2}, \frac{Q^2}{\mu_F^2}) f_{2,\bar{b}/h}(x_2, \mu_F^2)
\end{aligned} \tag{3.87}
$$

where $\sigma_0(\tau_h, Q^2) = \dfrac{4\pi\alpha^2}{3N_C s}$ is the Born cross section and

$$
\tau_h = \frac{Q^2}{s}, \quad z = \frac{\tau_h}{x_1 x_2} \tag{3.88}
$$

the kinematical variables that we frequently will use. The perturbative expansion of the hard coefficient is

$$
\omega_{ab} = \sum_n \left(\frac{\alpha_s}{\pi}\right)^n \omega_{ab}^{(n)} \tag{3.89}
$$

where the normalization of the cross section is chosen in such a way that $\omega_{ab}^{(0)} = \delta_{ab}\delta(1-z)$. Similar to DIS, the NLO hard function can be determined by first exploiting the factorization of the amplitude into a leptonic and partonic part. The latter requires the computation of virtual contributions to the initial $q\bar{q}$ channel due

to self-energy and vertex corrections. After performing the two-dimensional phase space integration the virtual ϵ-dependent piece of the hard coefficient is

$$h_{q\bar{q}}^{(1),v}(z,\alpha_s(\mu_R^2),\frac{Q^2}{\mu_R^2},\frac{Q^2}{\mu_F^2}) = C_F\left(\frac{4\pi\mu^2}{Q^2}\right)^\epsilon \frac{\Gamma(1-\epsilon)}{\Gamma(1-2\epsilon)}\left(-\frac{1}{\epsilon^2}-\frac{3}{2\epsilon}+\frac{\pi^2}{3}-4\right) \quad (3.90)$$

Real contributions both in the quark anti-quark channel due to the emission of a real gluon

$$h_{q\bar{q}}^{(1),r}(z,\alpha_s(\mu_R^2),\frac{Q^2}{\mu_R^2},\frac{Q^2}{\mu_F^2}) = C_F\left(\frac{4\pi\mu^2}{Q^2}\right)^\epsilon \left\{\frac{1}{\epsilon^2}\delta(1-z)-\frac{1}{\epsilon}(z^2+1)\left[\frac{1}{1-z}\right]_+ \right. \quad (3.91)$$

$$\left. -(z^2+1)\ln z\left[\frac{1}{1-z}\right]_+ + 2(z^2+1)\left[\frac{\ln(1-z)}{1-z}\right]_+\right\} \quad (3.92)$$

and the indistinguishable gluon-quark channel completes the NLO calculation. Still the final partonic result

$$h_{q\bar{q}}^{(1)}(z,\alpha_s(\mu_R^2),\frac{Q^2}{\mu_R^2},\frac{Q^2}{\mu_F^2}) = \left(\frac{4\pi\mu^2}{q^2}\right)^\epsilon\left(R_{q\bar{q}}(z)-\frac{1}{\epsilon}P_{qq}^{(0)}(z)\right) \quad (3.93)$$

$$h_{qg}^{(1)}(z,\alpha_s(\mu_R^2),\frac{Q^2}{\mu_R^2},\frac{Q^2}{\mu_F^2}) = C_F\left(\frac{2N_C}{N_C^2-1}\right)\left(\frac{4\pi\mu^2}{Q^2}\right)^\epsilon\left(R_{qg}(z)-\frac{1}{2\epsilon}P_{qg}^{(0)}(z)\right) \quad (3.94)$$

with

$$R_{q\bar{q}}(z) = CF\left\{\left(-4+\frac{\pi^2}{3}\right)\delta(1-z)+2(1+z^2)\left[\frac{\ln(1-z)}{1-z}\right]_+ - \left(\frac{1+z^2}{1-z}\right)\ln z\right\} \quad (3.95)$$

$$R_{qg}(z) = -\frac{1}{2}P_{qg}^{(0)}(z)\ln\frac{z}{(1-z)^2}-\frac{T_R}{4}(7z^2-6z-1) \quad (3.96)$$

suffers from collinear singularities in the splitting $q\to qg$ and in the splitting $g\to q\bar{q}$ of the initial state. These can be rendered finite in a similar fashion as in DIS. The partonic equivalent to the factorization formula Eq. (3.87)

$$h_{ab}(x_1,x_2,\alpha_s(\mu_R^2),\frac{Q^2}{\mu_R^2},\frac{Q^2}{\mu_F^2},\epsilon) = \sum_{c,d}\int_{x_1}^1\frac{\mathrm{d}\xi_1}{\xi_1}\int_{x_2}^1\frac{\mathrm{d}\xi_2}{\xi_2}$$

$$\times f_{1,c/a}(\xi_1,\mu_F^2,\epsilon)\omega_{ab}(\frac{x_1}{\xi_1},\frac{x_2}{\xi_2},\alpha_s(\mu_R^2),\frac{Q^2}{\mu_R^2},\frac{Q^2}{\mu_F^2})f_{2,d/b}(\xi_2,\mu_F^2,\epsilon) \quad (3.97)$$

enables us by using the parton-in-parton densities Eqs. (3.71) to determine the finite partonic hard scattering cross section. Expanding Eq. (3.97) in terms of the strong coupling on both sides gives the relation

$$\omega_{ab}^{(0)}(x_1,x_2,\alpha_s(\mu_R^2),\frac{Q^2}{\mu_R^2},\frac{Q^2}{\mu_F^2}) = h_{ab}^{(0)}(x_1,x_2,\alpha_s(\mu_R^2),\frac{Q^2}{\mu_R^2},\frac{Q^2}{\mu_F^2},\epsilon) \tag{3.98}$$

$$\tag{3.99}$$

and at one loop

$$\omega_{ab}^{(1)}(x_1,x_2,\alpha_s(\mu_R^2),\frac{Q^2}{\mu_R^2},\frac{Q^2}{\mu_F^2}) = h_{ab}^{(1)}(x_1,x_2,\alpha_s(\mu_R^2),\frac{Q^2}{\mu_R^2},\frac{Q^2}{\mu_F^2},\epsilon) \tag{3.100}$$

$$+\frac{1}{\epsilon}\left(\frac{4\pi\mu^2}{Q^2}\right)^{\epsilon}\sum_c\int_{x_1}^1\frac{\mathrm{d}\xi_1}{\xi_1}P_{c/a}^{(0)}(\xi_1)h_{cb}^{(0)}(\frac{x_1}{\xi_1},x_2,\alpha_s(\mu_R^2),\frac{Q^2}{\mu_R^2},\frac{Q^2}{\mu_F^2},\epsilon) \tag{3.101}$$

$$+\frac{1}{\epsilon}\left(\frac{4\pi\mu^2}{Q^2}\right)^{\epsilon}\sum_d\int_{x_2}^1\frac{\mathrm{d}\xi_2}{\xi_2}P_{d/b}^{(0)}(\xi_2)h_{ad}^{(0)}(x_1,\frac{x_2}{\xi_2},\alpha_s(\mu_R^2),\frac{Q^2}{\mu_R^2},\frac{Q^2}{\mu_F^2},\epsilon). \tag{3.102}$$

For completeness we list the final result at one loop order in Drell–Yan [56]

$$W(\tau_h,\alpha_s(\mu_R^2),\frac{Q^2}{\mu_R^2},\frac{Q^2}{\mu_F^2}) = \int_{\tau_h}^1\frac{\mathrm{d}\tau}{\tau}\left\{\sum_q Q_q^2\frac{\mathrm{d}\mathcal{L}^{q\bar{q}}}{\mathrm{d}\tau}\left[\delta(1-z)+\frac{\alpha_s(\mu_R^2)}{\pi}\omega_{q\bar{q}}^{(1)}(z,\alpha_s(\mu_R^2),\frac{Q^2}{\mu_R^2},\frac{Q^2}{\mu_F^2})\right]\right. \tag{3.103}$$

$$\left.+\sum_{q\bar{q}}Q_q^2\frac{\mathcal{L}^{gq}}{\mathrm{d}\tau}\frac{\alpha_s(\mu_R^2)}{\pi}\omega_{gq}^{(1)}(x_1,x_2,\alpha_s(\mu_R^2),\frac{Q^2}{\mu_R^2},\frac{Q^2}{\mu_F^2})\right\} \tag{3.104}$$

with

$$\omega_{q\bar{q}}^{(1)}(z,\alpha_s(\mu_R^2),\frac{Q^2}{\mu_R^2},\frac{Q^2}{\mu_F^2}) = -P_{qq}^{(0)}(z)\ln\frac{\mu_F^2 z}{Q^2} + C_F\left\{2\left[\frac{\pi^2}{6}-2\right]\delta(1-z)+2(1+z^2)\left[\frac{\ln(1-z)}{1-z}\right]_+\right\} \tag{3.105}$$

$$\omega_{qg}^{(1)}(z,\alpha_s(\mu_R^2),\frac{Q^2}{\mu_R^2},\frac{Q^2}{\mu_F^2}) = -\frac{1}{2}P_{qg}^{(0)}(z)\ln\frac{\mu_F^2 z}{Q^2(1-z)^2}+\frac{T_R}{4}(1+6z-7z^2) \tag{3.106}$$

Here we defined the parton luminosities as

$$\frac{\mathrm{d}\mathcal{L}^{a\bar{b}}}{\mathrm{d}\tau} = \int_\tau^1\frac{\mathrm{d}x}{x}\left[f_{a/h1}(x,\mu_F^2)f_{\bar{b}/h2}(\frac{\tau}{x},\mu_F^2)+f_{\bar{b}/h1}(x,\mu_F^2)f_{a/h2}(\frac{\tau}{x},\mu_F^2)\right] \tag{3.107}$$

Although the hard scattering coefficients are free of divergences due to the infrared safety and the renormalization of the bare PDF's we notice the appearance of plus distributions both in DIS and in DY.This is a common property of higher order perturbation theory. These distributions show a singluar behavior for $z \to 1$ and spoil the convergence of the perturbative expansion in this region. Near the partonic threshold the initial state has just enough energy to produce the final state without any further gluon emission forcing the gluons to be soft. At first sight this may cause severe problems to the asymptotic convergence of the perturbative expansion. Thus, the knowledge of higher order corrections especially in the soft gluon region is highly desired. Fixed order calculations up to now only allow the determination of the hard coefficients of the respective process up to a limited order. However, it was found [71] that the coefficients of the leading plus distributions show a recurrent behavior which lead to the basis for resumming the enhanced terms up to all orders. The construction of factorization theorems in this kinematical region as well as exploiting the independence of the cross section of the unphysical scale μ is called threshold resummation or soft gluon resummation. The upcoming sections are devoted to illuminate the technical aspect of resummation near the partonic threshold.

2 Threshold Resummation in QCD

In the previous subsection we identified the sources of large logarithmical contributions in DIS and DY, namely the plus distributions. In this section we describe two methods which consistently resum soft gluon effects. While the first work presented in Ref. [72] assumes a factorization of the different sources of the enhanced contributions, the second [73] moreover presumes a kinematical and dynamical factorization that eventually leads to the same results. The resummation is carried out in Mellin space where the partonic cross section factorizes multiplicatively instead of having an integral convolution form as it can be inferred from the DY cross section

$$\begin{aligned} h_{ab}(N, \alpha_s(\mu_R^2), \frac{Q^2}{\mu_R^2}, \frac{Q^2}{\mu_F^2}, \epsilon) &= \int_0^1 \mathrm{d}z z^{N-1} h_{ab}(z, \alpha_s(\mu_R^2), \frac{Q^2}{\mu_R^2}, \frac{Q^2}{\mu_F^2}, \epsilon) \\ &= \sum_{c,d} f_{1,c/a}(N, \mu^2, \epsilon) \omega_{ab}(N, \alpha_s(\mu_R^2), \frac{Q^2}{\mu_R^2}, \frac{Q^2}{\mu_F^2}) f_{2,d/b}(N, \mu, \epsilon). \end{aligned} \tag{3.108}$$

In the following subsections we try to give an although technical introduction to the resummation in the Drell–Yan process.

2.1 Exponentiation of leading large logarithms

The foundation to both resummation techniques was laid due to the observation that one is able to resum the leading logarithmical contributions up to all orders [71]. In addition, factorization theorems enables one to systematically isolate the different sources of these large logarithms. In particular, the resummation of the latter can be performed by exploiting the renormalization group independence of the all-order resummation formula. In the following subsection we review the factorization and resummation based on the method described in Ref. [72]

2.1.1 Factorization near the partonic threshold in DY

As we have seen in previous sections factorization theorems play an essential role in separating long distance from short distance effects, e.g. in DIS and DY. The factorization formula in case of DY, Eq. (3.87) is valid for any kind of kinematical region. However, as explained above, the basis of resummation is to first find and isolate the source of the logarithmically enhanced terms. Without any proof we will heuristically explain the main assumptions which lead to the factorization formula

for $z \to 1$. Similar to Eq. (3.97) light-cone parton-in-parton densities are used not only to separate the universal collinear divergences from the hard scattering cross section but also to isolate the soft-collinear sources of large logarithms. In the region $z \to 1$ the quark-in-quark parton density defined in the center of mass frame at fixed energy reads [74]

$$\psi_{q/q}(x, 2p_0/\mu, \epsilon) = \frac{1}{2\pi 2^{3/2}} \int_{-\infty}^{\infty} \mathrm{d}y_0 \mathrm{e}^{-ixp_0y_0} \langle q(p)|\bar{q}(y_0, \mathbf{0}) \frac{1}{2} v \cdot \gamma q(0)|q(p)\rangle \tag{3.109}$$

where q denotes the quark field and p its momentum. The matrix element is evaluated in Coulomb gauge, $G_0 = 0$, with ζ being a gauge fixing vector, thus Eq. (3.109) depends on the gauge fixing. The vector v^μ is light-like and oriented in the opposite direction to p^μ. At LO $\psi_{q/q}$ is normalized to $\delta(1-x)$. Likewise the anti-quark-in-anti-quark-density can be derived [74]

$$\psi_{\bar{q}/\bar{q}}(x, 2p_0/\mu, \epsilon) = \frac{1}{2\pi 2^{3/2}} \int_{-\infty}^{\infty} \mathrm{d}y_0 \mathrm{e}^{-ixp_0y_0} \langle \bar{q}(p)|\mathrm{Tr}\left[\frac{1}{2} v \cdot \gamma q(y_0, \mathbf{0}) \bar{q}(0)\right]|\bar{q}(p)\rangle \tag{3.110}$$

which fulfills $\psi_{q/q} = \psi_{\bar{q}/\bar{q}}$ as a consequence of charge conjugation conservation. We note that only flavor diagonal parton-in-parton densities are considered since off-diagonal parton functions show no singular behavior as $z \to 1$. Furthermore, the remaining piece of the scattering coefficient can further be decomposed into a part that includes the wide-angle soft gluon radiation as well as into a part H that is not singular for $z \to 1$. Near the partonic threshold the general factorization form is [72]

$$\begin{aligned} h_{q\bar{q}}(\omega, \alpha_s(\mu_R^2), \frac{Q^2}{\mu_R^2}, \frac{Q^2}{\mu_F^2}, \epsilon) = H\left(\frac{p_1}{\mu}, \frac{p_2}{\mu}, \zeta_1, \zeta_2\right) \int \frac{\mathrm{d}w}{w} \frac{\mathrm{d}w_1}{w_1} \frac{\mathrm{d}w_2}{w_2} \\ \times \psi_{q/q}\left(\frac{p_1 \cdot \zeta_1}{\mu}, w_1 \frac{Q}{\mu}\right) \psi_{\bar{q}/\bar{q}}\left(\frac{p_2 \cdot \zeta_2}{\mu}, w_2 \frac{Q}{\mu}\right) \\ \times U_{q\bar{q}}\left(w_2 \frac{Q}{\mu}, v_1, v_2, \zeta_1\zeta_2\right) \delta(w - w_1 - w_2 - w_s). \end{aligned} \tag{3.111}$$

The δ-function contained in (3.111) fixes the $n+2$ dimensional phase space of the final state by the invariant mass of the lepton pair and the emission of n radiated gluons in the initial state as

$$\delta\left[Q^2 - \left(p_1 + p_2 - \sum_i^n k_i\right)^2\right] = \frac{1}{s}\delta\left(-(1-z)x_1x_2 + 2\frac{\sum_i^n k_i^0}{s^{1/2}} + \mathcal{O}\left([1-z]^2\right)\right)$$

$$= \frac{1}{s}\delta\left(w - w_1 - w_2 - w_s + \mathcal{O}(w^2)\right) \tag{3.112}$$

where the weights are denoted as $w = 1-z$, $w_1 = 1-x_1$, $w_2 = 1-x_2$ and $w_s = 2\frac{\sum_i^n k_i^0}{s^{1/2}}$ with $\sum_i^n k_1^0$ the energy of the emitted gluons. Transforming Eq. (3.111) into Mellin space gives the multiplicative formula

$$\begin{aligned}\tilde{h}_{ab}(N, \alpha_s(\mu_R^2), \frac{Q^2}{\mu_R^2}, \frac{Q^2}{\mu_F^2}, \epsilon) &= \int_0^1 \mathrm{d}z z^{N-1} h_{ab}(z, \alpha_s(\mu_R^2), \frac{Q^2}{\mu_R^2}, \frac{Q^2}{\mu_F^2}, \epsilon) \\ &= \tilde{H}\left(\frac{p_1}{\mu}, \frac{p_2}{\mu}, \frac{Q}{\mu}, \alpha_s(\mu^2)\right) \tilde{U}\left(\frac{Q}{N\mu}, \alpha_s(\mu^2), v_1, v_2, \zeta_1, \zeta_2\right) \\ &\times \tilde{\psi}_{q/q}\left(\frac{p_1\cdot\zeta_1}{\mu}, \frac{Q}{\mu N}\right) \tilde{\psi}_{\bar{q}/\bar{q}}\left(\frac{p_2\cdot\zeta_2}{\mu}, \frac{Q}{\mu N}\right)\end{aligned} \tag{3.113}$$

The comparison of Eq. (3.108) and Eq. (3.113) helps us to extract the infrared safe hard scattering coefficient in Mellin space

$$\tilde{\omega}_{qq}(N, \alpha_s(\mu_R^2), \frac{Q^2}{\mu_R^2}, \frac{Q^2}{\mu_F^2}) = \left[\frac{\tilde{\psi}_{q/q}(N, \mu^2, \epsilon)}{\tilde{f}_{q/q}(N, \mu^2, \epsilon)}\right]^2 \tilde{H}\left(\frac{Q}{\mu}, \alpha_s(\mu^2)\right) \tilde{U}\left(\frac{Q}{N\mu}, \alpha_s(\mu^2)\right) \tag{3.114}$$

The ratio of the modified ψ and the general f parton distribution serves to render this quantity finite. Since these distributions can be determined within perturbation theory, as we have seen in DIS, the Sudakov resummation is subject to the next section.

2.1.2 From RG-invariance to Sudakov resummation

With the disentangled form in Eq. (3.114) we are now ready to exploit the independence of the all-order cross section both of the scale μ and of the gauge vectors ζ_i

$$\frac{\mathrm{d}}{\mathrm{d}\ln\mu}\tilde{h}_{q\bar{q}}(N) = 0 \tag{3.115}$$

$$\frac{\mathrm{d}}{\mathrm{d}(p_i\cdot\zeta_i)}\tilde{h}_{q\bar{q}}(N) = 0 \tag{3.116}$$

The solution to both equations leads to the Sudakov-exponentiation. One important assumption is that of the multiplicative renormalizability of the hard H, soft U and

soft-collinear ψ functions. Hence, the scale dependence is determined by a set of anomalous dimensions

$$\mu\frac{\mathrm{d}}{\mathrm{d}\mu}\ln\tilde{H}\left(\frac{p_1}{\mu},\frac{p_2}{\mu},\frac{Q}{\mu},\alpha_s(\mu^2)\right)=-\gamma_H(\alpha_s(\mu)) \tag{3.117}$$

$$\mu\frac{\mathrm{d}}{\mathrm{d}\mu}\ln\tilde{U}\left(\frac{Q}{N\mu},v_1,v_2,\zeta_1,\zeta_2,\alpha_s(\mu^2)\right)=-\gamma_U(\alpha_s(\mu)) \tag{3.118}$$

$$\mu\frac{\mathrm{d}}{\mathrm{d}\mu}\ln\tilde{\psi}_i\left(\frac{p_i\cdot\zeta_i}{\mu},\frac{Q}{\mu N},\alpha_s(\mu^2)\right)=-\gamma_{\psi_i}(\alpha_s(\mu)) \tag{3.119}$$

where we used the notation $\psi_1=\psi_{q/q}$ and $\psi_2=\psi_{\bar{q}/\bar{q}}$. We further assume that the anomalous dimensions are independent of the Mellin momentum N and of the gauge vector ζ but dependent on the strong coupling at the scale μ. Henceforth, Eqs. (3.117), (3.118), (3.119) require that the sum of the anomalous dimensions is zero

$$\gamma_H+\sum_i\gamma_{\psi_i}+\gamma_U=0 \tag{3.120}$$

The solution of the soft function is

$$U\left(\frac{Q}{N\mu},v_1,v_2,\zeta_1,\zeta_2,\alpha_s(\mu^2)\right)=U\left(1,v_1,v_2,\zeta_1,\zeta_2,\alpha_s(\mu^2)\right)\exp\left[\int_\mu^{Q/N}\frac{\mathrm{d}\lambda}{\lambda}\gamma_U(\alpha_s(\lambda^2))\right] \tag{3.121}$$

where the initial soft scale $\frac{Q}{N}$ is chosen in a natural way such that $U\left(1,v_1,v_2,\zeta_1,\zeta_2,\alpha_s(\mu^2)\right)$ contains no large logarithmic contributions. Eq. (3.121) correctly resums the single logarithmic terms in the soft function U. The jet function contains double logarithms. Solving Eq. (3.119)

$$\psi_i\left(\frac{p_i\cdot\zeta_i}{\mu},\frac{Q}{\mu N},\alpha_s(\mu^2)\right)=\psi_i\left(\frac{p_i\cdot\zeta_i}{\mu},1,\alpha_s(\mu^2)\right)\exp\left[\int_\mu^{Q/N}\frac{\mathrm{d}\lambda}{\lambda}\gamma_{\psi_i}(\alpha_s(\lambda^2))\right] \tag{3.122}$$

only resums the single logarithmic contributions. The entire N-dependence of ψ can be covered by exploiting the invariance of equation (3.119) under variation of the combination $p_i\cdot\zeta_i$

$$\frac{\mathrm{d}}{\mathrm{d}\ln\mu}\frac{\mathrm{d}}{\mathrm{d}\ln(p_i\cdot\zeta_i)}\ln\psi_i=0 \tag{3.123}$$

as well as using Eq. (3.116) leading to a set of Sudakov anomalous dimensions

$$\frac{\mathrm{d}}{\mathrm{d}\ln\mu}G\left(\frac{p_i\cdot\zeta_i}{\mu},\alpha_s(\mu^2)\right)=\gamma_K\left(\alpha_s(\mu^2)\right) \tag{3.124}$$

$$\frac{\mathrm{d}}{\mathrm{d}\ln\mu}\tilde{K}\left(\frac{Q}{N\mu},\alpha_s(\mu^2)\right)=-\gamma_K\left(\alpha_s(\mu^2)\right) \tag{3.125}$$

with

$$G=-\frac{\partial}{\partial(p_i\cdot\zeta_i)}\ln H \tag{3.126}$$

$$\tilde{K}=-\frac{\partial}{\partial(p_i\cdot\zeta_i)}\ln U. \tag{3.127}$$

Due to gauge changes the jet functions exchange contributions with the soft part via $\tilde{K}$ and with the hard part via H. Solving Eqs. (3.126) and (3.127) gives

$$G\left(\frac{p_i\cdot\zeta_i}{\mu},\alpha_s(\mu^2)\right)+\tilde{K}\left(\frac{Q}{N\mu},\alpha_s(\mu^2)\right)=G\left(1,\alpha_s(Q^2/N^2)\right)+\tilde{K}\left(1,\alpha_s((p_i\cdot\zeta_1)^2)\right)$$
$$-\int_{Q/N}^{p_i\cdot\zeta_i}\frac{\mathrm{d}\xi}{\xi}\gamma_K\left(\alpha_s(\xi)\right) \tag{3.128}$$

The scales of the first two terms ins Eq. (3.128) are still unrelated. By using the RGE equation (3.19) on $\tilde{K}$ Eq. (3.128) reads

$$G\left(\frac{p_i\cdot\zeta_i}{\mu},\alpha_s(\mu^2)\right)+\tilde{K}\left(\frac{Q}{N\mu},\alpha_s(\mu^2)\right)=A'\left(\alpha_s\left((p_i\cdot\zeta_i)^2\right)\right)-\int_{Q/N}^{p_i\cdot\zeta_i}\frac{\mathrm{d}\xi}{\xi}A\left(\alpha_s(\xi)\right) \tag{3.129}$$

where we denoted the functions A and A' by

$$A\left(\alpha_s(\mu^2)\right)=\gamma_K\left(\alpha_s(\mu^2)\right)+\beta(g)\frac{\partial}{\partial g}\tilde{K}\left(1,\alpha_s(\mu^2)\right), \tag{3.130}$$

and

$$A'\left(\alpha_s(\mu^2)\right)=\tilde{K}\left(1,\alpha_s(\mu^2)\right)+G\left(1,\alpha_s(\mu^2)\right) \tag{3.131}$$

Together with Eq. (3.122) the entire solution of the jet functions can be derived as

$$\psi_i\left(\frac{p_i\cdot\zeta_i}{\mu},\frac{Q}{\mu N},\alpha_s(\mu^2)\right)=\psi_i\left(1,1,\alpha_s(\mu^2)\right)\exp\left[-\int_{Q/N}^{\mu}\frac{\mathrm{d}\lambda}{\lambda}\gamma_{\psi_i}(\alpha_s(\lambda^2))\right]$$
$$\times\exp\left[-\int_{Q/N}^{p_i\cdot\zeta_i}\frac{\mathrm{d}\xi}{\xi}\left\{\int_{Q/N}^{\lambda}A\left(\alpha_s(\xi^2)\right)-A'\left(\alpha_s(\lambda^2)\right)\right\}\right] \tag{3.132}$$

Finally, the solutions of the hard, soft and soft-collinear functions in Eqs. (3.121) and (3.132) give the Sudakov resummation formulas

$$\begin{aligned} h_{ab}(N,\alpha_s(\mu_R^2),\frac{Q^2}{\mu_R^2},\frac{Q^2}{\mu_F^2},\epsilon) = & H\left(1,\alpha_s(Q^2)\right) \\ & \times \psi_{qq}\left(1,1,\alpha_s\left(\frac{Q^2}{N^2}\right)\right)\psi_{\bar{q}\bar{q}}\left(1,1,\alpha_s\left(\frac{Q^2}{N^2}\right)\right) \\ & \times U\left(1,\alpha_s\left(\frac{Q^2}{N^2}\right)\right) \\ & \times \exp\left[-\int_{Q/N}^{Q}\frac{\mathrm{d}\xi}{\xi}\left\{\int_{Q/N}^{\lambda} A\left(\alpha_s(\xi^2)\right) - B\left(\alpha_s(\lambda^2)\right)\right\}\right] \end{aligned} \tag{3.133}$$

where we have set $p_i \cdot \zeta_i$ and μ equal to Q. Eq. (3.133) provides an all-order resummation formula for the DY cross section and attributes double logarithmic contributions to the function A and single logarithmic contributions in

$$B\left(\alpha_s(\mu^2)\right) = -\frac{1}{2}\gamma_U\left(\alpha_s(\mu^2)\right) - \sum_{i=1,2}\frac{1}{2}\gamma_{\psi_i}\left(\alpha_s(\mu^2)\right) + A'\left(\alpha_s(\mu^2)\right) \tag{3.134}$$

Both functions can be determined by matching formula (3.133) with fixed-order results. For practical reasons an alternative Sudakov exponentiation turns out to be more efficient which we will describe in the next subsection.

2.1.3 Explicit calculation in DY and general organization of large logarithms

Referring to [75] the general form of Eq. (3.133) obeys the Sudakov evolution equation in Mellin space

$$\frac{\mathrm{d}}{\mathrm{d}\ln Q^2}\tilde{h}_{qq}(N,\alpha_s(\mu),\frac{Q^2}{\mu},\epsilon) = W_{qq}(N,\alpha_s(\mu),\frac{Q^2}{\mu},\epsilon)\tilde{h}_{qq}(N,\alpha_s(\mu),\frac{Q^2}{\mu},\epsilon) \tag{3.135}$$

The solution of Eq. (3.135) is

$$h_{qq}(N,\alpha_s(\mu),\frac{Q^2}{\mu},\epsilon) = \exp\left[\int_0^1 \mathrm{d}z z^{N-1}\int_0^{Q^2/\mu^2}\frac{\mathrm{d}\lambda}{\lambda}W_i(z,\lambda,\alpha_s(\mu^2),\epsilon)\right] \tag{3.136}$$

where we used the boundary condition $\tilde{h}_{qq}(N, \alpha_s(\mu), \frac{Q^2}{\mu} = 0, \epsilon) = 1$. Furthermore, we use the RG invariance of W_{qq} under a rescaling of the parameter λ and expand in a power series in α_s leading to

$$\tilde{h}_{qq}(N, \alpha_s(\mu), \frac{Q^2}{\mu}, \epsilon) = \exp\left[\int_0^1 \mathrm{d}z z^{N-1} \int_0^{Q^2/\mu^2} \frac{\mathrm{d}\lambda}{\lambda} \left\{ \frac{\alpha_s(\lambda, \mu^2, \epsilon)}{\pi} W_{qq}^{(1)}(z, 1, \epsilon) \right.\right.$$
$$\left.\left. + \frac{\alpha_s^2(\lambda, \mu^2, \epsilon)}{\pi^2} W_{qq}^{(2)}(z, 1, \epsilon) \right\}\right] \tag{3.137}$$

This equation requires the solution of the d-dimensional RGE of the strong coupling

$$\lambda^\epsilon \alpha_s(\lambda, \alpha_s(\mu^2), \epsilon) = \alpha_s(\mu^2) + \gamma(\lambda^\epsilon, \epsilon)\alpha_s^2(\mu^2) + \mathcal{O}(\alpha_s^3) \tag{3.138}$$

where we denote $\gamma(\lambda^\epsilon, \epsilon) = \frac{\beta_0}{4\pi\epsilon}(\lambda^{-\epsilon} - 1)$. Expanding (3.137) on left hand side in a power series of α_s the coefficients W_{qq} can now be matched to the fixed oder coefficients at one and two loops via

$$W_{qq}^{(1)}(N, 1, \epsilon) = \left(\frac{Q^2}{\mu^2}\right)^\epsilon Q^2 \frac{\partial}{\partial Q^2} \tilde{h}_{qq}^{(1)}(N, \frac{Q^2}{\mu^2}, \epsilon), \tag{3.139}$$

and

$$W_{qq}^{(2)}(N, 1, \epsilon) = \left(\frac{Q^2}{\mu^2}\right)^{2\epsilon} \left\{ Q^2 \frac{\partial}{\partial Q^2} \left(\tilde{h}_{qq}^{(2)}(N, \frac{Q^2}{\mu^2}, \epsilon) - \frac{1}{2}\left[\tilde{h}_{qq}^{(1)}(N, \frac{Q^2}{\mu^2}, \epsilon)\right]^2 \right) \right. \tag{3.140}$$
$$\left. - \gamma\left(\left(Q^2/\mu^2\right)^\epsilon, \epsilon\right) Q^2 \frac{\partial}{\partial Q^2} \tilde{h}_{qq}^{(1)}(N, \frac{Q^2}{\mu^2}, \epsilon) \right\} \tag{3.141}$$

The general form at one loop in DY can be summarized as

$$W_{qq}^{(1)}(z, 1, \epsilon) = \delta(1-z) f_{qq}^{(1)}(\epsilon) + z^\epsilon \left(\frac{g_{qq}^{(1)}(z, \epsilon)}{(1-z)^{1+2\epsilon}} \right)_+ + r^{(1)}(z, \epsilon) \tag{3.142}$$

where inferring from Eqs. (3.90) and (3.92) the regular functions at $z = 1$ read

$$f_{qq}^{(1)}(\epsilon) = C_F \left(\frac{1}{2} - \frac{\pi^2}{3}\right)\epsilon \tag{3.143}$$
$$g_{qq}^{(1)}(z, \epsilon) = C_F \left(1 + z^2\right) \tag{3.144}$$
$$r^{(1)}(z, \epsilon) = 0 \tag{3.145}$$

The term $\delta(1-z) f_{qq}^{(1)}(\epsilon)$ generates those coefficients which are constant for large N when we perform an explicit integration over λ. On the other side the integration

of the plus distribution causes double and single logarithmically enhanced terms. Treating the plus distributions as in Eq. (3.62) and rescaling the lambda integration in order to absorb the factor $(1-z)^{-2\epsilon}$ into the integration measure we obtain

$$\begin{aligned} h_{qq} &= h_{qq}(N, \alpha_s(\mu), \frac{Q^2}{\mu}, \epsilon) \\ &\times \exp\left[C_F \int_0^1 \mathrm{d}z \left(\frac{z^{N-1+\epsilon}-1}{1-z}\right)(1+z^2) \int_0^{Q^2(1-z)^2/\mu^2} \frac{\mathrm{d}\lambda}{\lambda} \frac{\alpha_s(\lambda, \alpha_s(\mu^2), \epsilon)}{\pi}\right] \\ &\times \exp\left[-\frac{\alpha_s(\mu^2)}{\pi} C_F (\frac{1}{2} - \frac{\pi^2}{3})\right] \end{aligned} \tag{3.146}$$

Although the r term is zero in Drell–Yan, we can safely neglect contributions of this functions since they are of order $\mathcal{O}(1/N^4)$. Finally the universal ϵ collinear singularity can be cancelled by the mass factorization formula (3.114) with [75]

$$f_{qq}(N, Q^2, \epsilon) = \exp\left[\frac{C_F}{2} \int_0^1 \left(\frac{z^{N-1}-1}{1-z}\right)(1+z^2) \int_0^{Q^2/\mu^2} \frac{\mathrm{d}\lambda}{\lambda} \frac{\alpha_s(\lambda, \alpha_S(\mu^2), \epsilon)}{\pi} + \cdots\right] \tag{3.147}$$

The result in DY can be written in a generalized form

$$\omega_{qq}(N, \alpha_s(Q^2)) = A_{qq}(\alpha_s(Q^2)) I_{qq}(N, \alpha_s(Q^2)) \tag{3.148}$$

where the N-independent terms are contained in A and the Sudakov exponential is

$$I_{qq}(N, \alpha_s(Q^2)) = \exp\left[-\int_0^1 \mathrm{d}z \frac{z^{N-1}-1}{1-z} \left\{\int_{(1-z)^2}^{(1-z)} \frac{\mathrm{d}\lambda}{\lambda} g_1[(\alpha_s(\lambda Q^2)] + g_2[\alpha_s(Q^2)]\right\}\right]. \tag{3.149}$$

The functions g have the expansion

$$g_1[\alpha] = \sum_{n=1}^{\infty} \left(\frac{\alpha_s}{\pi}\right)^n g_1^{(n)}, \quad g_2[\alpha_s] = \sum_{n=1}^{\infty} \left(\frac{\alpha_s}{\pi}\right)^n g_2^{(n)} \tag{3.150}$$

where the finite coefficients in the $\overline{\text{MS}}$-scheme are [76]

$$g_1^{(1)} = 2C_F, \quad g_2^{(1)} = 0 \tag{3.151}$$

$$g_1^{(2)} = C_A C_F \left(\frac{67}{18} - \zeta_2\right) + N_f C_F \left(-\frac{5}{9}\right) \tag{3.152}$$

$$g_2^{(2)} = C_A C_F \left(\frac{101}{27} - \frac{11}{3}\zeta_2 - \frac{7}{2}\zeta_3 \right) + N_f C_F \left(-\frac{14}{27} + \frac{2}{3}\zeta_2 \right) \tag{3.153}$$

The coefficient $g_1^{(1)}$ can easily be read off from Eqs. (3.146) and (3.147). Expression Eq. (3.149) organizes all large logarithms in the perturbative series, e.g. an expansion in the strong coupling generates terms of the kind $(\alpha_s/\pi)^n(Q^2)\ln^m N$, $n = 0, \ldots, \infty$, $m \leq n+1$ in the exponent. Terms with $m = n+1$ are called leading logarithms (LL), terms with $m = n$ next-to-leading (NLL) and the ones with $m < n$ subdominant. In the convention of (3.149) the coefficient $g_1^{(1)}$ contributes to LL while $g_1^{(2)}$ and $g_2^{(1)}$ contribute to NLL.

2.2 Alternative method and extension to subleading logarithms

Similar to the method presented in [72] a factorization theorem underlies the resummation of large infrared singularities. The partonic cross section can be decomposed into a soft part W which is logarithmically enhanced due to the plus distributions and into a part which contains only hard virtual corrections due to the delta-distributions [73]. For further discussions we neglect the latter since we saw that the virtual contributions only lead to a constant behavior for large N. In the following we only concentrate on the flavor non-singlet part ($a = q$, $b = \bar{q}$) of W due to the flavor conservation of the soft gluons. At one-loop the radiative factor in the center of mass frame reads

$$\tilde{\omega}_{ab}\left(z, \alpha_s(\mu_R^2), \frac{Q^2}{\mu_R^2}, \frac{Q^2}{\mu_F^2}\right) = -\int \mathrm{d}w_{\mathrm{DY}}^{(1)}(q)\delta(1-z) + \int \mathrm{d}w_{DY}^{(1)}(q)\delta\left(1 - z - \frac{\omega}{E}\right) \tag{3.154}$$

where the momenta of the initial state partons are $p_1^0 = p_2^0 = E \sim \sqrt{Q^2}/2$. q represents the momentum of the radiated gluon while ω denotes its energy. The first term in Eq. (3.154) is the one-loop eikonal cross section for a virtual emission of a soft gluon, fixed by the soft gluon unitarity. The second term depicts the real radiation with the kinematical constraint of a single-emission phase space. The real gluon emission probability $\mathrm{d}w$ is defined as

$$\mathrm{d}w_{\mathrm{DY}}^{(1)}(q) = -\frac{\mathrm{d}^3 q}{4\pi\omega}|J_{\mathrm{DY}}(q)|^2. \tag{3.155}$$

where J_{DY} is the eikonal current. The square of the latter can be calculated as

$$J_{\mathrm{DY}}^{\mu}(q) = -C_F \frac{2p_1 \cdot p_2}{p_1 \cdot q p_2 \cdot q}. \tag{3.156}$$

Higher-order calculations are more involved since non-Abelian correlations are present. These correlations, however, cancel by gauge-invariance and the exponentiation of the leading logarithms in the leading IR-approximation takes place. Transformed into Mellin space the exponentiation of the single-gluon emission probability then can be derived as

$$\begin{aligned}\ln\tilde{\omega}_{q\bar{q}}^{\mathrm{s-c}} =& \ln\tilde{\omega}_{q\bar{q}}\left(z,\alpha_s(\mu_R^2),\frac{Q^2}{\mu_R^2},\frac{Q^2}{\mu_F^2}\right)\\ =&\int \mathrm{d}q_{\mathrm{DY}}^{(1)}(q)\frac{\alpha_s(q_T^2)}{\pi}\left[\left(1-\frac{\omega}{E}\right)^{N-1}\right]\theta(E-\omega)\\ =&2\frac{C_F}{\pi}\int_0^1\frac{z^{N-1}-1}{1-z}\int_{\mu_F^2}^{(1-z)^2Q^2}\frac{\mathrm{d}q_T^2}{q_T^2}\alpha_s(q_T^2)+\mathcal{O}\left((\alpha_s\ln N)\right).\end{aligned} \tag{3.157}$$

where we notice that the scale of the running coupling has been set to q_T^2 since this choice resums the leading IR-singularities. Exploiting the RGE the strong coupling can be expressed as

$$\alpha_s\left[(1-z)q^2\right]=\alpha_s(q^2)\left[1-\frac{\beta_0}{2\pi}\alpha_s(q^2)\ln(1-z)+\mathcal{O}(\alpha_s^2)\right]. \tag{3.158}$$

Subleading soft gluon radiation can be included into Eq. (3.157) due to the formal replacement

$$\frac{\alpha_s}{\pi}C_F\to A_{\mathrm{DY}}(\alpha_s) \tag{3.159}$$

where the function A_{DY} possesses the following perturbative expansion

$$A_{\mathrm{DY}}(\alpha_s)=\sum_{k=1}^{\infty}\left(\frac{\alpha_s}{\pi}\right)^k A_{\mathrm{DY}}^{(k)} \tag{3.160}$$

Thus the all-order resummation formula of the soft-collinear radiative factor can be written as

$$\begin{aligned}\ln\tilde{\omega}_{q\bar{q}}^{\mathrm{s-c}} =& \ln\tilde{\omega}_{q\bar{q}}\left(z,\alpha_s(\mu_R^2),\frac{Q^2}{\mu_R^2},\frac{Q^2}{\mu_F^2}\right)\\ =&\left\{\int_0^1\mathrm{d}z\frac{z^{N-1}-1}{1-z}\int_{\mu_F^2}^{(1-z)^2Q^2}\frac{\mathrm{d}q_T^2}{q_T^2}A_{\mathrm{DY}}\left(\alpha_s(q_T^2)\right)\right\}\end{aligned} \tag{3.161}$$

Large angle soft gluon radiation can be included by modifying Eq. (3.157) with the additional factor

$$\ln\tilde{\omega}_{q\bar{q}}^{\mathrm{int}} =\ln\tilde{\omega}_{q\bar{q}}\left(z,\alpha_s(\mu_R^2),\frac{Q^2}{\mu_R^2},\frac{Q^2}{\mu_F^2}\right)$$

$$= \left\{ \int_0^1 \mathrm{d}z \frac{z^{N-1}-1}{1-z} D_{\mathrm{DY}} \left(\alpha_s((1-z)^2 q_T^2) \right) \right\} \tag{3.162}$$

where the function D_{DY} obeys the perturbative expansion

$$D_{\mathrm{DY}}(\alpha_s) = \sum_{k=2}^{\infty} \left(\frac{\alpha_s}{\pi} \right)^k D_{\mathrm{DY}}^{(k)} \tag{3.163}$$

The combination of soft-collinear and wide-angle soft-gluon effects up to all orders can be cast into the following form

$$\tilde{\omega}_{q\bar{q}} = \exp \left\{ \int_0^1 \mathrm{d}z \frac{z^{N-1}-1}{1-z} \left[\int_{\mu_F^2}^{(1-z)^2 Q^2} \frac{\mathrm{d}q_T^2}{q_T^2} A_{\mathrm{DY}} \left(\alpha_s(q_T^2) \right) + D_{\mathrm{DY}} \left(\alpha_s((1-z)^2 q_T^2) \right) \right] \right\} \tag{3.164}$$

We notice that the radiative factor in Eq. (3.164) is consistent with the one in Eq. (3.149) as it has been demonstrated in Ref. [77]. In Chapter 5 we will utilize the formalism and method described in this subsection to apply the soft gluon resummation to the gluon fusion process.

Chapter 4

Gluon fusion for scalar and pseudoscalar Higgs

1 Fixed order QCD calculations

As mentioned briefly in section 1.3 the dominant production mechanism for a SM Higgs is the gluon fusion. Historically, all relevant production processes and decays for a scalar Higgs boson at hadron colliders were first calculated in Ref. [78]. The calculations did, however, not involve the loop induced gluonic Higgs couplings which was later pointed out in Ref. [79] in the context of Higgs decay into gluons. The authors of Ref. [80] then calculated the leading-order diagram and studied the numerical impact of the latter in hadron-hadron-collisions leading eventually to the key observation of the dominance over the entire mass range at the LHC. In this section we want to review the perturbative QCD corrections beyond leading order for a scalar as well as for a pseudoscalar Higgs boson. We also deal with effective Higgs theories which play an essential role in the determination of QCD corrections at NLO and beyond.

1.1 Leading-order cross section and notations

The leading-order diagrams of the partonic subprocess $gg \to h, A$ are depicted in Fig. 4.1. The Feynman rules can be inferred from Figs. 3.1, 2.1 and Eq. 2.49 in order to compute the process at LO. The partonic cross section then reads

$$\hat{\sigma}_{ab\Phi}(\hat{s}, M_\Phi^2) = \sigma_0^\Phi \Delta_{ab\Phi}(z) \tag{4.1}$$

where $\hat{\sigma}_{ab\Phi}$ is the partonic cross section for the process $ab \to \Phi + X$. The field Φ can either be H for a scalar Higgs or A for a pseudoscalar Higgs. The partonic labels a, b

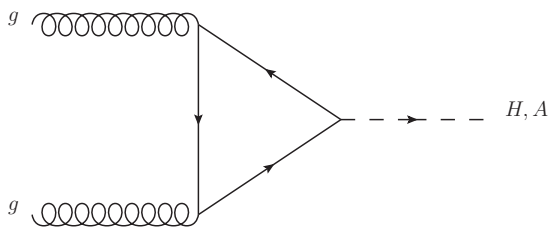

Figure 4.1: Leading order diagram for the process $gg \to H, A$

denote the partons in the initial state and X can be any numbers of parton in the final state. Throughout this section and for later issues we will use the convention where the DY variable z

$$z = \frac{\tau_\Phi}{x_1 x_2},\ \tau_\Phi = \frac{M_\Phi^2}{s} \tag{4.2}$$

is extracted from the partonic cross section, i.e.

$$\Delta_{ab\Phi}(z) = z\, G_{ab\Phi}(z) \tag{4.3}$$

The coefficient function $G_{ab\Phi}$ obeys an expansion in order α_s and is computable within perturbation theory

$$G_{ab}(z; \alpha_s(\mu_R^2), \frac{M_H^2}{\mu_F^2}; \frac{M_H^2}{\mu_F^2}) = \alpha_s^2(\mu_R^2) \sum_{n=0}^{+\infty} \left(\frac{\alpha_s(\mu_R^2)}{\pi}\right)^n\ G_{ab}^{(n)}(z; \frac{M_H^2}{\mu_F^2}; \frac{M_H^2}{\mu_F^2}) \tag{4.4}$$

The Born factor σ_0^Φ in both scalar and pseudoscalar cases is defined as

$$\sigma_0^\Phi = \frac{\sqrt{2} G_F}{256\pi} \left| \sum_{q=t,b,c} A_q^\Phi(\tau_q^\Phi) \right|^2, \quad \tau_q^\Phi = 4m_q^2/m_\Phi^2 \tag{4.5}$$

where $G_F = 1/(\sqrt{2}v^2)$. The mass dependence of the Born term on the heavy quarks is included in the scalar form factor

$$A_q^H(\tau_q^H) = g_q^H \tau_q^H [1 + (1 - \tau_q^H) f(\tau_q^H)], \tag{4.6}$$

respectively for a pseudoscalar Higgs

$$A_q^A(\tau_q^A) = g_q^A \tau_q^A f(\tau_q^A) \tag{4.7}$$

where the function $f(\tau)$ is

$$f(\tau) = \begin{cases} \arcsin^2 \frac{1}{\sqrt{\tau}}, & \tau \geq 1, \\ -\frac{1}{4} \left[\ln \frac{1+\sqrt{1-\tau}}{1-\sqrt{1-\tau}} - i\pi \right]^2, & \tau < 1 \end{cases} \tag{4.8}$$

At LO the normalization due to the Born term is chosen in such a way that the leading order coefficient $G_{ab}^{(0)}$ is determined as

$$G_{ab\Phi}^{(0)}(z) = \delta_{ag}\delta_{bg}\delta(1-z) \tag{4.9}$$

where the Kronecker-symbols δ_{ag} respectively δ_{bg} signals the presence of the gluon-gluon channel at the lowest order. In the next subsection we will proceed with the coefficient $G_{ab\Phi}^{(1)}$ where also additional gq and $q\bar{q}$ channels, open up that contribute to $\mathcal{O}(\alpha_s)$ corrections.

Φ		g_u^Φ	g_d^Φ
SM	H	1	1
MSSM	A	$1/\tan\beta$	$\tan\beta$

Table 1: Higgs couplings to SM fermions

1.2 Next-to-leading order calculations and effective theory

In decays $H \to \gamma\gamma$ it has been observed that with the knowledge of the UV-behavior of the theory one is able to determine the amplitude in the low energy region region, i.e. for energies much lower than the masses in the loop [78, 81] This leads to the conclusions that the heavy particles in the loop do not decouple from the theory but lead to an effective coupling instead. Similar to the Higgs decay into two photons the same analysis can be repeated for the $gg \to H$ coupling. Considering only the heavy top-quark in the triangle and assuming that the mass of the Higgs is much smaller than the heavy quark ($M_\Phi^2 \ll M_t^2$) the latter can be integrated out from the theory. The effective Lagrangian can then be obtained with different methods for a scalar Higgs and a pseudoscalar Higgs.

$$\mathcal{L}_{ggH}^{\text{eff}} = -\frac{1}{4v}C_1 H G^{a,\mu\nu}G_{a,\mu\nu} \quad \mathcal{L}_{ggA}^{\text{eff}} = -\frac{A}{v}\left(\tilde{C}_1 O_1 + \tilde{C}_2 O_2\right) \tag{4.10}$$

where

$$O_1 = -\frac{1}{8}\epsilon_{\mu\nu\lambda\sigma}G_a^{\mu\nu}G_a^{\lambda\sigma}, \quad O_2 = -\frac{1}{2}\partial^\mu \sum_{i=1}^{N_f}\bar{q}_i\gamma_\mu\gamma_5 q_i \tag{4.11}$$

The Standard Model Wilson coefficients C_1 was determined up to four loop level in α_s [82, 22, 23, 83, 84, 85, 86]. The result up to three loop level is

$$\begin{aligned} C_1(\mu^2) = &- \frac{\alpha_s(\mu^2)}{3\,\pi} \left\{ 1 + \left(\frac{\alpha_s(\mu^2)}{\pi}\right) \frac{11}{4} \right. \\ &+ \left(\frac{\alpha_s(\mu^2)}{\pi}\right)^2 \left[\frac{19}{16}\, L_t + \frac{2777}{288} + N_f \left(\frac{1}{3}\, L_t - \frac{67}{96} \right) \right] \\ &+ \left(\frac{\alpha_s(\mu^2)}{\pi}\right)^3 \left[\frac{897943}{9216}\, \zeta_3 + \frac{209}{64}\, L_t^2 + \frac{1733}{288}\, L_t - \frac{2892659}{41472} \right. \\ &+ N_F \left(-\frac{110779}{13824}\, \zeta_3 + \frac{23}{32}\, L_t^2 + \frac{55}{54}\, L_t + \frac{40291}{20736} \right) \\ &\left. \left. + N_F^2 \left(-\frac{1}{18}\, L_t^2 + \frac{77}{1728}\, L_t - \frac{6865}{31104} \right) \right] + \mathcal{O}(\alpha_s^4) \right\}, \end{aligned} \tag{4.12}$$

where $L_t = \ln \frac{\mu_R^2}{M_t^2}$. The Wilson coefficients for the effective coupling to a pseudoscalar Higgs can be read off from Eqs. (15) and (19) in Ref. [87].

Next-to-leading order corrections were first calcluated in the context of heavy quark effective theory (HQET) in [22, 23] for a scalar SM Higgs and in Ref. [40, 88] for a pseudoscalar Higgs. The full massive calculation has been published in [89, 24], later confirmed by Refs. [90] and [91]. At next-to-leading order in QCD the gg-channel receives virtual and real corrections due to diagrams of the form shown in Fig. 4.2. After adding the real and virtual contributions the IR-divergences cancel leaving

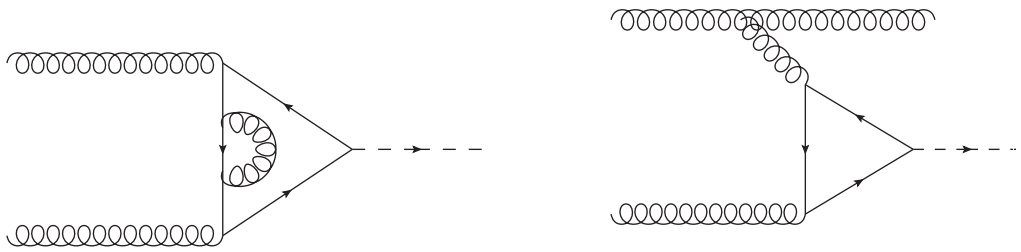

Figure 4.2

over UV-divergences as well as collinear divergences which can be absorbed into the bare parton densities. After subtracting the UV-poles by the counterterms the NLO gg-coefficient can be separated into three types of contributions

$$G_{gg\Phi}^{(1)} = G_{gg\Phi}^{(1),\delta} + G_{gg\Phi}^{(1),+} + G_{gg\Phi}^{(1),\mathrm{reg}} \tag{4.13}$$

where the superscripts δ, $+$ and R denote the δ-, plus- and regular contributions. The former two can be summarized into a soft and virtual part $G^{(1),\mathrm{SV}}_{ab\Phi}(z)$, i.e. into terms which are singular for $z \to 1$. The regular contributions contain terms which are purely collinear and next-to-dominant or next-to-soft in the threshold region. For the scalar SM Higgs H and the pseudoscalar MSSM Higgs A the coefficients then are [24]

$$\begin{aligned} G^{(1)}_{gg\Phi}(z; M^2_\Phi/\mu^2_R; M^2_\Phi/\mu^2_F) =& G^{(1),\mathrm{SV}}_{gg\Phi}(z; M^2_\Phi/\mu^2_R; M^2_\Phi/\mu^2_F, M^2_\Phi/M^2_q) \\ &+ G^{(1),\mathrm{reg}}_{gg\Phi}(z; M^2_\Phi/\mu^2_R; sM^2_\Phi/\mu^2_F, M^2_\Phi/M^2_q) \end{aligned} \tag{4.14}$$

with

$$\begin{aligned} G^{(1),\mathrm{SV}}_{gg\Phi} =& \delta(1-z)\left(c_\Phi(\tau^\Phi_q) + 6\zeta(2) + \frac{33-2N_f}{6}\ln\frac{\mu^2_R}{\mu^2_F}\right) \\ &+ 12\mathcal{D}_1(z) + 6\mathcal{D}_0(z)\ln\frac{M^2_\Phi}{\mu^2_F} \end{aligned} \tag{4.15}$$

$$\begin{aligned} G^{(1),\mathrm{reg}}_{gg\Phi} =& G^{(1),\mathrm{reg}}_{gg\Phi}(z; M^2_\Phi/\mu^2_R; M^2_\Phi/\mu^2_F; M^2_\Phi/M^2_q) \\ =& P^{\mathrm{reg}}_{gg}(z)\,\ln\frac{(1-z)^2M^2_\Phi}{z\mu^2_F} - 6\frac{\ln z}{1-z} + d^\Phi_{gg}(z,\tau^\Phi_q)\,, \end{aligned} \tag{4.16}$$

The gq and $q\bar{q}$-channels contribute to the same level in α_s but do not contain logarithmically enhanced terms or delta distributions in the limit $z \to 1$. Their coefficient functions can be summarized as [24]

$$\begin{aligned} G^{(1)}_{gq\Phi} =& G^{(1),\mathrm{reg}}_{gq\Phi}(z; M^2_\Phi/\mu^2_R; M^2_\Phi/\mu^2_F, M^2_\Phi/M^2_q) \\ =& \frac{1}{2}P_{gq}(z)\ln\frac{(1-z)^2M^2_\Phi}{z\mu^2_F} + d^\Phi_{gq}(z,\tau^\Phi_q)\,, \end{aligned} \tag{4.17}$$

$$\begin{aligned} G^{(1)}_{q\bar{q}\Phi} =& G^{(1),\mathrm{reg}}_{q\bar{q}\Phi}(z; M^2_\Phi/\mu^2_R; M^2_\Phi/\mu^2_F, M^2_\Phi/M^2_q) \\ =& d^\Phi_{q\bar{q}}(z,\tau^\Phi_q) \end{aligned} \tag{4.18}$$

The full mass dependence of the coefficients $c(\tau^\Phi_q)$, $d^\Phi_{ab}(z,\tau^\Phi_q)$ can be found in Eq. (B.2) in appendix B, respectively in Eq. (C.4) in appendix C of Ref. [24]

$$\begin{aligned} d^\Phi_{q\bar{q}}(z,\tau^\Phi_q) &= \frac{2}{3\left|\sum_Q F^\Phi_0(\tau^\Phi_q)\right|^2}\frac{(1-z)^3}{z}\left|\sum_Q \mathcal{A}^\Phi_{qqg}(S)\right|^2 \\ d^\Phi_{gq}(z,\tau^\Phi_q) &= \frac{2}{3}z + \frac{2}{3}z\int_0^1\frac{dv}{v}\left\{-1-2\frac{1-z}{z^2}\right. \\ &\quad \left. + \frac{1+(1-z)^2(1-v)^2}{z^2}\left|\frac{3}{4\sum_Q F^\Phi_0(\tau^\Phi_q)}\sum_Q \mathcal{A}^\Phi_{qqg}(T)\right|^2\right\} \end{aligned}$$

$$d_{gg}^{\Phi}(z,\tau_q^{\Phi}) = \frac{3}{(1-z)z}\int_0^1 \frac{dv}{v}\left\{ z^4 \frac{\mathcal{A}_{ggg}^{\Phi}(S,T,U)}{\left|\sum_Q F_0^{\Phi}(\tau_q^{\Phi})\right|^2} - 1 - z^4 - (1-z)^4 \right\} \quad (4.19)$$

where the function F_0^{Φ} can be extracted from Eq. (A.5) in appendix A whereas $\mathcal{A}_{qqg}^{\Phi}$ and $\mathcal{A}_{ggg}^{\Phi}$ are given in Eq. (C.5) in appendix C of Ref. [24]. In the limit of a heavy top-quark $M_t^2 \gg m_H^2$ the universal coefficients d simplify to the following expressions

$$c^H(\tau_q^H) \to \frac{11}{2},\ c^A(\tau_q^A) \to 6, \quad (4.20)$$

$$d_{gg}^{\Phi}(z,\tau_q^{\Phi}) \to -\frac{11}{2}\frac{(1-z)^3}{z}, \quad (4.21)$$

$$d_{gq}^{\Phi}(z,\tau_q^{\Phi}) \to -\frac{1}{z} + 2 - \frac{z}{3}, \quad (4.22)$$

$$d_{q\bar{q}}^{\Phi}(z,\tau_q^{\Phi}) \to \frac{32}{27}\frac{(1-z)^3}{z}. \quad (4.23)$$

We want to conclude this subsection with the analysis of the impact of the NLO corrections as well as to compare the full massive with the effective theory approach. Due to the factorization formula in hadron collisions the total inclusive hadronic cross section for the Standard Model Higgs and the pseudoscalar MSSM Higgs can be written as

$$\sigma^{\Phi}(s,M_{\Phi}^2,M_Q^2) = \sum_{a,b}\int_0^1 dx_1\, dx_1\, f_{a/h_1}(x_1,\mu_F^2)\, f_{b/h_2}(x_2,\mu_F^2) \int_0^1 dz\, \delta\left(z - \frac{\tau_{\Phi}}{x_1 x_2}\right)$$
$$\cdot\, \sigma_0^{\Phi}\Delta_{ab\Phi}(z; M_Q^2, \alpha_s(\mu_R^2), M_{\Phi}^2/\mu_R^2; M_{\Phi}^2/\mu_F^2, M_{\Phi}^2/M_q^2)\ . \quad (4.24)$$

We define the K-factor in the usual way as the ratio of the NLO cross section over the LO cross section while the K_{∞}-factor represents the equivalent ratio in the limit of a heavy top quark.

$$K^{NLO} = \frac{\sigma^{\Phi}(s,M_{\Phi}^2)^{NLO}}{\sigma^{\Phi}(s,M_{\Phi}^2,M_Q^2)^{LO}} \quad (4.25)$$

$$K_{\infty}^{NLO} = \left.\frac{\sigma^{\Phi}(s,M_{\Phi}^2)^{NLO}}{\sigma^{\Phi}(s,M_{\Phi}^2,M_Q^2)^{LO}}\right|_{m_t\to\infty, m_b=0, m_c=0} \quad (4.26)$$

For our analysis we used the FORTRAN 77 program HIGLU [92]. The NLO contributions in the limit of a heavy top quark are also included in a separate Mathematica program which has been checked against HIGLU. For the evaluation of (4.24) at next-to-leading order we used the NLO MSTW08 PDF's [93] in HIGLU, respectively

the Mathematica interface. With a center-of-mass energy of $\sqrt{s} = 14$ TeV and only including top mass effects at NLO with $m_t = 172.5$ GeV the K-factor amounts to $1.5 - 1.9$ thus proving sizeable. Within the HQET it was observed [24] that the full massive NLO result can be approximated by the K_∞-factor rescaled with the massive LO Born term

$$\sigma^\Phi(s, M_\Phi^2) = \sigma_0^\Phi K_\infty^{NLO} \tag{4.27}$$

within an accuracy of about $\mathcal{O}(1\%)$ for a Higgs mass $M_H = 125$ GeV. For larger Higgs masses at around $M_H = 600$ GeV the deviation is about $\mathcal{O}(10\%)$. In case of a pseudoscalar Higgs the K-factor amounts to approximately $1.5 - 1.7$ for small values of $\tan\beta$ whereas for larger values of $\tan\beta$ the K-factor is close to unity.

Both for a SM Higgs and pseudoscalar MSSM Higgs boson the comparison between the full massive and effective theory approach is depicted in Figs. 4.3 and 4.4. The good numerical agreement of both approaches thus gives good reasons to rely on the HQET-calculations. The bulk of the next-to-leading and higher-order corrections originates from the region of soft and collinear gluons which do not resolve the effective coupling [84]. In the next subsection the NNLO and N^{3}LO contributions will be reviewed in the context of a heavy top-quark in the triangle loop.

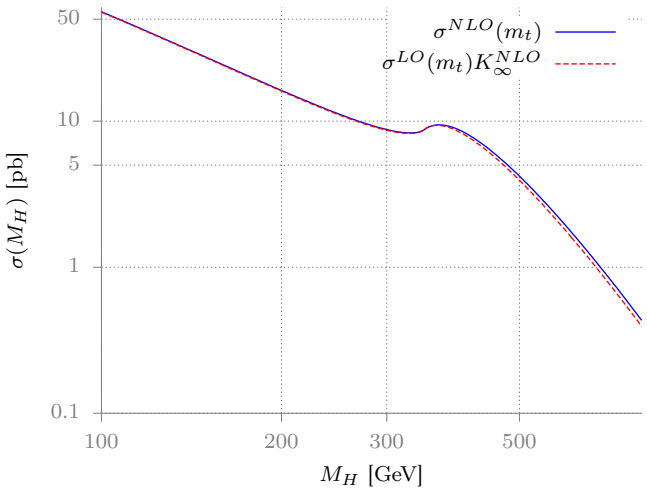

Figure 4.3: Comparison between the full massive NLO result (the solid blue line) with the effective theory approach as defined in (4.26) (the dashed red line) in case of a SM Higgs with center of mass energy $\sqrt{s} = 14$ TeV and $M_t = 172.5$ GeV.

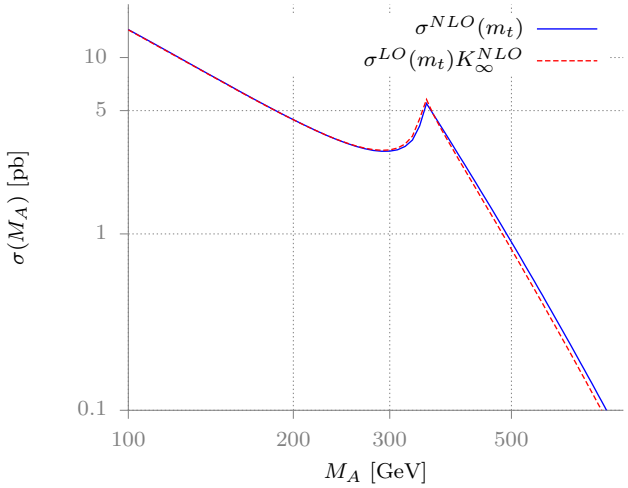

Figure 4.4: Comparison between the full massive NLO result (the solid blue line) with the effective theory approach as defined in (4.26) (the dashed red line) in case of a pseudoscalar MSSM Higgs with center of mass energy $\sqrt{s} = 14$ TeV and $M_t = 172.5$ GeV and $\tan\beta = 3$.

1.3 Contributions beyond next-to-leading order in HQET

The next-to-leading order soft+virtual contributions to the gluon fusion process in the SM within the HQET have first been calculated in Refs. [94, 95]. Later terms originating from the collinear region have been derived by the authors in Ref. [96]. Additionally to the gg-,gq- and $\bar{q}q$-channels the qq and $q_i q_j$ $(i \neq j)$ channels open up. The full NNLO calculations were first presented in Refs. [97], [96] and [43]. The coefficient function associated with the soft contributions, the terms proportional to $\mathcal{D}_i(z)$, $0 \leq i \leq 3$, and the virtual contributions, the terms proportional to $\delta(1-z)$ can be summarized into

$$
\begin{aligned}
G_{ggH}^{(2)\mathrm{SV}} =& G_{ggH}^{(2)\mathrm{SV}}(z; \frac{M_H^2}{\mu_F^2}, \frac{M_H^2}{\mu_F^2}) \\
=& \delta(1-z) \left[\frac{11399}{144} + \frac{133}{2}\zeta(2) - \frac{9}{20}\zeta(2)^2 - \frac{165}{4}\zeta(3) \right. \\
&+ \left(\frac{19}{8} + \frac{2}{3}N_f\right) \ln\frac{M_H^2}{M_t^2} + N_f \left(-\frac{1189}{144} - \frac{5}{3}\zeta(2) + \frac{5}{6}\zeta(3)\right) \\
&+ \frac{(33-2N_f)^2}{48} \ln^2\frac{\mu_F^2}{\mu_R^2} - 18\,\zeta(2)\ln^2\frac{M_H^2}{\mu_F^2} \\
&+ \left(\frac{169}{4} + \frac{171}{2}\zeta(3) - \frac{19}{6}N_f + (33-2N_f)\,\zeta(2)\right) \ln\frac{M_H^2}{\mu_F^2} \\
&\left. + \left(-\frac{465}{8} + \frac{13}{3}N_f - \frac{3}{2}\,(33-2N_f)\,\zeta(2)\right) \ln\frac{M_H^2}{\mu_R^2} \right] \\
&+ \mathcal{D}_0(z) \left[-\frac{101}{3} + 33\zeta(2) + \frac{351}{2}\zeta(3) + N_f \left(\frac{14}{9} - 2\zeta(2)\right) + \right. \\
&\left(\frac{165}{4} - \frac{5}{2}N_f\right) \ln^2\frac{M_H^2}{\mu_F^2} \\
&\left. - \frac{3}{2}\,(33-2N_f) \ln\frac{M_H^2}{\mu_F^2}\, \ln\frac{M_H^2}{\mu_R^2} + \left(\frac{133}{2} - 45\zeta(2) - \frac{5}{3}N_f\right) \ln\frac{M_H^2}{\mu_F^2} \right] \\
&+ \mathcal{D}_1(z) \left[133 - 90\zeta(2) - \frac{10}{3}N_f + 36\ln^2\frac{M_H^2}{\mu_F^2} \right. \\
&\left. + (33-2N_f) \left(2\ln\frac{M_H^2}{\mu_F^2} - 3\ln\frac{M_H^2}{\mu_R^2}\right) \right] \\
&+ \mathcal{D}_2(z) \left[-33 + 2N_f + 108\ln\frac{M_H^2}{\mu_F^2} \right]
\end{aligned}
$$

$$+ 72\,\mathcal{D}_3(z) \quad . \tag{4.28}$$

The remaining regular terms in the gg-, gq-,qq-, $q\bar{q}$- and q_iq_j-channel can be found in Eqs. (47-57) of Ref. [97] for $\mu_R = \mu_F = M_H$ or in Eqs. (A.1-A.30) of Ref. [43] for $\mu = \mu_R = \mu_F \neq M_H$. We have extended the Mathematica program by evolving the scale dependence of the strong coupling on μ_F up to values of μ_R (see Appendix C) and checking the numerical results against HIGLU.

In the case of a pseudoscalar Higgs the soft+virtual contributions have been calculated in Ref. [42] whereas to full NNLO coefficient functions were published in Ref. [43, 44, 96]. The difference of the soft+virtual coefficient functions at two loop level $G^{(2)}_{ggA-H} = G^{(2)}_{ggA} - G^{(2)}_{ggH}$ reads

$$\begin{aligned}
G^{(2)\mathrm{SV}}_{ggA-H} =& G^{(2)\mathrm{SV}}_{ggA-H}(z; \frac{M_H^2}{\mu_F^2}, \frac{M_H^2}{\mu_F^2}) \\
=& \left[\frac{1939}{144} - \frac{19}{8}\ln\frac{M_A^2}{M_t^2} + 3\zeta_2 \right. \\
& + N_f\left(\frac{21}{16} + \frac{1}{3}\ln\frac{M_A^2}{M_t^2}\right) \\
& \left.\left(+\frac{11}{4} - \frac{1}{6}N_f\right)\ln\frac{M_A^2}{\mu_F^2} + \left(-\frac{33}{8} + \frac{1}{4}N_f\right)\ln\frac{M_A^2}{\mu_R^2}\right]\delta(1-z) \\
& + 3\mathcal{D}_0(z)\ln\frac{M_A^2}{\mu_F^2} + 6\mathcal{D}_1(z)
\end{aligned} \tag{4.29}$$

Numerical studies of the impact of the two loop corrections both for a scalar Higgs and a pseudoscalar Higgs have been carried out in Refs. [97, 96, 43], respectively in Refs. [42, 43, 44]. It was observed that with respect to NLO results in the heavy top-quark limit the total hadronic cross section increases by about $\mathcal{O}(30\%)$ and the residual scale dependence is reduced to approximately $\mathcal{O}(15\%)$.

Quite recently N^{3}LO contributions in the threshold expansion for a scalar SM Higgs have been published. The coefficient functions in the soft+virtual region are given in Eq. (9) of Ref. [98] for $\mu_R = \mu_F = M_H$. The partonic cross sections differs from the one in Eq. (4.1) but can be transformed to our convention by

$$G^{\mathrm{SV}}_{abH}(z) = (3\pi)^2 \left[C(\mu^2)\right]^2 \eta_{ij}(z) \tag{4.30}$$

Furthmore, the same authors presented terms arising from the collinear region in Ref. [99] and then completed the effective three loop calculation in Ref. [100]. The authors stated a further increase of the cross section of around $\mathcal{O}(2.2\%)$ for $\mu_R = \mu_F = M_H/2$ with respect to the previous order and noted that the scale dependence amounts to $\mathcal{O}(3\%)$. Thus the residual theoretical uncertainties are parametric ones due the strong coupling and the parton densities.

2 Electroweak contributions

Two-loop electroweak contributions to the gluon-fusion process in the SM involve the computation of diagrams in excerpts shown in Fig. 4.5. The first diagram is a order $\mathcal{O}(\alpha)$-correction to the Born diagram whereas the second depicts the situation of two vector bosons fusing into a Higgs. Apart from the difference in the couplings to the Higgs both kinds of diagrams contribute to $\mathcal{O}(\alpha_s^2\alpha)$ corrections when interfered with the Born term. In Ref. [101, 102, 103] only a gauge invariant subset of diagrams of the second type of diagrams depicted in Fig. 4.5 where the quark in the box is considered to be massless. In addition, in Ref. [104], both kind of contributions in Fig. 4.5 in the limit $M_H^2 \ll 4M_W^2$ were presented. Finally, the full NLO electroweak

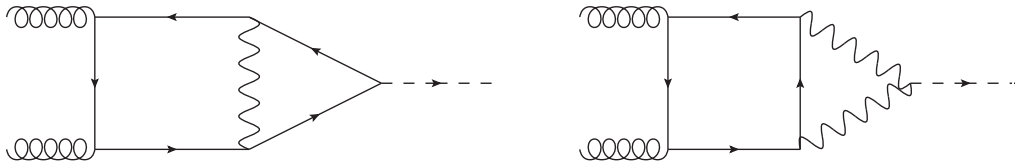

Figure 4.5: Diagrams contributing to the NLO electroweak corrections to the gluon fusion

corrections were published in Refs. [105, 106]. It is furthermore assumed that the electroweak contributions factorize from the QCD effects. Two kinds of factorization schemes have already been proposed in [103, 105].

- Complete factorization

$$\sigma_0^H \Delta_{abH} \to \sigma_0^H (1 + \delta_{\text{EW}}) \Delta_{abH} \tag{4.31}$$

- Partial factorization

$$\sigma_0^H \Delta_{abH} \to \sigma_0^H (\Delta_{abH} + \delta_{\text{EW}} \alpha_s^2(\mu_R^2) \Delta_{abH}^{(0)}) \tag{4.32}$$

where δ_{EW} contains all NLO electroweak corrections to the partonic cross section $\hat{\sigma}(gg \to H)$

$$\hat{\sigma}_{abH}(\hat{s}, M_\Phi^2) = \alpha_s^2(\mu_R^2) \sigma_0^H (1 + \delta_{\text{EW}}) \Delta_{abH}^{(0)} \tag{4.33}$$

Refering to [103] the complete factorization of electroweak contributions from QCD corrections relies on the fact that higher-order terms starting at the three-loop level are small. Nevertheless, approximate mixed QCD-electroweak contributions have been calculated in Ref. [107]. The program HIGLU provides both NLO-electroweak

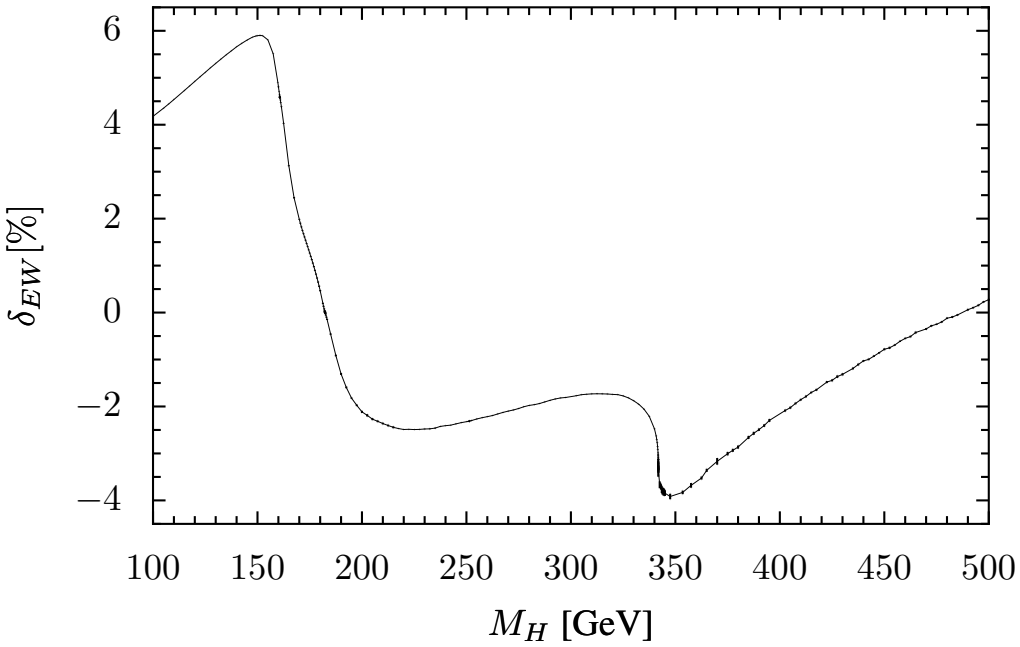

Figure 4.6: Electroweak percentage corrections at NLO to the partonic cross sections as in Eq. (4.33) from [105]

corrections generated by a grid file and mixed QCD-electroweak corrections. For a Higgs mass $M_H = 125$ GeV the electroweak corretions are further increasing the cross section by about $\mathcal{O}(5\%)$. At Higgs masses larger than $M_H = 180$ GeV the corrections become negative of around $\mathcal{O}(-4\%)$ at the threshold of a $t\bar{t}$-pair. Mixed QCD-electroweak corrections only amount at the per-mille level.

Chapter 5

Threshold Resummation in Gluon fusion

1 Introduction and previous work

Based on the two methods described in Section (2) the soft and collinear resummation to the gluon fusion process in the SM has been first applied at NLL accuracy in Ref. [84]. Further work extended the resummation to NNLL level [108], respectively in Refs. [109, 110, 111, 112, 113]. Mass effects have also been incorporated into the resummation [114]. Approximate N^3LO results have been derived in Refs. [115, 116, 117, 118] due to the knowledge of the threshold expansion, published in Ref. [98]. In case of the pseudoscalar Higgs the resummation of soft and collinear gluons has only be performed at NNLL level [45] in the limit of a heavy top quark.

In the following sections we set up the basis of the soft-virtual-collinear gluon resummation up to N^3LL level for a scalar Higgs, respectively at NNLL level for the pseudoscalar Higgs. The inclusion of the leading collinear logarithms turns out to be numerically relevant [84]. In addition to previous work we also study the analytical inclusion and numerical impact of the subleading collinear gluons in the gluon fusion processes by providing an alternative approach to Ref. [118]. Furthermore, we consistently treat mass effects within the resummation method. Besides analytical derivations we deal with the numerical implementation and matching of the resummed and fixed-order result. Finally we present numerical results for both scalar and pseudoscalar Higgs.

2 Soft and collinear gluon resummation at N^{3}LL accuracy

Following our notation of the total hadronic cross section in Eq. (4.24) the Mellin moment is defined as

$$\sigma_N^\Phi(M_\Phi^2, M_Q^2) \equiv \int_0^1 d\tau_H \; \tau_\Phi^{N-1} \; \sigma^\Phi(s, M_\Phi^2, M_Q^2). \; . \tag{5.1}$$

Instead of an integral convolution form as in Eq. (4.24) the partonic cross section as well the parton densities factorize multiplicatively in Mellin space

$$\begin{aligned}\sigma_{N-1}^\Phi(M_\Phi^2, M_Q^2) =& \sigma^{(0)} \sum_{a,b} \tilde{f}_{a/h_1}(N, \mu_F^2) \; \tilde{f}_{b/h_2}(N, \mu_F^2) \\ & \times \tilde{G}_{ab\Phi}\left(N; \alpha_s(\mu_R^2), \frac{M_\Phi^2}{\mu_F^2}; \frac{M_\Phi^2}{\mu_F^2}; \frac{M_\Phi^2}{M_t^2}\right) \; ,\end{aligned} \tag{5.2}$$

where $G_{ab,\,N}$ obeys the analogous perturbative expansion in α_s as in Eq. (4.4). Going back to Sec. 1 only the initial gg-channel contains soft+virtual contributions at every perturbative order. The virtual contributions include terms proportional to $\delta(1-z)$ whereas the soft contributions include terms which are proportional to the plus distributions $\mathcal{D}_i(z)$. We further saw that the limit $z \to 1$ in x-space corresponds to the large N limit in Mellin space. The plus distributions generate large logarithms $\ln^i N$ that spoil the convergence in this particular kinematical region. The delta distributions simply become constants in the large N limit. All other regular contributions are of order $\mathcal{O}(1/N)$ and thus can safely be neglected. Near the partonic threshold the hard coefficient functions $G_{ab,\,N}$ then can be resummed as

$$\begin{aligned}\tilde{G}_{gg\Phi}\left(N, \alpha_s(\mu_R^2), \frac{M_\Phi^2}{\mu_F^2}; \frac{M_\Phi^2}{\mu_F^2}\right) =& \alpha_s^2 \left\{1 + \sum_{n=1}^{+\infty} \alpha_s^n \sum_{m=0}^{2n} G_H^{(n,m)} \ln^m N\right\} \\ & + \mathcal{O}(1/N) \\ =& G_{gg\Phi,\,N}^{(\text{res})} + \mathcal{O}(1/N) \; ,\end{aligned} \tag{5.3}$$

$$\tilde{G}_{ab\Phi}\left(N, \alpha_s(\mu_R^2), \frac{M_\Phi^2}{\mu_F^2}; \frac{M_\Phi^2}{\mu_F^2}\right) = \mathcal{O}(1/N) \qquad (ab \neq gg) \; , \tag{5.4}$$

The first application of the soft and collinear gluon resummation to the gluon fusion process was performed in Ref. [84] in the limit of a heavy top quark. Due to kinematical similarities to the Drell-Yan process the same resummation procedure can be repeated in a fully analogous way as in section 2.1.3 where one simply has to

replace the subscript qq by Φ. The main difference to the Drell–Yan process stems from the fact that the one loop coefficients $W_\Phi^{(1)}$ are not universal. They can be written as

$$W_\Phi^{(1)}(z,1,\epsilon) = \delta(1-z) f_\Phi^{(1)}(\epsilon) + z^\epsilon \left(\frac{g^{(1)}(z,\epsilon)}{(1-z)^{1+2\epsilon}} \right)_+ + h^{(1)}(z,\epsilon) \,, \tag{5.5}$$

where the regular functions $f_\Phi^{(1)}$, $g^{(1)}$ and $h^{(1)}$ read

$$f_{h,H}^{(1)}(\epsilon) = -C_A \epsilon \left(\frac{11}{6\epsilon} + \frac{203}{36} + \frac{\pi^2}{3} \right) , \tag{5.6}$$

$$f_A^{(1)}(\epsilon) = f_{h,H}^{(1)}(\epsilon) - 2C_A\epsilon, \tag{5.7}$$

$$g^{(1)}(z,\epsilon) = C_A \left(1 + z^4 + (1-z)^4 \right) , \tag{5.8}$$

$$h^{(1)}(z,\epsilon) = C_A \epsilon \frac{11}{6} z^\epsilon (1-z)^{3-2\epsilon}. \tag{5.9}$$

The authors of Ref. [84] also included collinear logarithms of the kind $\ln^i N/N$ by evaluating the combination $(z^{N-1}-1)g^{(1)}(z,\epsilon)$ in the following way

$$\begin{aligned} \frac{1}{C_A}(z^{N-1}-1)g^{(1)}(z,\epsilon) \to & (z^{N-1}-1)\ 2 - (1-z)(2z^2-4z-2z^3) \\ & - 4z^{N-1}(1-z)\,. \end{aligned} \tag{5.10}$$

This results in an exponentiation of the leading and next-to-leading logarithms as well as the constant terms and the collinear logarithms. At NLL accuracy the all order resummation formula is

$$\begin{aligned} \tilde{G}_{gg\Phi} =& \tilde{G}_{gg} \left(N, \alpha_s(\mu_R^2), \frac{M_\Phi^2}{\mu_F^2}; \frac{M_\Phi^2}{\mu_F^2}, 0 \right) \\ =& \alpha_s^2(\mu_R^2) \exp\left\{ \frac{\alpha_s(\mu_R^2)}{\pi} \left(G_{gg\Phi,N}^{(1)\mathrm{SV}-N} + 2C_A \frac{\ln N}{N} \right) \right\} \end{aligned} \tag{5.11}$$

where $G_{gg,N}^{(1)}$ can be inferred from Eq. (E.11) in Appendix E. The soft and collinear resummation has been extended to NNLL accuracy in Ref. [108] based on the earlier work in DY [73, 77], that we described in Sec. 2.2. Following along the notation in Ref. [108] we extend the soft gluon resummation to N^{3}LL accuracy. The all order resummation formula can be cast into the following form [95]

$$\tilde{G}_{gg\Phi}^{(\mathrm{res})} = \tilde{G}_{gg\Phi}^{(\mathrm{res})} \left(N, \alpha_s(\mu_R^2), \frac{M_\Phi^2}{\mu_F^2}; \frac{M_\Phi^2}{\mu_F^2} \right) \tag{5.12}$$

$$= \alpha_s^2(\mu_R^2)\,\overline{C}_{gg\Phi}\left(\alpha_s(\mu_R^2), \frac{M_\Phi^2}{\mu_R^2}; \frac{M_\Phi^2}{\mu_F^2}; \frac{M_\Phi^2}{M_t^2}\right)$$
$$\cdot\,\Delta^H\left(N, \alpha_s(\mu_R^2), \frac{M_\Phi^2}{\mu_R^2}; \frac{M_\Phi^2}{\mu_F^2}\right) + \mathcal{O}(1/N)\,. \tag{5.13}$$

where $\overline{C}_{gg}$ contains all the constant terms. The Sudakov radiative factor Δ_N^H is universal for scalar and pseudoscalar Higgs boson production and has the following integral representation

$$\begin{aligned}\Delta^H &= \Delta^H\left(N, \alpha_s(\mu_R^2), \frac{M_\Phi^2}{\mu_R^2}; \frac{M_\Phi^2}{\mu_F^2}\right)\\ &= \exp\left\{\int_0^1 dz\,\frac{z^{N-1}-1}{1-z}\right.\\ &\left.\times\left[2\int_{\mu_F^2}^{(1-z)^2M_\Phi^2}\frac{dq^2}{q^2}\,A(\alpha_s(q^2)) + D(\alpha_s((1-z)^2M_\Phi^2))\right]\right\}\,,\end{aligned} \tag{5.14}$$

where $A(\alpha_s)$ and $D(\alpha_s)$ are perturbative functions

$$\begin{aligned}A(\alpha_s) &= \sum_{n=1}^{+\infty}\left(\frac{\alpha_s}{\pi}\right)^n A^{(n)} = \frac{\alpha_s}{\pi}A^{(1)} + \left(\frac{\alpha_s}{\pi}\right)^2 A^{(2)} + \left(\frac{\alpha_s}{\pi}\right)^3 A^{(3)} + \left(\frac{\alpha_s}{\pi}\right)^3 A^{(4)}\\ &+ \mathcal{O}(\alpha_s^4)\,,\end{aligned} \tag{5.15}$$

$$D(\alpha_s) = \sum_{n=2}^{+\infty}\left(\frac{\alpha_s}{\pi}\right)^n D^{(n)} = \left(\frac{\alpha_s}{\pi}\right)^2 D^{(2)} + \left(\frac{\alpha_s}{\pi}\right)^2 D^{(3)} + \mathcal{O}(\alpha_s^3)\,. \tag{5.16}$$

The functions $A^{(i)}$ contain all soft+collinear gluon effects in the initial state and the functions $D^{(i)}$ contain all the wide angle soft-gluon effects in the final state. Explicit expressions can be found in Eqs. (E.1), (E.2), (E.3) and (E.4) in Appendix E. By solving the integrals in Eq. (5.14) one obtains a convenient form which systematically organizes all singular and constant contributions

$$\begin{aligned}\tilde{G}_{gg}^{(\mathrm{res})}(N; \alpha_s(\mu_R^2), \frac{M_\Phi^2}{\mu_F^2}; \frac{M_\Phi^2}{\mu_F^2}) &= \alpha_s^2(\mu_R^2)\,C_{gg\Phi}\left(\alpha_s(\mu_R^2), \frac{M_\Phi^2}{\mu_R^2}; \frac{M_\Phi^2}{\mu_F^2}, \frac{M_\Phi^2}{M_t^2}\right)\\ &\cdot \exp\left\{\mathcal{G}_H\left(\alpha_s(\mu_R^2), \ln N; \frac{M_\Phi^2}{\mu_R^2}), \frac{M_\Phi^2}{\mu_F^2}\right)\right\}\,.\end{aligned} \tag{5.17}$$

The constant function $C_{gg\Phi}$ contains contributions which originate from the terms in front of the delta distribution $\delta(1-z)$ as well as from non-logarithmic terms emerging from the Mellin transformations. The perturbative expansion of $C_{gg\Phi}$ is

$$C_{gg\Phi} = C_{gg\Phi}\left(\alpha_s(\mu_R^2), \frac{M_\Phi^2}{\mu_R^2}; \frac{M_\Phi^2}{\mu_F^2}, \frac{M_\Phi^2}{M_t^2}\right)$$

$$= 1 + \sum_{n=1}^{+\infty} \left(\frac{\alpha_s(\mu_R^2)}{\pi}\right)^n C_{gg\Phi}\left(\frac{M_\Phi^2}{\mu_R^2}; \frac{M_\Phi^2}{\mu_F^2}, \frac{M_\Phi^2}{M_t^2}\right) \quad . \tag{5.18}$$

The difference between $C_{gg\Phi}$ and $\overline{C}_{gg\Phi}$ is that one can put either terms into the radiative factor Δ_N^H or into the constant terms. The threshold expansion of the Laurent series in [98] allows us to determine the constant terms $C_{gg\Phi}$ in the limit of a heavy top quark. The restauration of the scale dependence is described in detail in Appendix C whereas the coefficient functions $C_{gg\Phi}^{(i)}$ are given in Eqs. (E.14), (E.15) and (E.18). We notice that $C_{gg\Phi}$ generally depends on the ratio $\frac{M_\Phi^2}{M_t^2}$ and we postpone the discussion about mass effects to section 3 . The singular contributions are all included in the resummed kernel $\mathcal{G}_\Phi$ which can be expanded in the following way

$$\begin{aligned}
\mathcal{G}_\Phi &= \mathcal{G}_\Phi\left(\alpha_s(\mu_R^2), \ln N; \frac{M_\Phi^2}{\mu_R^2}, \frac{M_\Phi^2}{\mu_F^2}\right) \\
&= \sum_{n=1}^{+\infty} \alpha_s^n \sum_{m=1}^{n+1} \mathcal{G}_H^{(n,m)} \ln^m N \\
&= \ln N \; g_H^{(1)}(b_0 \alpha_s(\mu_R^2) \ln N) \\
&+ g_H^{(2)}\left(b_0 \alpha_s(\mu_R^2) \ln N, \frac{M_\Phi^2}{\mu_R^2}; \frac{M_\Phi^2}{\mu_F^2}\right) \\
&+ \alpha_s(\mu_R^2) \; g_H^{(3)}\left(b_0 \alpha_s(\mu_R^2) \ln N, \frac{M_\Phi^2}{\mu_R^2}; \frac{M_\Phi^2}{\mu_F^2}\right) \\
&+ \alpha_s^2(\mu_R^2) \; g_H^{(4)}\left(b_0 \alpha_s(\mu_R^2) \ln N, \frac{M_\Phi^2}{\mu_R^2}; \frac{M_\Phi^2}{\mu_F^2}\right) \\
&+ \sum_{n=5}^{+\infty} \left[\alpha_s(\mu_R^2)\right]^{n-2} \; g_H^{(n)}\left(b_0 \alpha_s(\mu_R^2) \ln N, \frac{M_\Phi^2}{\mu_R^2}; \frac{M_\Phi^2}{\mu_F^2}\right) \quad ,
\end{aligned} \tag{5.19}$$

The term $\ln N \; g_H^{(1)}$ resums all leading logarithms $\alpha_s^n \ln^{2n} N$ while sub-leading logarithms are contained in the functions $g_H^{(2)}$, $g_H^{(3)}$ and $g_H^{(4)}$. The functions $g_H^{(i)}$ can be inferred from Eqs. (E.7), (E.8), (E.9), (E.10) in Appendix E. Expanding Eq. (5.19) in terms of the strong coupling the soft+virtual approximation at fixed order can be written as

$$\begin{aligned}
\tilde{G}_{gg\Phi}^{(\mathrm{res})} = \alpha_s^2(\mu_R^2) \Bigg[1 &+ \frac{\alpha_s(\mu_R^2)}{\pi} \tilde{G}_{gg\Phi,N}^{(1)\,\text{SV-}N} + \left(\frac{\alpha_s(\mu_R^2)}{\pi}\right)^2 \tilde{G}_{gg\Phi,N}^{(2)\,\text{SV-}N} \\
&+ \left(\frac{\alpha_s(\mu_R^2)}{\pi}\right)^3 \tilde{G}_{gg\Phi,N}^{(3)\,\text{SV-}N} + \mathcal{O}(\alpha_s^4)\Bigg] \quad .
\end{aligned} \tag{5.20}$$

where the hard scattering coefficient function in Mellin space $G^{(i)\text{SV-}N}_{gg\Phi,N}$, $i = 1, 2, 3$ can be found in Eqs. (E.11), (E.12) and (E.13). These soft+virtual approximations can be obtained by transforming the expressions in Eqs. (4.15) and (4.28) into Mellin space.

3 Collinear and mass effects

We want to note that the all order resummation formula in Eq. (5.11) is consistent with Eq. (5.17) at NLL level apart from the inclusion of terms arising from collinear regions. Following the discussion in Ref. [95], the origin of the leading collinear terms $\ln^{2n-1} N/N$ can be attributed to the initial state collinear radiation up to a maximal value of transverse momentum of the gluon $q_T^{\max} \sim (1-z)^2 M_\Phi^2$. Similar to the conjecture in [84] we observed that one has to add to the soft-collinear function $A^{(1)}$ the regular part of the Altarelli–Parisi splitting kernel $P_{gg}^{(1)\mathrm{reg}}(z)$ in the limit $z \to 1$ in order to incorporate the leading collinear terms into the resummation formula (5.14)

$$\begin{aligned}\frac{z^{N-1}-1}{1-z}\, A^{(1)} \to\ & \frac{z^{N-1}-1}{1-z}\, A^{(1)} + z^{N-1} \lim_{z\to 1} \frac{1}{2} P_{gg}^{(1)\mathrm{reg}}(z) = \\ & = \left[\frac{z^{N-1}-1}{1-z} - z^{N-1}\right] A^{(1)} \quad . \end{aligned} \tag{5.21}$$

This replacement leads to the same exponentiated form as in Eq. (5.11) which is equivalent to the substitution [108]

$$C_{gg\Phi}^{(1)} \to C_{gg\Phi}^{(1)} + 2C_A \frac{\ln N}{N} \tag{5.22}$$

Both schemes correctly predict all leading collinear logarithms, the next-to-soft terms (NS), of the form $\alpha_s^n \ln^{2n-1} N/N$ up to all orders but do not cover the subleading logarithms of this kind in the soft-virtual-collinear (SVC-N) approximation. The soft-virtual-collinear contributions in x-space in the threshold region read

$$G_{gg\Phi}^{(1)\,\mathrm{SVC}-x} = G_{gg\Phi}^{(1)\,\mathrm{SV}-x}\left(z; \frac{M_\Phi^2}{\mu_R^2}; \frac{M_\Phi^2}{\mu_F^2}; \frac{M_\Phi^2}{M_t^2}\right) - 12\, \ln(1-z) \quad , \tag{5.23}$$

$$\begin{aligned} G_{gg\Phi}^{(2)\,\mathrm{SVC}-x} =& G_{gg\Phi}^{(2)\,\mathrm{SV}-x}\left(z; \frac{M_\Phi^2}{\mu_R^2}; \frac{M_\Phi^2}{\mu_F^2}\right) - 72\, \ln^3(1-z) \quad . \\ & + \left(-108 \ln \frac{M_\Phi^2}{\mu_F^2} + \frac{345}{2} - 2N_F\right) \ln^2(1-z), \end{aligned} \tag{5.24}$$

where we also considered terms proportional to $\ln^2(1-z)$. The SVC-N coefficient $G_{ggH}^{(2)\mathrm{SVC}-N(\mathrm{res})}$, obtained by expanding Eq. (5.17) with the formal replacement in Eq. (5.22), differs from the coefficient, determined by computing the Mellin moments of Eq. (5.24), in subleading collinear terms. The correct form of the SVC contribution $G_{ggH}^{(2)\mathrm{SVC}-N}$ up to next-to-next-to-soft terms (NNS) in Mellin space is

$$\tilde{G}_{gg\Phi}^{(2)\,\mathrm{SVC}-N}\left(z; \frac{M_\Phi^2}{\mu_R^2}; \frac{M_\Phi^2}{\mu_F^2}\right) = \tilde{G}_{gg\Phi}^{(2)\,\mathrm{SV}-N}\left(z; \frac{M_\Phi^2}{\mu_R^2}; \frac{M_\Phi^2}{\mu_F^2}\right) + 36 \frac{\ln^3 N}{N}$$

$$- \frac{54 \ln^2 N \ln\left(\frac{M_\Phi^2}{\mu_F^2}\right)}{N} - \frac{N_F \ln^2 N}{N} + \frac{108 \gamma_E \ln^2 N}{N} + \frac{48 \ln^2 N}{N} \quad . \tag{5.25}$$

We have observed that the NNS terms can correctly be reproduced within the resummation formula by the formal replacement

$$\begin{aligned} C_{gg\Phi}^{(1)} &\to C_{gg\Phi}^{(1)} + 6 \frac{\tilde{L}}{N} \\ C_{gg\Phi}^{(2)} &\to C_{gg\Phi}^{(2)} + (48 - N_F) \frac{\tilde{L}^2}{N} \end{aligned} \tag{5.26}$$

with the extended logarithm

$$\tilde{L} = \ln \frac{N e^{\gamma_E} \mu_F}{M_H} = \ln N + \gamma_E - \frac{1}{2} \ln \frac{M_\Phi^2}{\mu_F^2}. \tag{5.27}$$

With this replacement we are able to predict the correct collinear logarithms $\ln^3 N/N$ and $\ln^2 N/N$ in Eq. (5.25). At N^{3}LO we can exactly reproduce the terms $\ln^k N/N$, $k = 4, 5$.

Previous work on the soft and collinear gluon resummation in the gluon fusion was first performed in the limit of a heavy top quark. Returning to Eq. (5.18) mass effects can be included consistently into the resummation due to the following observation: The only mass dependence in the threshold terms appears in virtual coefficient function C_{gg} in Mellin space [114]

$$C_{gg\Phi}^{(1)} = \delta C_{gg\Phi}^{(1)} + 6(\gamma_E^2 + \zeta_2) - 6\gamma_E \ln \frac{M_\Phi^2}{\mu_F^2}, \tag{5.28}$$

$$\delta C_{gg\Phi}^{(1)} = c_\Phi(\tau_t^\Phi) + 6\zeta_2 + \frac{33 - 2N_F}{6} \ln \frac{\mu_R^2}{\mu_F^2}. \tag{5.29}$$

All other mass dependent regular coefficients, e.g. $G_{gg\Phi}^{(1)\text{reg}}$, $G_{gq\Phi}^{(1)\text{reg}}$, $G_{q\bar{q}\Phi}^{(1)\text{reg}}$ in Eqs. (4.16), (4.17) and (4.18) can safely be neglected in the incorporation of mass effects since they are not logarithmically enhanced, consistent with the all order resummation formula (5.17). The NNLO and N^{3}LO coefficient functions $C_{gg}^{(2)}$ and $C_{gg}^{(3)}$ have only been computed in the limit of a heavy top quark. This allows us only to include the mass effects of the top quark at NLL accuracy only. We note that we do not include the full mass dependence of the bottom and charm loops in the resummation due to the following reason: In case of the bottom quark the virtual coefficient $c^H(\tau_b^H)$ behaves in the limit $M_H^2 \gg m_b^2$ as [24]

$$c_H(\tau_b^H) \to \frac{C_A - C_F}{12} \ln^2 \frac{M_H^2}{m_b^2} - C_F \ln \frac{M_H^2}{m_b^2} \tag{5.30}$$

where we notice the appearance of large double and single logarithms of the ratio M_H^2/m_b^2. The double logarithmic contributions at LO come from infrared sensitive regions where the fermion line of the bottom quark opposite to the $Hb\bar{b}$-vertex is soft. The Abelian parts, scaling with C_F in Eq. (5.30), have been resummed at LL and NLL accuracy in case of the $H\gamma\gamma$ form factor [119, 120]. The assumption leading to the resummation is that the $H\gamma\gamma$ form factor factorizes into an off-shell $Hb\bar{b}$ vertex and an off-shell amplitude $b\bar{b} \to \gamma\gamma$. The latter does not contain any double and single logarithmic contributions as well as self-energy contributions to the fermion lines up to all orders in α_s. Soft gluons in the $Hb\bar{b}$ vertex can be organized in general ladder diagrams leading to the Sudakov form factor [121], [122], [123] which then can be used to resum the large logarithms. The resummation of the non-Abelian part proportional to the Casimir factor C_A has not been performed so far. As mentioned above, the origin of this type of logarithms in Eq. (5.30) is very different from the one of soft and collinear gluons near the partonic threshold which do not resolve the Hgg-form factor. For a SM Higgs the bottom quark contributions result in very different sizes of the QCD corrections, thus a resummation of these effects is mandatory in order to obtain reliable results. In case of a pseudoscalar Higgs the virtual coefficient $c^A(\tau_b^A)$ scales with $\tan\beta$. For large values of $\tan\beta$ bottom quark contributions are dominating over the top quark contributions. For the above mentioned reasons we neglect bottom quark mass effect and only perform the threshold resummation by imbedding top-quark contributions in the resummation formula for a scalar and pseudoscalar Higgs.

4 Numerical implementation and Matching

In this section we will describe the numerical implementation of the all-order resummation formula in Eq. (5.17) and the improvement of the physical cross section by matching the resummed to the fixed-order result. The total hadronic cross section in momentum space can be obtained by the inverse Mellin transform of the resummed expression $\tilde{G}_{ab,\,\mathrm{res}}$ as

$$\sigma(s, M_\Phi^2) = \sigma^{(0)} \sum_{a,b} \int_{C_N} \frac{dN}{2\pi i} \left(\frac{M_\Phi^2}{s}\right)^{-N+1} \tilde{f}_{a/h_1}(N, \mu_F^2)\, \tilde{f}_{b/h_2}(N, \mu_F^2) \times \tilde{G}_{ab,\,\mathrm{res}}\left(N; \alpha_s(\mu_R^2), \frac{M_\Phi^2}{\mu_R^2}; \frac{M_\Phi^2}{\mu_F^2}; \frac{M_\Phi^2}{M_t^2}\right), \tag{5.31}$$

where C_N denotes the contour in the complex N-plane. The integrand in Eq. (5.31), however, possesses non-perturbative singularities which come from the parton densities and the resummed exponent $\mathcal{G}_H$. As we will discuss later, the general functional form of the parton densities at the input scale $\mu_{F,0}$ is given by the expression $x f_{i/h_i}(x\mu_F^2) = \sum_l A_l x^{\gamma_l}(1-x)^{\delta_l}$, where the coefficients A_l, γ_l and δ_l are obtained from a fitting-procedure in DIS. The Mellin transformation of the parton densities then results in a combination of Euler beta-functions $B(a,b)$ of the following form

$$f_{i/h_{1,2},\,N}(\mu_{F_0}^2) = \sum_l A_l B(N + \gamma_l - 1, 1 + \delta_l). \tag{5.32}$$

The singularities associated with the beta-functions lie on the left real axis in the complex N-plane. Furthermore, the resummed exponent in $\mathcal{G}_H$ contains a Landau pole for values $\lambda = 1/2$, i.e. $N_L = \exp\frac{1}{2\alpha_s b_0}$. As proposed in [124], the contour has to be chosen in the following way

$$\sigma(s, M_\Phi^2) = \sigma^{(0)} \sum_{a,b} \int_{C_{MP}-i\infty}^{C_{MP}+i\infty} \frac{dN}{2\pi i} \left(\frac{M_\Phi^2}{s}\right)^{-N+1} \tilde{f}_{a/h_1}(N, \mu_F^2)\, \tilde{f}_{b/h_2}(N, \mu_F^2) \times \tilde{G}^{(\mathrm{res})}_{ab,\,N}\left(\alpha_s(\mu_R^2), \frac{M_\Phi^2}{\mu_R^2}; \frac{M_\Phi^2}{\mu_F^2}; \frac{M_\Phi^2}{M_t^2}\right), \tag{5.33}$$

with

$$C_f < C_{\mathrm{MP}} < N_L = \exp\frac{1}{2\alpha_s b_0} \tag{5.34}$$

such that C_{MP} lies between the rightmost singularity C_f of the parton densities and the Landau pole N_L. In this way factorially growing terms and power like ambiguities can be avoided in the perturbative expansion of the resummed result.

In principle one could choose an integration contour $\mathcal{C}_0$ which is perpendicular to the real exis with the abcissa C_{MP} depicted in Figure 5.1. For numerical stability reasons we have chosen the deformed contour $\mathcal{C}_1$ which can be split into an upper and lower branch, parametrized by

$$N = C_{MP} + ye^{\pm i\phi} \tag{5.35}$$

with $0 \leq y < \infty$ for the upper and $\infty > y \geq 0$ for the lower branch. We observe that we can obtain fast numerical convergence for $\phi > \pi/2$. Since the integrand $\tilde{G}_{ab,\,\mathrm{res}}$ obeys the relation $\tilde{G}^*_{ab,\,\mathrm{res}}(N) = \tilde{G}_{ab,\,\mathrm{res}}(N*)$ we can rewrite Eq. (5.31) as

$$\begin{aligned}\sigma(s, M_\Phi^2) = \sigma^{(0)}\, \frac{1}{\pi} \sum_{a,b} \tau_H \int_0^\infty \mathrm{d}y\, \mathrm{Im}\Big[& \tau_H^{-C_{MP}-ye^{i\phi}} \\ & \tilde{f}_{a/h_1}\left(C_{MP} + ye^{i\phi}, \mu_F^2\right)\, \tilde{f}_{b/h_2}\left(C_{MP} + ye^{i\phi}, \mu_F^2\right) \\ & \times \tilde{G}_{ab}^{(\mathrm{res})}\left(C_{MP} + ye^{i\phi}; \alpha_s(\mu_R^2), \frac{M_\Phi^2}{\mu_R^2}; \frac{M_\Phi^2}{\mu_F^2}; \frac{M_\Phi^2}{M_t^2}\right)\Big] \;,\end{aligned} \tag{5.36}$$

which is the form we used together with the integration routine VEGAS [125] for the implementation in our Fortran 95 subroutine HIGLURES.

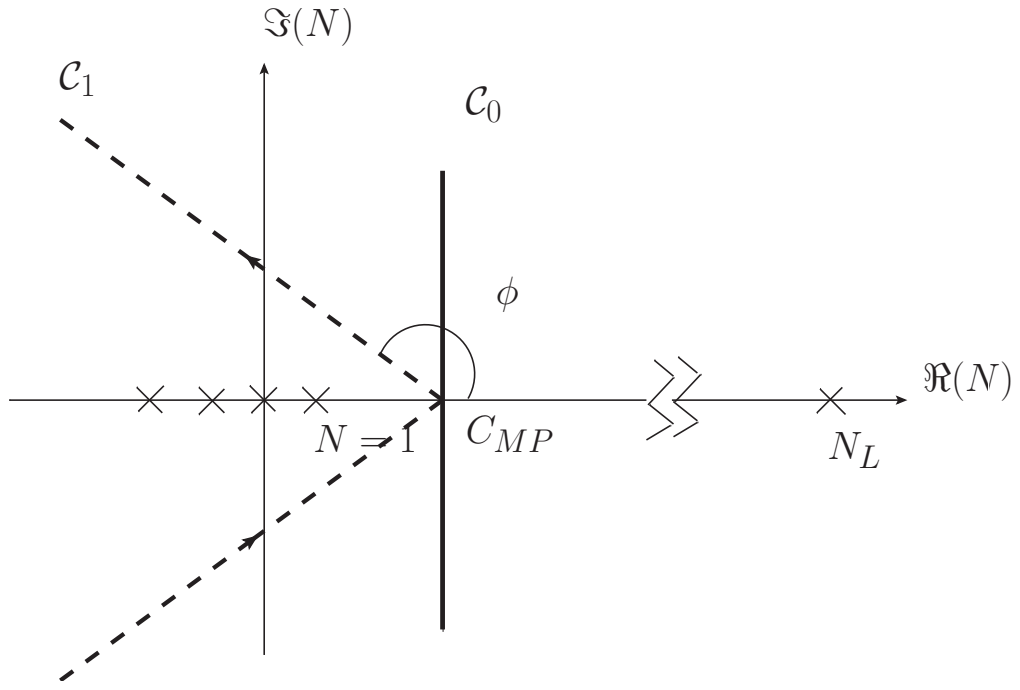

Figure 5.1: Possibilities to choose the contour for the Mellin inversion of the partonic cross section as proposed in Ref. [124].

The next two subsections are devoted to the investigation of the treatment of PDF's in Mellin and in x-space.

4.1 Parton densities in Mellin space

Common parton density groups do not provide parton distribution functions in Mellin space. One possibility, used in Ref. [108], is to fit combinations of $\sum_l A_l x^{\gamma_l}(1-x)^{\delta_l}$ to x-space PDF's for a fixed scale μ_F. This simplified form allows to Mellin-transform the fitted result for each scale choice μ_F separately. Another possibility is to evolve the parton densities at the input scale μ_{F_0} with the DGLAP evolution equations in Mellin space up to higher scales. In our work we used the program QCD-PEGASUS [126] which provides unpolarized and polarized PDF's in N-space and x-space. In the inclusive Higgs boson production via gluon fusion we only make use of the unpolarized NLO and NNLO PDF's provided by PEGASUS. We first will give a brief overview about the basis of the parton density evolution in Mellin space and then discuss the numerical implementation.

In Section 1.3 we discussed the general form of the Altarelli–Parisi splitting functions in Eq. (3.76). Since the splitting functions P_{ij} do only depend on the scale μ_F via the strong coupling $\alpha_s(\mu_F^2)$ we only need to evolve the strong coupling up to the renormalization scale μ_R with Eq. (C.4) in order to get the splitting functions in the case $\mu_R \neq \mu_F$ as

$$\begin{aligned}
P_{ij}(x,\mu_F,\mu_R) &= a_s(\mu_R^2)\, P_{ij}^{(0)}(x) \\
&+ a_s^2(\mu_R^2)\left(P_{ij}^{(1)}(x) - \beta_0 P_{\rm NS}^{(0)}(x) L\right) \\
&+ a_s^3(\mu_R^2)\left(P_{ij}^{(2)}(x) - 2\beta_0 L\, P_{ij}^{(1)}(x) - \left\{\beta_1 L - \beta_0^2 L^2\right\} P_{ij}^{(0)}(x)\right) \\
&+ a_s^4(\mu_R^2)\left(P_{ij}^{(3)}(x) - 3\beta_0 L\, P_{ij}^{(2)}(x) - \left\{2\beta_1 L - 3\beta_0^2 L^2\right\} P_{ij}^{(1)}(x)\right. \\
&\qquad \left. - \left\{\beta_2 L - 5/2\,\beta_1\beta_0 L^2 + \beta_0^3 L^3\right\} P_{ij}^{(0)}(x)\right) \qquad (5.37)
\end{aligned}$$

In Mellin space the DGLAP-equations (3.74) have the simple factorized form

$$\frac{\partial}{\partial \ln \mu_F^2} \tilde{f}_i(N,\mu_F^2) = P_{ij}(N,\mu_R^2,\mu_F^2)\tilde{f}_j(N,\mu_F^2) \qquad (5.38)$$

Expanding the r.h.s as a power expansion of $a_s = \alpha_s/(4\pi)$ we obtain

$$\frac{\partial \tilde{f}_i(N,a_s)}{\partial a_s} = -\frac{1}{a_s}\left[R_{ij}^{(0)}(N) + \sum_{k=1}^{\infty} a_s^k R_{ij}^{(K)}(N)\right]\tilde{f}_j(N,a_s)\ . \qquad (5.39)$$

where

$$R_{ij}^{(0)} \equiv \frac{1}{\beta_0} P_{ij}^{(0)} \quad , \quad R_{ij}^{(k)} \equiv \frac{1}{\beta_0} P_{ij}^{(k)} - \sum_{i=l}^{k} b_l \, R_{ij}^{(k-l)}. \tag{5.40}$$

Eq. (5.39) has then to be solved for both singlet and non-singlet combinations of partons where higher-order solutions can be derived as an expansion around the LO result. The solutions then have to be converted into the individual parton densities. The solution of the DGLAP evolution equations require the exact solution of the strong coupling α_s. Beyond LO one cannot solve the RGE of α_s in a closed form as it can inferred from the implicit solution at NLO

$$\frac{1}{a_s(\mu_R^2)} = \frac{1}{a_s(\mu_0^2)} + \beta_0 \ln\left(\frac{\mu_R^2}{\mu_0^2}\right) - b_1 \ln\left\{\frac{a_s(\mu_R^2)\,[1 + b_1 a_s(\mu_0^2)]}{a_s(\mu_0^2)\,[1 + b_1 a_s(\mu_R^2)]}\right\} \tag{5.41}$$

where $b_k = \beta_k/\beta_0$. QCD-PEGASUS solves Eq. (A.1) by a fourth order Runge-Kutta integration which differs from to the method used in Appendix B. The usage of the latter would result in a difference between Eqs. (3.74) and (5.39). Within PEGASUS the user has access to parton densities in x-space which is realized due to the Mellin inversion of the individual parton distribution in N-space. As mentioned earlier, the common functional form of the parton densities at the input-scale μ_{F_0} is the one in Eq. (5.32). Although QCD-Pegasus provides two different forms of the type as in Eq. (5.32) we used

$$x f_i(x, \mu_{F_0}^2) = N_i \, p_{i,1} \, x^{p_{i,2}} (1-x)^{p_{i,3}} \left[1 + p_{i,5} \, x^{p_{i,4}} + p_{i,6} \, x\right] \tag{5.42}$$

where N_i is the normalization of the PDF's at the reference scale μ_{F_0}. On the other hand the functional form in (5.42) matches the one used by the MSTW08 parton density group that reads

$$x u_v(x, \mu_{F_0}^2) = A_u \, x^{\eta_1} (1-x)^{\eta_2} (1 + \epsilon_u \sqrt{x} + \gamma_u \, x), \tag{5.43}$$

$$x d_v(x, \mu_{F_0}^2) = A_d \, x^{\eta_3} (1-x)^{\eta_4} (1 + \epsilon_d \sqrt{x} + \gamma_d \, x), \tag{5.44}$$

$$x S(x, \mu_{F_0}^2) = A_S \, x^{\delta_S} (1-x)^{\eta_S} (1 + \epsilon_S \sqrt{x} + \gamma_S \, x), \tag{5.45}$$

$$x \Delta(x, \mu_{F_0}^2) = A_\Delta \, x^{\eta_\Delta} (1-x)^{\eta_S + 2} (1 + \gamma_\Delta \, x + \delta_\Delta \, x^2), \tag{5.46}$$

$$x g(x, \mu_{F_0}^2) = A_g \, x^{\delta_g} (1-x)^{\eta_g} (1 + \epsilon_g \sqrt{x} + \gamma_g \, x) + A_{g'} \, x^{\delta_{g'}} (1-x)^{\eta_{g'}}, \tag{5.47}$$

$$x(s + \bar{s})(x, \mu_{F_0}^2) = A_+ \, x^{\delta_S} \, (1-x)^{\eta_+} (1 + \epsilon_S \sqrt{x} + \gamma_S \, x), \tag{5.48}$$

$$x(s - \bar{s})(x, \mu_{F_0}^2) = A_- \, x^{\delta_-} (1-x)^{\eta_-} (1 - x/x_0), \tag{5.49}$$

where the input parameters p_i can be fixed from the corresponding table in Ref. [93]. In case of the gluon densities we adapted the following form

$$x f_i(x, \mu_{F_0}^2) = N_i \, p_{i,1} \, x^{p_{i,2}} (1-x)^{p_{i,3}} \left[1 + p_{i,5} \, x^{p_{i,4}} + p_{i,6} \, x\right] + p_{i,7} \, x^{p_{i,8}} (1-x)^{p_{i,9}} \tag{5.50}$$

in QCD-PEGASUS by extending the relevant subroutines.

4.2 Parton derivative method

The total hadronic cross section for the inclusive Higgs boson production via gluon fusion in Eq. (4.24) can be written as

$$\sigma(s, M_\Phi^2) = \sigma^{(0)} \tau_H \sum_{a,b} \int_{\tau_H}^{\infty} \frac{\mathrm{d}z}{z} \int_{\tau_H/z}^{1} \frac{\mathrm{d}x}{x} f_{a/h_1}(x, \mu_F^2) f_{b/h_2}(\frac{\tau_H}{xz}, \mu_F^2) \tag{5.51}$$

$$\times G_{ab}^{(\mathrm{res})} \left(z; \alpha_s(\mu_R^2), \frac{M_\Phi^2}{\mu_R^2}; \frac{M_\Phi^2}{\mu_F^2}; \frac{M_\Phi^2}{M_t^2} \right) \tag{5.52}$$

where the resummed cross section $G_{ab}^{(\mathrm{res})}(z)$ is the Mellin inverted form of the corresponding partonic cross section in Mellin space

$$G_{ab}^{(\mathrm{res})} \left(z; \alpha_s(\mu_R^2) \right., \left. \frac{M_\Phi^2}{\mu_R^2}; \frac{M_\Phi^2}{\mu_F^2}; \frac{M_\Phi^2}{M_t^2} \right) = \frac{1}{2\pi i} \int_{C_{\mathrm{MP}}} \mathrm{d}N z^{-N} \tilde{G}_{ab}^{(\mathrm{res})} \left(N; \alpha_s(\mu_R^2), \frac{M_\Phi^2}{\mu_R^2}; \frac{M_\Phi^2}{\mu_F^2}; \frac{M_\Phi^2}{M_t^2} \right). \tag{5.53}$$

We notice the different integration limits of the variable z in Eqs. (5.52) and (4.24). The upper limit $z = \infty$ in Eq. (5.52) instead of $z = 1$ corresponds the fact that within the Minimal Prescrition formula the partonic cross section in Mellin space is not vanishing for values of $z > 1$ due to the presence of the Landau pole. However, we observed that the partonic cross section decreases rapidly for $z > 1$. Mainly due to the plus distributions the integrand in Eq. (5.52) is strongly oscillating for large N. These oscillation can be damped by the introduction of modified parton luminosities. The trick of the method proposed in Ref. [127] is to multiply the total hadronic cross section by $1 = (N-1)^{2k}/(N-1)^{2k}$, $k = 1, 2, 3, \ldots$. This leads to the following form of Eq. (5.33)

$$\sigma(s, M_\Phi^2) = \sigma^{(0)} \sum_{a,b} \int_{C_{MP}-i\infty}^{C_{MP}+i\infty} \frac{dN}{2\pi i} \left(\frac{M_\Phi^2}{s} \right)^{-N+1}$$

$$\times \left[(N-1)^k \tilde{f}_{a/h_1}(N, \mu_F^2) \right] \left[(N-1)^k \tilde{f}_{b/h_2}(N, \mu_F^2) \right]$$

$$\times \tilde{G}_{ab}^{(\mathrm{res})} \left(N; \alpha_s(\mu_R^2), \frac{M_\Phi^2}{\mu_R^2}; \frac{M_\Phi^2}{\mu_F^2}; \frac{M_\Phi^2}{M_t^2} \right) / (N-1)^{2k} \,, \tag{5.54}$$

Now we introduce the modified parton luminosities $f_{a/h_1}^{(k)}$ as the Mellin inversion of $(N-1)^k f_{a/h_1}(N, \mu_F^2)$ defined by

$$f_{a/h_i}^{(k)}(x, \mu_F^2) = \frac{1}{2\pi i} \int_{\mathrm{C_{MP}}} \mathrm{d}N x^{-N} (N-1)^k \tilde{f}_{a/h_i}(N, \mu_F^2) \quad i = 1, 2 \tag{5.55}$$

We identify the modified luminosities as derivatives acting on the the x-space PDF's. For $k = 1$ we can rewrite Eq. (5.55) by integration by parts

$$\begin{aligned}(N-1) f_{a/h_i}(N,\mu_F^2) &= \int_0^1 \mathrm{d}x (N-1) x^{N-1} f_{a/h_i}(x,\mu_F^2) \\ &= \int_0^1 \mathrm{d}x\; x f_{a/h_i}(x,\mu_F^2) \frac{\mathrm{d}}{\mathrm{d}x} x^{N-1} \\ &= \int_0^1 \mathrm{d}x\; x^{N-1} \left[-\frac{\mathrm{d}}{\mathrm{d}x} x f_{a/h_i}(x,\mu_F^2) \right] \end{aligned} \tag{5.56}$$

and exploiting the fact that the parton densities vanish for $x = 1$. The general form due to the large N-damping can be derived as

$$f_{a/h_i}^{(k)}(x,\mu_F^2) = -\frac{\mathrm{d}}{\mathrm{d}x}\left[x f_{a/h_i}^{(k-1)}(x,\mu_F^2) \right] \tag{5.57}$$

$$f_{a/h_i}^{(0)}(x,\mu_F^2) = f_{a/h_i}(x,\mu_F^2) \tag{5.58}$$

We observed that it is possible to implement the derivatives of the parton densities up to order $k = 2$. Beyond that we are not able to obtain numerically stable results for the modified luminosities beginning with $k = 3$. As we can infer from Eq. (5.54) the oscillation of the partonic cross section for large N are suppressed by a factor $1/(N-1)^{2k}$. The Mellin inversion of Eq. (5.52) then reads

$$\begin{aligned}\sigma(s,M_\Phi^2) = \sigma^{(0)} \tau_H \sum_{a,b} \int_{\tau_H}^\infty \frac{\mathrm{d}z}{z} \int_{\tau_H/z}^1 \frac{\mathrm{d}x}{x} f_{a/h_1}^{(k)}(x,\mu_F^2) f_{b/h_2}^{(k)}(\frac{\tau_H}{xz},\mu_F^2) \\ \times \tilde{G}_{ab}^{(k)(\mathrm{res})}\left(z; \alpha_s(\mu_R^2), \frac{M_\Phi^2}{\mu_R^2}; \frac{M_\Phi^2}{\mu_F^2}; \frac{M_\Phi^2}{M_t^2} \right) \end{aligned} \tag{5.59}$$

where

$$\begin{aligned}&\tilde{G}_{ab}^{(k)(\mathrm{res})}\left(z; \alpha_s(\mu_R^2), \frac{M_\Phi^2}{\mu_R^2}; \frac{M_\Phi^2}{\mu_F^2}; \frac{M_\Phi^2}{M_t^2} \right) \\ &= \frac{1}{2\pi i} \int_{C_{\mathrm{MP}}} \mathrm{d}N z^{-N} \tilde{G}_{ab}^{(\mathrm{res})}\left(N; \alpha_s(\mu_R^2), \frac{M_\Phi^2}{\mu_R^2}; \frac{M_\Phi^2}{\mu_F^2}; \frac{M_\Phi^2}{M_t^2} \right) / (N-1)^{2k}. \end{aligned} \tag{5.60}$$

As was noticed in Ref. [127], the introduction of higher-order derivatives turns out to be necessary in gluon initiated processes. We observed as well that in the inclusive gluon fusion process only the second derivative on the parton densities leads to stable results for the z-integration between τ_H and 1. Furthermore, the integration between $1 < z < \infty$ is negligible.

4.3 Matching

The resummed result in Eq. (5.31) can be matched to the fixed order expression in Eq. (4.24) as follows:

$$
\begin{aligned}
\sigma^{(\text{res})}(s, M_\Phi^2) =& \sigma_{tt}^{(0)\Phi} \int_{C_{MP}-i\infty}^{C_{MP}+i\infty} \frac{dN}{2\pi i} \left(\frac{M_\Phi^2}{s}\right)^{-N+1} \tilde{f}_{g/h_1}(N, \mu_F^2)\, \tilde{f}_{g/h_2}(N, \mu_F^2) \\
&\times \Bigg\{ \tilde{G}^{(\text{res})}_{gg\Phi,\,(\text{N})\text{NNLL}} \left(N; \alpha_s(\mu_R^2), \frac{M_\Phi^2}{\mu_F^2}; \frac{M_\Phi^2}{\mu_F^2}; 0\right) \\
&- \left[\tilde{G}^{(\text{res})}_{gg\Phi,\,(\text{N})\text{NNLL}} \left(N; \alpha_s(\mu_R^2), \frac{M_\Phi^2}{\mu_F^2}; \frac{M_\Phi^2}{\mu_F^2}; 0\right)\right]_{(\text{f.o.})} \Bigg\} \\
&+ \sigma_{tt}^{(0)\Phi} \int_{C_{MP}-i\infty}^{C_{MP}+i\infty} \frac{dN}{2\pi i} \left(\frac{M_\Phi^2}{s}\right)^{-N+1} \tilde{f}_{g/h_1}(N, \mu_F^2)\, \tilde{f}_{g/h_2}(N, \mu_F^2) \\
&\times \Bigg\{ \tilde{G}^{(\text{res})}_{gg\Phi,\,\text{NLL}} \left(N; \alpha_s(\mu_R^2), \frac{M_\Phi^2}{\mu_F^2}; \frac{M_\Phi^2}{\mu_F^2}; \frac{M_\Phi^2}{M_t^2}\right) \\
&- \left[\tilde{G}^{(\text{res})}_{gg\Phi,\,\text{NLL}} \left(N; \alpha_s(\mu_R^2), \frac{M_\Phi^2}{\mu_F^2}; \frac{M_\Phi^2}{\mu_F^2}; \frac{M_\Phi^2}{M_t^2}\right)\right]_{(\text{NLO})} \Bigg\} \\
&- \sigma_{tt}^{(0)\Phi} \int_{C_{MP}-i\infty}^{C_{MP}+i\infty} \frac{dN}{2\pi i} \left(\frac{M_\Phi^2}{s}\right)^{-N+1} \tilde{f}_{g/h_1}(N, \mu_F^2)\, \tilde{f}_{g/h_2}(N, \mu_F^2) \\
&\times \Bigg\{ \tilde{G}^{(\text{res})}_{gg\Phi,\,\text{NLL}} \left(N; \alpha_s(\mu_R^2), \frac{M_\Phi^2}{\mu_F^2}; \frac{M_\Phi^2}{\mu_F^2}; 0\right) \\
&- \left[\tilde{G}^{(\text{res})}_{gg\Phi,\,\text{NLL}} \left(N; \alpha_s(\mu_R^2), \frac{M_\Phi^2}{\mu_F^2}; \frac{M_\Phi^2}{\mu_F^2}; 0\right)\right]_{(\text{NLO})} \Bigg\} \\
&+ \sigma^{\text{NNLO}}_{t+b+c}(s, M_\Phi^2, M_t^2) \quad , \qquad (5.61)
\end{aligned}
$$

where $\sigma_{tt}^{(0)\Phi}$ denotes the LO Born factor $\sigma^{(0)\Phi}$ of Eq. (4.5) including only the top quark contributions. The index (N)NNLL shall indicate that the soft collinear gluon resummation for a scalar Higgs can be performed at NNNLL whereas for a pseudoscalar Higgs the resummation procedure can only be applied at NNLL. Moreover, in Eq. (5.61) we also use the index (f.o.) for the soft collinear contributions of $\tilde{G}^{(\text{res})}_{gg\Phi}$ at fixed order as in Eqs. (E.11), (E.12) and (E.13). By evaluating the first integral in Eq. (5.61) we convolve the integrand with (N)NNLO α_s (see appendix B) and NNLO parton densities due to the non-necessity of N^{3}LO PDF's [128], while the second and third integrand has to evaluated with NLO α_s and NLO PDF's consistently. Finally we add the fixed order result at NNLO as it is implemented in HIGLU [92] as

$$
\sigma^{\text{NNLO}}_{t+b+(c)}(s, M_\Phi^2) = \sigma^{\text{NNLO}}_{\infty}(s, M_\Phi^2) + \sigma^{\text{NLO}}_{t+b+c}(s, M_\Phi^2) - \sigma^{\text{NNLO}}_{\infty}(s, M_\Phi^2) \qquad (5.62)
$$

with the individual fixed-order contributions denoted by

$$\sigma_{\infty}^{\mathrm{NNLO}}(s, M_{\Phi}^2) = \sigma_{tt}^{(0)\Phi} K_{\infty}^{\Phi,\mathrm{NNLO}} \tag{5.63}$$

$$\sigma_{\infty}^{\mathrm{NLO}}(s, M_{\Phi}^2) = \sigma_{tt}^{(0)\Phi} K_{\infty}^{\Phi,\mathrm{NLO}} \tag{5.64}$$

$$\sigma_{t+b+(c)}^{\mathrm{NLO}}(s, M_{\Phi}^2) = \sigma_{t+b+(c)}^{(0)\Phi} K_{t+b+(c)}^{\Phi,\mathrm{NLO}}. \tag{5.65}$$

where the $K_{\infty}^{\Phi\mathrm{NLO}}$-factor is defined in Eq. (4.26) and analogously the $K_{\infty}^{\Phi\mathrm{NNLO}}$ represents the ratio of the NNLO cross section over the LO one in the limit of a heavy top quark

$$K_{\infty}^{\Phi,\mathrm{NNLO}} = \left. \frac{\sigma^{\Phi}(s, M_{\Phi}^2)^{\mathrm{NNLO}}}{\sigma^{\Phi}(s, M_{\Phi}^2)^{\mathrm{LO}}} \right|_{m_t \to \infty, m_b = 0, m_c = 0} \tag{5.66}$$

The full massive NLO cross section $\sigma_{t+b+(c)}^{\mathrm{NLO}}$ can be obtained from Eqs. (4.24), respectively the NLO coefficients from Eqs. (4.4), (4.15), (4.16), (4.17) and (4.18) while the full massive $K_{t+b+(c)}^{\Phi,\mathrm{NLO}}$-factor is defined in Eq. (4.25). We evaluate the NNLO part with NNLO α_s and PDF's and the NLO part with NLO α_s and PDF's consistently in HIGLU. With the matching been set up we are able to present numerical results for a scalar and pseudoscalar Higgs.

5 Numerical results

For our analysis we performed the Mellin inversion in Eq. (5.36) and Eq. (5.52) with the integration routine VEGAS [125]. The off-set parameter has been chosen as $C = 2.5$. In case of the parton derivative method we have set the angle ϕ as $3\pi/4$ for the z-integration from τ_H to 1, respectively as $\pi/4$ for the z-integration from 1 to ∞. For the Mellin inversion in Eq. (5.36) we used parton densities from QCD-PEGASUS and fixed the angle ϕ as $3\pi/4$. In both events we performed checks for a variation of C within the interval $C_f < C < N_L$ and for a variation of the angle ϕ and obtained a numerical independence of our results.

For the calculation of the total hadronic cross section we set the heavy quark masses to $M_t = 172.5$ GeV, $M_b = 4.75$ GeV and $M_c = 1.40$ GeV consistently with the MSTW08 set. All predictions of observables have been made for a center-of-mass energy $\sqrt{s} = 14$ TeV and in the case of a pseudoscalar Higgs we have chosen the value of $\tan\beta$ as 3. Throughout our analysis we used the MSTW08 parton densities for the convolution with the partonic cross section. The total hadronic cross section is obtained by the matched result in Eq. (5.61) where we also added NLO electroweak contributions in the complete factorization scheme as in Eq. (4.31).

5.1 Comparison between the derivative method and QCD PEGASUS

We start with the comparison of the PDF's in x-space between the publicly available MSTW08 densities and the ones we obtained for the same input parameters with QCD-PEGASUS.

For small Bjorken-x we find an agreement of all parton densities within 0.1%. In the large x-region we observed a discrepancy between MSTW08- and QCD-PEGASUS-PDF's, in particular for the gluon densities, that is related to an inconsistency of the PDF-evolution up to higher scales. In Fig. 5.2 the ratio of the NNLO parton densities of QCD-PEGASUS and MSTW08 is depicted for a factorization scale $\mu_F = 800$ GeV.

The MSTW08 group has provided us with a corrected version of the parton distribution functions which we denote as MSTW08*. With this improved version we observe a larger deviation of 2% for small values of x in case of the gluon distribution functions, contrary to the former MSTW08 densities. However, for large Bjorken-x we find a better agreement within 6%, see Fig. 5.3.

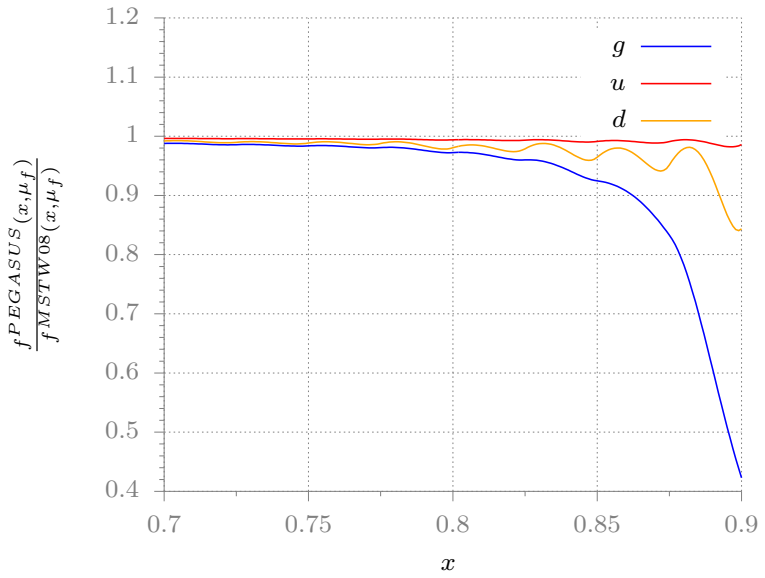

Figure 5.2: Ratio of the NNLO QCD-PEGASUS and MSTW08 parton distribution functions of the valence up and down quarks and the gluon for a renormalization scale $\mu_F = 800$ GeV

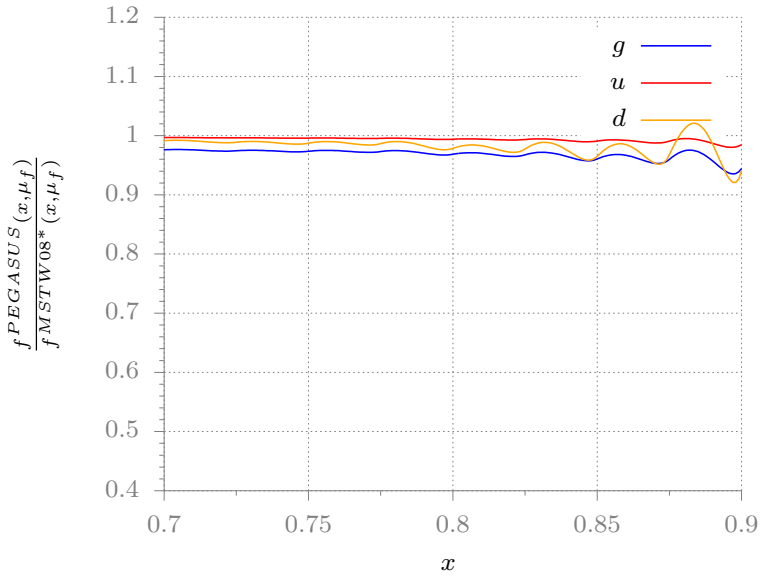

Figure 5.3: Ratio of the NNLO QCD-PEGASUS and MSTW08* parton distribution functions of the valence up and down quarks and the gluon for a renormalization scale $\mu_F = 800$ GeV

5.2 Collinear and mass effects

As mentioned in the previous chapter the inclusion of collinear logarithms turns out to be numerically relevant as we will demonstrate in the following. In Fig. 5.4 the total hadronic cross section at NLO is depicted. The red line represents the full massive result obtained by HIGLU. The soft-virtual approximation in Mellin space, the dashed blue line, only agrees with the fixed order result within 5%. With the formal replacement (5.22) the soft+virtual+collinear approximation is in good agreement with the NLO result within 0.1%. Furthermore, we observed that the incorporation of subleading collinear effects in Eq. (5.22) leads to a slight increase of the total hadronic cross section at the per-mille level. The embeddding of top quark mass effects into the resummation formula results in a decrease at the per-mille level.

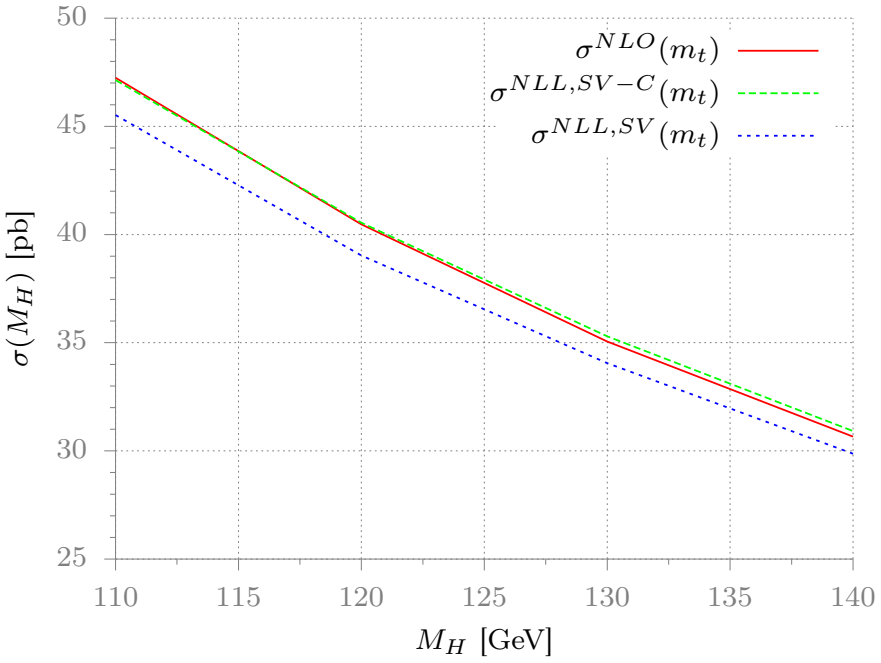

Figure 5.4: Comparison of the total hadronic cross section of the gluon fusion process at NLO between the full massive result and the SV and SVC approximations

5.3 Scale dependence

In this subsection we present the phenomenological results of the total hadronic cross section for a scalar SM Higgs and a pseudoscalar MSSM Higgs. We first study

the scale dependence by varying the factorization and renormalization scale around the value M_Φ.

In Fig. 5.5 (Fig. 5.6) we present the scale variation of the factorization (renormalization scale) $\mu_F = \chi_F M_H$ ($\mu_R = \chi_R M_H$) by fixing the other scale at the default value $M_H = 125$ GeV. Merely due to the scaling behavior of the strong coupling α_s the total hadronic cross section decreases for larger values of the renormalization scale μ_R. The opposite behavior for the factorization scale μ_F is observed due to sensitivity of the cross section to the partons at small Bjorken-x. The simultaneous variation of both scales, $\mu_R = \mu_F$, leads to compensation of both behaviors (see Fig. 5.7). With respect to NNLO we obtain a slight reduction of the renormalization scale dependence due to our extension to N^{3}LL accuracy. The variation w.r.t. the factorization scale is marginally stronger after including the resummation effects. Referring to Figs. 5.8, 5.9 and 5.10 the scale variation in the pseudoscalar case for a Higgs mass of $M_A = 400$ GeV shows the analogous behavior as for a scalar Higgs.

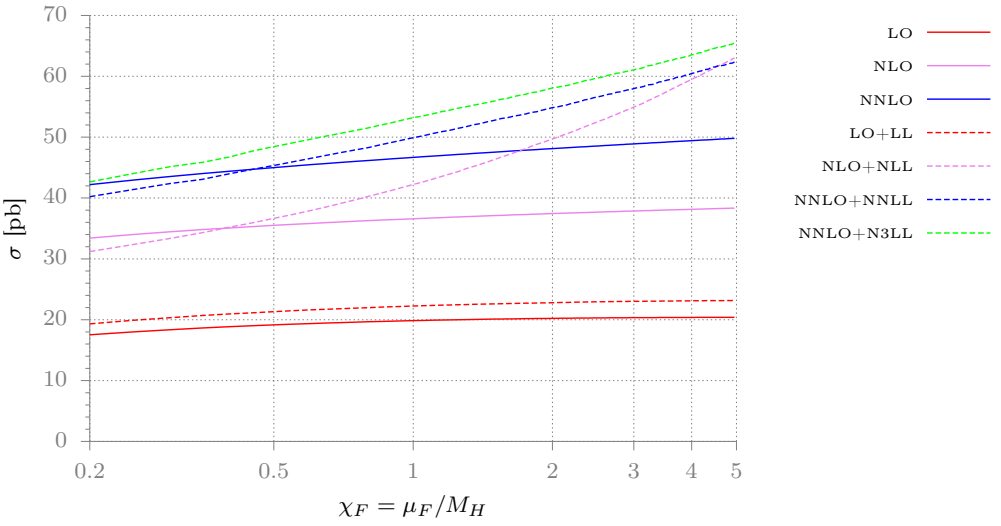

Figure 5.5: Factorization scale dependence of the total hadronic SM cross section via gluon fusion for $M_H = 125$ GeV, $\mu_R = M_H$.

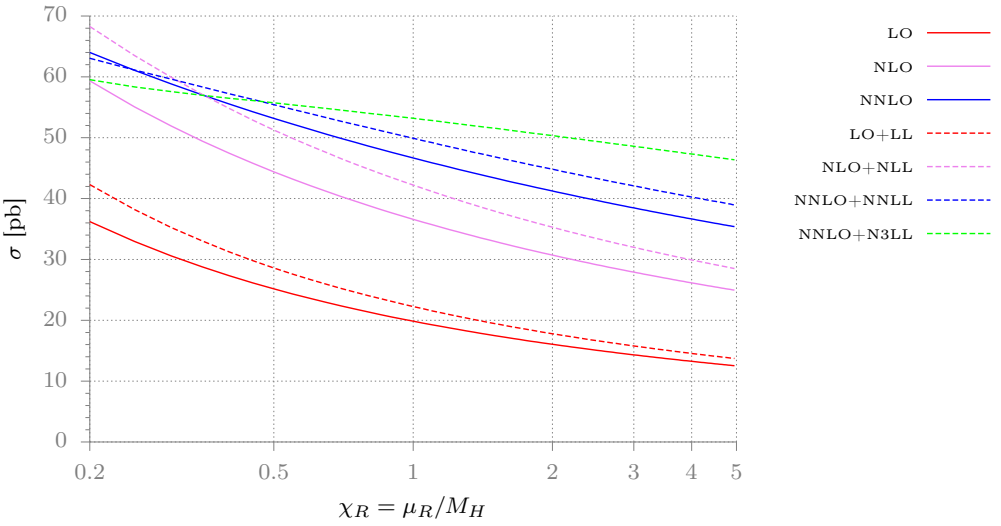

Figure 5.6: Renormalization scale dependence of the total hadronic SM cross section via gluon fusion for $M_H = 125$ GeV, $\mu_F = M_H$.

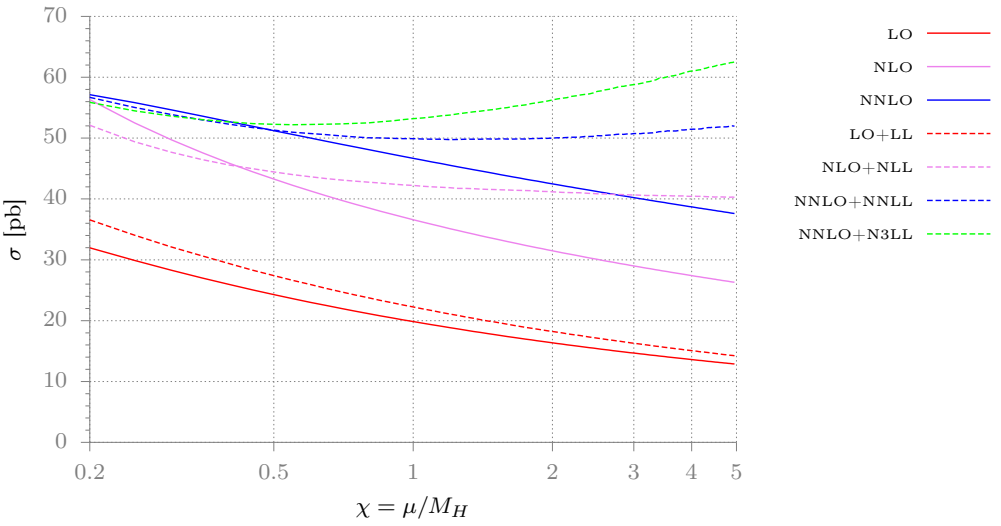

Figure 5.7: Scale dependence of the total hadronic SM cross section via gluon fusion for $M_H = 125$ GeV, $\mu = \mu_F = \mu_R$.

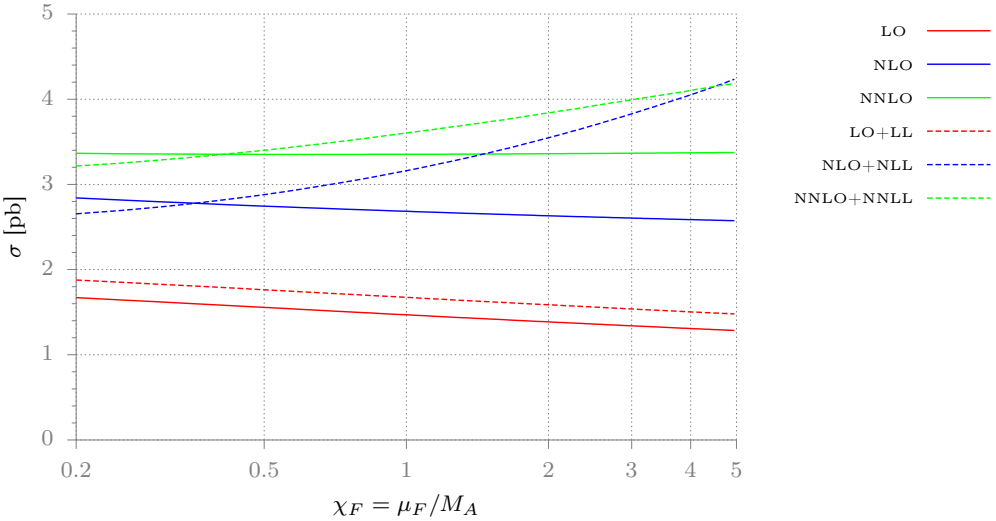

Figure 5.8: Factorization scale dependence of the total hadronic pseudoscalar cross section for $M_A = 400$ GeV, $\mu_F = M_A$ and $\tan\beta = 3$.

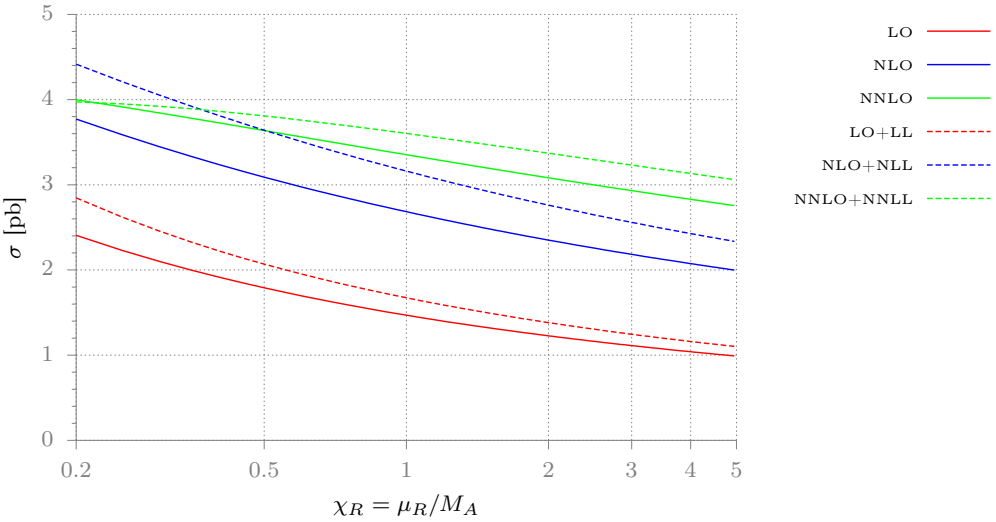

Figure 5.9: Renormalization scale dependence of the total hadronic pseudoscalar cross section for $M_A = 400$ GeV, $\mu_R = M_A$ and $\tan\beta = 3$.

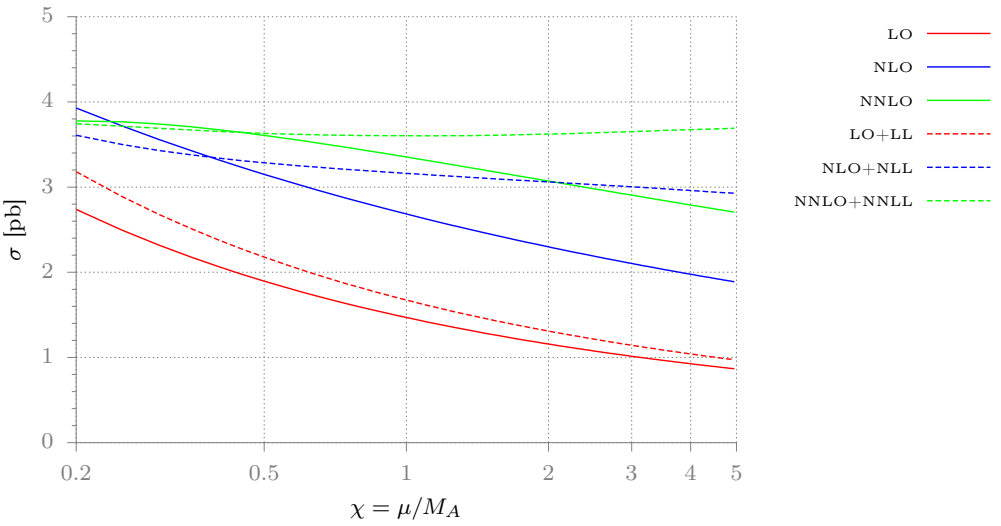

Figure 5.10: Scale dependence of the total hadronic pseudoscalar cross section for $M_A = 400$ GeV, $\mu = \mu_F = \mu_R$

5.4 Total hadronic cross section for scalar and pseudoscalar Higgs

In Fig. 5.11 (Fig.5.12) we present the total hadronic cross section for a scalar Higgs at fixed values $\mu_R = \mu_F = M_H$ ($\mu_R = \mu_F = M_H/2$). With respect to NNLO the inclusion of N^{3}LL resummation effects results in an increase of the cross section by an amount of $\mathcal{O}(10\%)$ for a renormalization and factorization scale equal to the Higgs mass of 125 GeV. Neglecting electroweak contributions we find an agreement with the exact N^{3}LO result [99] within $\mathcal{O}(4\%)$. For $\mu_R = \mu_F = M_H/2$ the Higgs cross section increases only by an amount of $\mathcal{O}(2\%)$ with respect to NNLO. We notice an agreement with Ref. [99] within $\mathcal{O}(0.3\%)$ for this corresponding scale choice. In Tab. 1 we compare the total hadronic cross section at N^{3}LL accuracy obtained by using MSTW08, MSTW08* and QCD-PEGASUS PDF's where we varied the scales μ_R and μ_F in the range $0.5M_H \leq \mu_R, \mu_F \leq 2M_H$, with the constraint $0.5 \leq \mu_R/\mu_F \leq 2M_H$. We notice a discrepancy for large Higgs masses between the MSTW08-densities and QCD-PEGASUS due to the mentioned reasons in Sec. 5.1 Although using the same set of input parameters we obtain a sizeable difference of the total hadronic cross section between the corrected version MSTW08* and QCD-Pegasus for Higgs mass of $M_H = 800$ GeV.

In an analogous way we performed a comparison of the NNLO with the NNLL renormalization group improved result for a pseudoscalar Higgs with $M_A = 400$ GeV. For $\mu_R = \mu_F = M_A$ the resummed cross section further increases with respect to NNLO by $\mathcal{O}(5-10\%)$. For a scale choice $\mu_R = \mu_F = M_A/2$ the increase amounts to less than $\mathcal{O}(1\%)$. As mentioned in Sec. 1 the pseudoscalar cross section is singular near the $t\bar{t}$-threshold due to the presence of a Coulomb-singularity.

M_H	$\sigma^H(s, M_H^2)_{\text{MSTW08}}$ [pb]	$\sigma^H(s, M_H^2)_{\text{MSTW08}^*}$ [pb]	$\sigma^H(s, M_H^2)_{\text{PEGASUS}}$ [pb]
125 GeV	$52.9594^{+5.75\%}_{-1.34\%}$	$53.2922^{+6.01\%}_{-1.36\%}$	$53.1792^{+4.80\%}_{-1.47\%}$
800 GeV	$0.581164^{+5.20\%}_{-3.59\%}$	$0.582321^{+5.26\%}_{-3.54\%}$	$0.560591^{+3.60\%}_{-1.95\%}$

Table 1: Comparison of the total hadronic cross section for a SM Higgs boson using MSTW08, MSTW08* and QCD-PEGASUS PDF's.

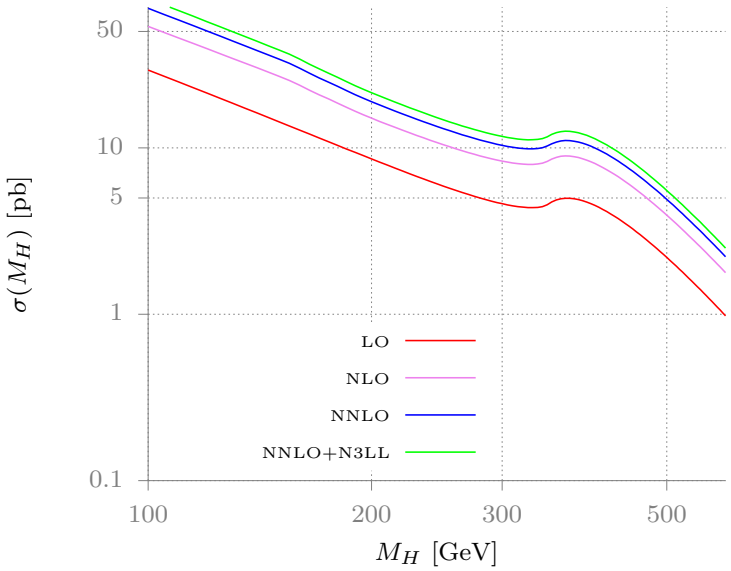

Figure 5.11: Comparison of the LO, NLO, NNLO and N^{3}LL cross section for a SM Higgs boson ($\mu_R = \mu_F = M_H$) using MSTW08* parton densities.

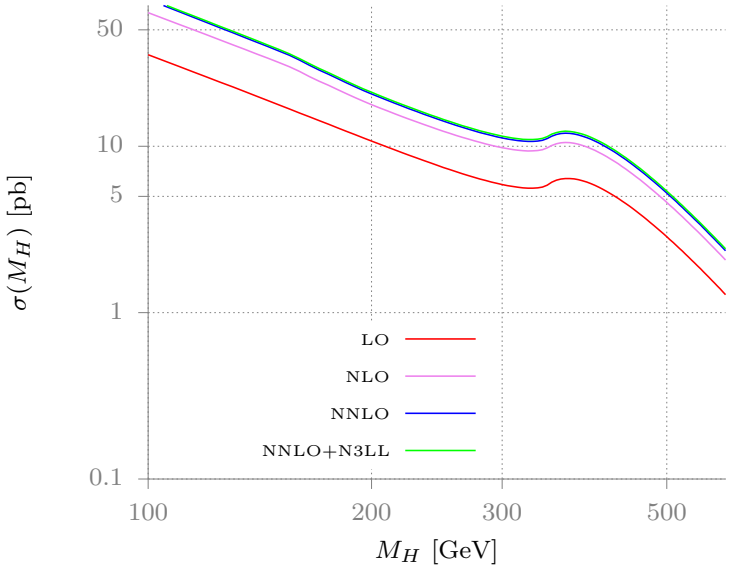

Figure 5.12: Comparison of the LO, NLO, NNLO and N^{3}LL cross section for a SM Higgs boson ($\mu_R = \mu_F = M_H/2$) using MSTW08* parton densities.

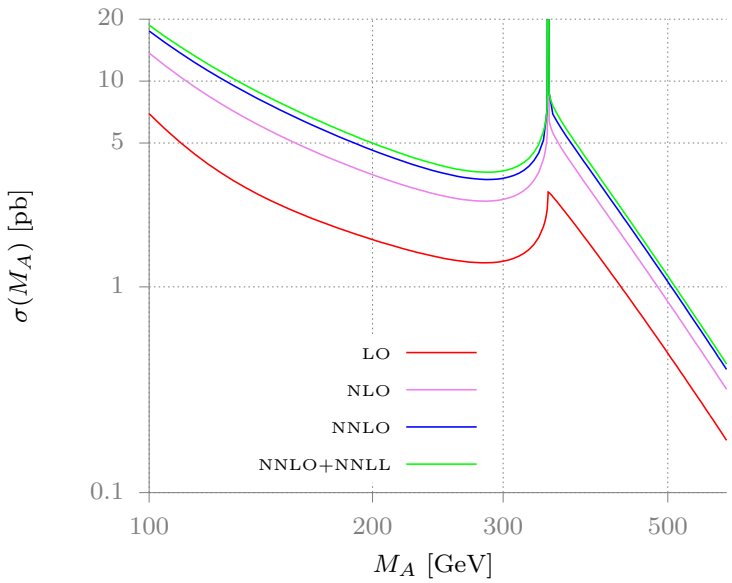

Figure 5.13: Comparison of the LO, NLO, NNLO and NNLL cross section for a pseudoscalar Higgs ($\mu_R = \mu_F = M_A$, $\tan\beta = 3$) using MSTW08* parton densities.

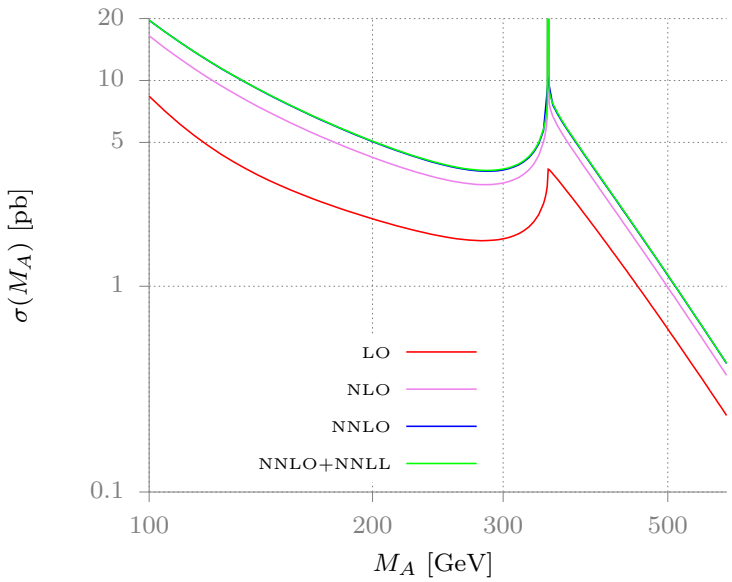

Figure 5.14: Comparison of the LO, NLO, NNLO and NNLL cross section for a pseudoscalar Higgs ($\mu_R = \mu_F = M_A/2$, $\tan\beta = 3$) using MSTW08* parton densities.

Chapter 6

Conclusions and Outlook

After the discovery of the Higgs boson the Large Hadron Collider has now passed a new milestone in collider physics by having reached a center-of-mass energy of 13 TeV. The detailed analysis of the scalar Higgs properties has now to be performed in order to find deviations of its coupling to SM fermions. We started this thesis by giving a brief overview about the production and the decay channels for a scalar and pseudoscalar Higgs. Fixed-order QCD calculations are needed to obtain precise theoretical predictions to the observable Higgs cross sections. Among these the gluon fusion process is the dominant production mechanism that also provides an excellent source to extract the Yukawa couplings to the heaviest quarks. We showed that, within the theoretical framework of QCD, information about residual higher-orders can be obtained due to the resummation of large contributions of the partonic cross section. The sources of the latter have to be carefully isolated by means of factorization theorems. We discussed two possible methods in conventional QCD which enabled us to apply the soft gluon resummation to the gluon fusion process. In this thesis we extended the methods to the highest known accuracy by including soft gluon resummation effects up to $\mathrm{N^3LL}$ level. A careful numerical analysis in this thesis showed the necessity of the inclusion of collinear logarithms. In this context we provided an alternative approach to the imbedding of subleading collinear sources. Top quark mass effects, an essential component of this thesis, have been included consistenly into the resummation procedure. Apart from theoretical developments in our work the detailed numerical analysis has been content to this thesis to large extent. In particular, we have set up a computer program which carries out the numerical Mellin inversion of the partonic cross section. The treatment of parton distribution functions showed that, although using the same set of input parameters, the evolution up to higher scales differs significantly in particular regions of the momentum fraction of the partons. Nevetheless we provided three different results for the SM Higgs boson production via gluon fusion. We were able to show

that for a renormalization and factoriation scale equal to the half of the Higgs mass our resummed N^{3}LL result agrees with the full N^{3}LO prediction within $\mathcal{O}(0.3\%)$. However, other scale choices only lead to an agreement of $\mathcal{O}(4\%)$. Furthermore we repeated the same analysis for a pseudoscalar Higgs. We have found an analytical difference between our NNLO resummed cross section and the publicly available results in literature which affects the pseudoscalar Higgs cross section for scale choice unequal the Higgs mass. Top quark mass effects have been incorporated into the resummation for the first time which enables us to present the most precise theoretical prediction. However, the sizeable PDF uncertainties have to be analysed carefully as well cross-checks of our result with the results published in literature have to be performed. The remaining uncertainties due to bottom quark mass effects in the resummation formula has to be studied and analysed in order to consistently derive predictions for the scalar and pseudoscalar Higgs cross sections.

Appendix A

QCD Beta-function and DGLAP-splitting kernels

The QCD β-function has been calculated up to one- [129, 130, 131], two-[132, 133, 134], three- [135, 134] and four-loop [136, 137] level. By using the conventional expansion of the 4-dimensional β-function

$$\frac{\partial a_s}{\partial \ln \mu^2} = \beta(a_s) = -\beta_0 a_s^2 - \beta_1 a_s^3 - \beta_2 a_s^4 - \beta_3 a_s^5 + \mathcal{O}(a_s^6) \tag{A.1}$$

in which $a_s = \alpha_s/(4\pi)$ the results are

$$\begin{aligned}
\beta_0 &= \frac{11}{3}C_A - \frac{4}{3}T_F n_f.\\
\beta_1 &= \frac{34}{3}C_A^2 - \frac{20}{3}C_A T_F n_f - 4C_F T_F n_f,\\
\beta_2 &= \frac{2857}{54}C_A^3 - \frac{1415}{27}C_A^2 T_F n_f + \frac{158}{27}C_A T_F^2 n_f^2 + \frac{44}{9}C_F T_F^2 n_f^2\\
&\quad - \frac{205}{9}C_F C_A T_F n_f + 2C_F^2 T_F n_f,\\
\beta_3 &= C_A C_F T_F^2 n_f^2 \left(\frac{17152}{243} + \frac{448}{9}\zeta_3\right)\\
&\quad + C_A C_F^2 T_F n_f \left(-\frac{4204}{27} + \frac{352}{9}\zeta_3\right)\\
&\quad + \frac{424}{243}C_A T_F^3 n_f^3 + C_A^2 C_F T_F n_f \left(\frac{7073}{243} - \frac{656}{9}\zeta_3\right)\\
&\quad + C_A^2 T_F^2 n_f^2 \left(\frac{7930}{81} + \frac{224}{9}\zeta_3\right) + \frac{1232}{243}C_F T_F^3 n_f^3
\end{aligned}$$

$$
\begin{aligned}
&+ C_A^3 T_F n_f \left(-\frac{39143}{81} + \frac{136}{3}\zeta_3\right) + C_A^4 \left(\frac{150653}{486} - \frac{44}{9}\zeta_3\right) \\
&+ C_F^2 T_F^2 n_f^2 \left(\frac{1352}{27} - \frac{704}{9}\zeta_3\right) \\
&+ 46 C_F^3 T_F n_f + n_f \frac{N(N^2+6)}{48} \left(\frac{512}{9} - \frac{1664}{3}\zeta_3\right) \\
&+ n_f^2 \frac{N^4 - 6N^2 + 18}{96N^2} \left(-\frac{704}{9} + \frac{512}{3}\zeta_3\right) \\
&+ \frac{N^2(N^2+36)}{24} \left(-\frac{80}{9} + \frac{704}{3}\zeta_3\right). \qquad \text{(A.2)}
\end{aligned}
$$

Along this thesis we also use the convention where all the factors $1/(4\pi)$ are absorbed into the coefficients of the β-function. The relation simply is

$$
b_i = \frac{1}{(4\pi)^{i+1}} \beta_i. \qquad \text{(A.3)}
$$

The one-loop Altarell–Parisi splitting functions read [62]

$$
P_{qq}(x) = C_F \left(\frac{1+x^2}{(1-x)_+} + \frac{3}{2}\delta(1-x)\right) \qquad \text{(A.4)}
$$

$$
P_{qg}(x) = C_F \left(\frac{1+(1-x)^2}{x}\right) \qquad \text{(A.5)}
$$

$$
P_{gq}(x) = T_R \left(x^2 + (1-x)^2\right) \qquad \text{(A.6)}
$$

$$
P_{gg}(x) = 2C_A \left(\frac{x}{(1-x)_+} + (1-x)(x+\frac{1}{x})\right) + \frac{11C_A - 4N_F T_R}{6}\delta(1-x) \qquad \text{(A.7)}
$$

Appendix B

Iterative solution of the strong coupling

Although the framework of perturbative QCD allows one to predict the variation of the running coupling with the unphysical renormalization scale μ_R the absolute value itself has to be determined by fitting the one parameter family of solutions to data at a reference scale, e.g. M_Z. The common appraoch is then to solve the RGE of α_s either numerically or analytically in order to deduce the values of the strong coupling at any large scale. However, for many purposes one introduces a dimensionful parameter Λ which also depends on the renormalization scheme used. This parameter represents the scale where the coupling gets strong at around 200 MeV. It has the advantage of providing a functional form for $\alpha_s(\mu_R^2)$ in case of solving the RGE iteratively [138]. Starting from

$$t = \int_{\alpha_s(\Lambda)}^{\alpha_s(\mu)} \frac{\mathrm{d}\alpha_s}{\beta(\alpha_s)}, \quad t = \ln\left(\frac{\mu}{\Lambda}\right), \tag{B.1}$$

expanding the β-function to sufficiently high orders in α_s and performing the integration the reference scale can be written as

$$\Lambda = \mu \exp\left[-\frac{2}{b_0\alpha_s(\mu)} + \frac{b_1}{b_0^2}\ln\left(\frac{1}{b_0\alpha_s(\mu)}\right) - \frac{b_2 b_0 - b_1^2}{b_0^3}\alpha_s(\mu) + C\right] \tag{B.2}$$

where C is an arbitrary integration constant. In the following we may choose $C = 0$ thus independent on the active flavors N_f which leads to the following expression

$$\frac{1}{\alpha_s(\mu)} = b_0 t + \Delta_1, \quad \Delta_1 = \frac{b_1}{2b_0}\ln\left(\frac{1}{\alpha_s(\mu)}\right) + \frac{b_2 b_0 - b_1^2}{4b_0^2}\alpha(\mu) + \mathcal{O}(\alpha_s^2) \tag{B.3}$$

The above formula can now be iteratively solved by inserting the solution for $\alpha_s(\mu)$ into Δ_1 giving the approximate analytically solution

$$\alpha_s(\mu) = \frac{1}{b_0 t}\left(1 - \frac{b_1}{b_0^2}\frac{\ln t}{t} + \frac{b_1^2(\ln^2 t - \ln t - 1) + b_0 b_2}{b_0^4 t^2} - \frac{b_1^3(\ln^3 t - \frac{5}{2}\ln^2 t - 2\ln t + \frac{1}{2}) + 3b_0 b_1 b_2 \ln t - \frac{1}{2}b_0^2 b_3}{b_0^6 t^3}\right) \tag{B.4}$$

Usually working groups on parton densities quote the strong coupling at respective order at the scale of the Z-mass. The corresponding Λ can be determined by eliminating α_s in Eq. (B.4) due to a redefinition like

$$\begin{aligned} b_0 =& \frac{1}{\alpha(\mu)A(\alpha(\mu))}, \quad b_1 = \frac{B(\alpha(\mu))}{\alpha^2(\mu)A(\alpha(\mu))} \quad , b_2 = \frac{C(\alpha(\mu))}{\alpha^3(\mu)A^2(\alpha(\mu))}, \\ b_3 =& \frac{D(\alpha(\mu))}{\alpha^4(\mu)A^3(\alpha(\mu))} \end{aligned} \tag{B.5}$$

leading to

$$t = \frac{A}{2}\left(1 + \sqrt{1 - 4B\Delta_2 \ln(t)}\right) \tag{B.6}$$

where

$$\Delta_2 = 1 + \frac{AB(\ln^2 t - \ln t - 1) + \frac{C}{B}}{t\ln(t)} - \frac{A^2B^2(\ln^3 t - \frac{5}{2}\ln^2 t - 2\ln t + \frac{1}{2}) + 3AC\ln t - \frac{D}{2B}}{t^2 \ln t} \tag{B.7}$$

Inserting Eq. (B.6) into (B.7) and solving the equation numerically up to a desired accuracy provides a fast and efficient method to convert M_Z into the appropriate Λ. At the end we want to mention that in general the coefficients of the β-function depend on the the flavor N_f of the quarks which are lighter than the renormalization scale μ_R. New flavor thresholds $\mu_R = m_{q_i}$ have to be treated as step functions in the beta coefficients, thus α_s is dis-continuous. In our case this is not necessary since we only work in the 5-flavor scheme.

Appendix C

Scale dependence

In Section 1.4 we noticed the appearance of scale-dependent logarithms after expanding the partonic cross section in ϵ and after carefully renormalizing the bare quantities as the strong coupling α_s and the parton densities f_i. However, the Laurent series for the total partonic cross section in [98] is given at the scale $\mu_R = \mu_F = m_h$ for which all scale-dependent logarithms of that kind vanish. In order to re-install the scale dependence we can exploit the renormalization group equations for the strong coupling and the parton densities as in Sec. 1 The scale translation of α_s from the initial scale μ_0 to μ_1 can be derived by solving

$$\frac{\partial \alpha_s(\mu^2)}{\partial \ln(\mu^2)} = \beta\left[\alpha_s(\mu^2)\right] \alpha_s(\mu^2) \tag{C.1}$$

where

$$\beta\left[\alpha_s(\mu^2)\right] = -\sum_{n=0} \beta_n \alpha^{n+1}(\mu^2) \tag{C.2}$$

is the QCD β-function with coefficients β_i taken from Sec. A and hence with solution

$$\alpha_s(\mu_1^2) = \alpha_s(\mu_0^2) + \int_{\ln(\mu_0^2)}^{\ln(\mu_1^2)} \mathrm{d}\ln(\mu^2)\beta[\alpha_s(\mu^2)]\alpha_s(\mu^2) \tag{C.3}$$

The trick to obtain logarithmic terms of the two different scales is to iteratively replace the solution by itself on the r.h.s. up to the desired order in α_s. This rather lengthy calculation leads to

$$\begin{aligned}\alpha_s(\mu_1^2) = \alpha_s(\mu_0^2) \\ - \beta_0 L \alpha_s^2(\mu_0^2) \\ - (\beta_1 L - \beta_0^2 L^2)\alpha_s^3(\mu_0^2)\end{aligned}$$

$$- (\beta_2 L - \frac{5}{2}\beta_0\beta_1 L^2 + \beta_0^3 L^3)\alpha_s^4(\mu_0^2) + \mathcal{O}(\alpha_s^5) \tag{C.4}$$

where $L = \ln\left(\frac{\mu_1^2}{\mu_0^2}\right)$. In a similar way the scale dependece of the parton densities can be restored by solving the DGLAP-equations

$$\frac{\partial f_i(\mu^2)}{\partial \ln(\mu^2)} = P_{ij}(\mu^2) \otimes f_j(\mu^2) \tag{C.5}$$

with the expansion of the splitting kernels as follows

$$P_{ij}(\mu^2) = \sum_{n=0} P_{ij}^{(n)} \alpha_s^{n+1}(\mu^2) \tag{C.6}$$

The solution

$$f_i(\mu_1^2) = f_i(\mu_0^2) + \int_{\ln(\mu_0^2)}^{\ln(\mu_1^2)} \mathrm{d}\ln(\mu^2) \left(P_{ij}(\mu^2) \otimes f_j(\mu^2)\right) \tag{C.7}$$

again can be replaced by itself on the r.h.s.. Repeatedly performing these steps gives the following expression for the scale translation of the parton densities

$$\begin{aligned}
f_i(\mu_1^2) = {} & f_i(\mu_0^2) \\
& + \alpha_s(\mu_0^2) L P_{ij}^{(0)} \otimes f_j(\mu_0^2) \\
& + \alpha_s^2(\mu_0^2) \left[L \left(P_{ij}^{(1)} \otimes f_j(\mu_0^2) \right) + \frac{1}{2} L^2 \left(P_{ik}^{(0)} \otimes P_{ij}^{(0)} - \beta_0 P_{ij}^{(0)} \right) \otimes f_j(\mu_0^2) \right] \\
& + \alpha_s^3(\mu_0^2) \left\{ L \left(P_{ij}^{(2)} \otimes f_j(\mu_0^2) \right) + \frac{1}{2} L^2 \left[\left(P_{ik}^{(0)} \otimes P_{kj}^{(1)} + P_{ik}^{(1)} \otimes P_{kj}^{(0)} \right) \otimes f_j(\mu_0^2) \right. \right. \\
& - 2\beta_0 \left(P_{ij}^{(1)} \otimes f_j(\mu_0^2) \right) - \beta_1 \left(P_{ij}^{(0)} \otimes f_j(\mu_0^2) \right) \Big] \\
& + \frac{1}{6} L^3 \left[P_{il}^{(0)} \otimes P_{kl}^{(0)} \otimes P_{lj}^{(0)} \otimes f_j(\mu_0^2) \right. \\
& \left. \left. - 3\beta_0 P_{ik}^{(0)} \otimes P_{kj}^{(0)} \otimes f_J(\mu_0^2) + 2\beta_0^2 P_{ij}^{(0)} \otimes f_j(\mu_o^2) \right] \right\} \\
& + \mathcal{O}(\alpha_s^4(\mu_0^2))
\end{aligned} \tag{C.8}$$

In Principle one could now start with expression in Ref. [97] exploiting equations (C.4) and (C.8) in order to restore the scale dependence. However, we are only interested in the large-x limit of the partonic cross section. Thus, it is convenient to work in Mellin space. The equivalent to the singlet splitting functions $P_{ij}^{(n)}$ in N-space are the singlet anomalous dimensions

$$\gamma_{ab}(N, \alpha_s) = -\int_0^1 \mathrm{d}x x^{N-1} P_{ab}(x, \alpha_s) \tag{C.9}$$

where the minus sign is the standard convention. The large-x behavior of the diagonal splitting functions [139] was found to behave as

$$\gamma_{aa}^{(n-1)} = A_n^a(\ln N + \gamma_e) - B_n^a - C_n^a \frac{\ln N}{N} + \mathcal{O}\left(\frac{1}{N}\right) \tag{C.10}$$

whereas the off-diagonal n-loop anomalous dimensions vanish like $\frac{1}{N}\ln^{2n-2} N$. The leading large-N gluon coefficients A_n^g are related to the quark coefficients A_n^q by

$$A_n^g = \frac{C_A}{C_F} A_n^q. \tag{C.11}$$

while the latter can be read off easily from Eq. (3.11) of Ref. [140]

$$\begin{aligned}
A_1^q &= 4\,C_F \\
A_2^q &= 8\,C_F\left[\left(\frac{67}{18} - \zeta_2\right)C_A - \frac{5}{9}\,N_f\right] \\
A_3^q &= 16\,C_F C_A^2\left(\frac{245}{24} - \frac{67}{9}\,\zeta_2 + \frac{11}{6}\,\zeta_3 + \frac{11}{5}\,\zeta_2^2\right) + 16\,C_F^2 N_f\left(-\frac{55}{24} + 2\,\zeta_3\right) \\
&\quad + 16\,C_F C_A N_f\left(-\frac{209}{108} + \frac{10}{9}\,\zeta_2 - \frac{7}{3}\,\zeta_3\right) + 16\,C_F N_f^2\left(-\frac{1}{27}\right) .
\end{aligned} \tag{C.12}$$

whereas the N-independent contributions B_n^g need to be extracted from the coefficients in front of the $\delta(1-x)$ terms in Eqs.(4.6), (4.10) and (4.15) of Refs. [141].

$$\begin{aligned}
B_1^g &= \frac{11C_A}{3} - \frac{2N_f}{3} \\
B_2^g &= 4C_A^2\left(3\zeta_3 + \frac{8}{3}\right) - \frac{8C_A N_f}{3} - 2C_F N_f \\
B_3^g &= 16C_A^3\left(\frac{11\zeta_2^2}{24} - \zeta_2\zeta_3 + \frac{\zeta_2}{6} + \frac{67\zeta_3}{6} - 5\zeta_5 + \frac{79}{32}\right) \\
&\quad - 16C_A^2 N_f\left(\frac{\zeta_2^2}{12} + \frac{\zeta_2}{6} + \frac{5\zeta_3}{3} + \frac{233}{288}\right) - \frac{241C_A C_F N_f}{18} \\
&\quad + \frac{29C_A N_f^2}{18} + C_F^2 N_f + \frac{11C_F N_f^2}{9}
\end{aligned}$$

One has to notice that due to the different expansion of the $n+1$-loop splitting function in Refs. [140],[141], namely

$$\mathcal{P}_{ab}(\alpha_s, x) = \sum_{n=0}\left(\frac{\alpha_s}{4\pi}\right)^{n+1}\mathcal{P}_{ab}^{(n)}(x) \tag{C.13}$$

the relation to our convention for the gluon splitting function is

$$P_{gg}^{(n)}(x) = \frac{1}{4^{n+1}} \mathcal{P}_{gg}^{(n)}(x) \tag{C.14}$$

This leads to a simplification of Eq. (C.8) for the gluon density since we are only interested in the gg-channel. From Eq. (5.1)

$$\sigma_{N-1}(m_h^2) = \sigma^{(0)} \left[f_{g/h_1}(N, m_h^2) \right] \left[f_{g/h_2}(N, m_h^2) \right] G_{gg,N}(\alpha_s(m_h^2), 1, 1) \tag{C.15}$$

the re-installation of the scale dependence can be attained by first replacing $f_{g/h_i}(N, m_h^2)$ by Eq. (C.8) in Mellin space and utilizing Eq. (C.4) to evolve α_s from the scales μ_f and m_h to the renormalization scale μ_R.

Appendix D

Mellin integrals

We define the Mellin moments of the plus distributions $\mathcal{D}_i$ as

$$I_n(N) = \int_0^1 \mathrm{d}z\, z^{N-1}\mathcal{D}_n(z) = \int_0^1 \mathrm{d}z \frac{z^{N-1}-1}{1-z} \ln^n(1-z). \tag{D.1}$$

The N-moments can be computed by using the following identity [108]

$$I_n(N) = \lim_{\epsilon\to 0}\left(\frac{\partial}{\partial\epsilon}\right)^n \left\{\frac{1}{\epsilon}\left[e^{-\epsilon\ln N}\Gamma(1+\epsilon)-1\right]\right\} + \mathcal{O}\left(\frac{1}{N}\right) \quad . \tag{D.2}$$

where we used the expression

$$\Gamma(1+\epsilon) = \exp\left\{-\gamma_E\,\epsilon + \sum_{n=2}^{+\infty}(-1)^n\frac{\zeta_2}{n}\,\epsilon^n\right\} \quad . \tag{D.3}$$

which can easily be expanded in a power series in ϵ. Here we give the solutions to Eq. (D.1) which are needed to compute the Mellin moments of the soft+virtual contributions

$$I_0(N) = -\ln N - \gamma_E + \mathcal{O}(1/N) \tag{D.4}$$

$$I_1(N) = \frac{\ln^2 N}{2} + \gamma_E \ln N + \frac{\zeta_2}{2} + \frac{\gamma_E^2}{2} + \mathcal{O}(1/N) \tag{D.5}$$

$$\begin{aligned} I_2(N) = {} & -\zeta_2 \ln N - \frac{1}{3}\ln^3 N - \gamma_E \ln^2 N - \gamma_E^2 \ln N \\ & -\gamma_E\zeta_2 - \frac{2\zeta_3}{3} - \frac{\gamma_E^3}{3} + \mathcal{O}(1/N) \end{aligned} \tag{D.6}$$

$$I_3(N) = \frac{3}{2}\zeta_2 \ln^2 N + 3\gamma_E\zeta_2 \ln N + 2\zeta_3 \ln N + \frac{\ln^4 N}{4}$$

$$
\begin{aligned}
& + \gamma_E \ln^3 N + \frac{3}{2}\gamma_E^2 \ln^2 N + \gamma_E^3 \ln N + \frac{3\zeta_2^2}{4} \\
& + \frac{3\gamma_E^2\zeta_2}{2} + 2\gamma_E\zeta_3 + \frac{3\zeta_4}{2} + \frac{\gamma_E^4}{4} + \mathcal{O}(1/N) \qquad \text{(D.7)} \\
I_4(N) \;=\; & -3\zeta_2^2 \ln N - 2\zeta_2 \ln^3 N - 6\gamma_E\zeta_2 \ln^2 N - 6\gamma_E^2\zeta_2 \ln N \\
& - 4\zeta_3 \ln^2 N - 8\gamma_E\zeta_3 \ln N - 6\zeta_4 \ln N - \frac{1}{5}\ln^5 N \\
& - \gamma_E \ln^4 N - 2\gamma_E^2 \ln^3 N - 2\gamma_E^3 \ln^2 N \\
& - \gamma_E^4 \ln N - 3\gamma_E\zeta_2^2 - 4\zeta_2\zeta_3 - 2\gamma_E^3\zeta_2 \\
& - 4\gamma_E^2\zeta_3 - 6\gamma_E\zeta_4 - \frac{24\zeta_5}{5} - \frac{\gamma_E^5}{5} + \mathcal{O}(1/N) \qquad \text{(D.8)} \\
I_5(N) \;=\; & \frac{15}{2}\zeta_2^2 \ln^2 N + 15\gamma_E\zeta_2^2 \ln N + 20\zeta_2\zeta_3 \ln N \\
& + \frac{5}{2}\zeta_2 \ln^4 N + 10\gamma_E\zeta_2 \ln^3 N + 15\gamma_E^2\zeta_2 \ln^2 N \\
& + 10\gamma_E^3\zeta_2 \ln N + \frac{20}{3}\zeta_3 \ln^3 N + 20\gamma_E\zeta_3 \ln^2 N \\
& + 20\gamma_E^2\zeta_3 \ln N + 15\zeta_4 \ln^2 N + 30\gamma_E\zeta_4 \ln N + 24\zeta_5 \ln N \\
& + \frac{\ln^6 N}{6} + \gamma_E \ln^5 N + \frac{5}{2}\gamma_E^2 \ln^4 N + \frac{10}{3}\gamma_E^3 \ln^3 N \\
& + \frac{5}{2}\gamma_E^4 \ln^2 N + \gamma_E^5 \ln N + \frac{5\zeta_2^3}{2} + \frac{15\gamma_E^2\zeta_2^2}{2} \\
& + 20\gamma_E\zeta_2\zeta_3 + 15\zeta_2\zeta_4 + \frac{5\gamma_E^4\zeta_2}{2} + \frac{20\zeta_3^2}{3} \\
& + \frac{20\gamma_E^3\zeta_3}{3} + 15\gamma_E^2\zeta_4 + 24\gamma_E\zeta_5 + 20\zeta_6 + \frac{\gamma_E^6}{6} + \mathcal{O}(1/N). \qquad \text{(D.9)}
\end{aligned}
$$

Appendix E

Resummation formulae

The functions $A^{(i)}$ can be inferred from [76, 142, 143, 144]

$$A^{(1)} = C_A \tag{E.1}$$

$$A^{(2)} = \frac{1}{2} C_A^2 \left(\frac{67}{18} - \frac{\pi^2}{6} \right) \tag{E.2}$$

$$\begin{aligned} A^{(3)} =& C_A \left[C_A^2 \left(\frac{11\zeta_2^2}{20} - \frac{67\zeta_2}{36} + \frac{11\zeta_3}{24} + \frac{245}{96} \right) \right. \\ & \left. - \frac{1}{2} N_F \left(C_A \left(\frac{7\zeta_3}{6} - \frac{5\pi^2}{54} + \frac{209}{216} \right) + C_F \left(\frac{55}{48} - \zeta_3 \right) \right) - \frac{N_F^2}{108} \right] \end{aligned} \tag{E.3}$$

The function $A^{(4)}$ yet has only been estimated numerically [145]

$$A^{(4)} = \frac{13977}{1024} \tag{E.4}$$

The NNLL coefficient $D^{(2)}$ has been evaluated in Refs. [95, 96] while the coefficient $D^{(3)}$ has been calculated in Ref. [109]:

$$D^{(2)} = C_A \left[C_A \left(-\frac{101}{27} + \frac{11}{3}\zeta_2 + \frac{7}{2}\zeta_3 \right) + N_F \left(\frac{14}{27} - \frac{2}{3}\zeta_2 \right) \right] \tag{E.5}$$

$$\begin{aligned} D^{(3)} =& \frac{1}{64} \left[C_A^3 \left(-\frac{2992\zeta_2^2}{15} - \frac{352\zeta_2\zeta_3}{3} \right. \right. \\ & \left. + \frac{98224\zeta_2}{81} + \frac{40144\zeta_3}{27} - 384\zeta_5 - \frac{594058}{729} \right) \\ & + C_A^2 N_F \left(\frac{736\zeta_2^2}{15} - \frac{29392\zeta_2}{81} - \frac{2480\zeta_3}{9} + \frac{125252}{729} \right) \\ & \left. + C_A C_F N_F \left(-\frac{64\zeta_2^2}{5} - 32\zeta_2 - \frac{608\zeta_3}{9} + \frac{3422}{27} \right) \right. \end{aligned}$$

$$+C_A N_F^2 \left(\frac{640\zeta_2}{27} + \frac{320\zeta_3}{27} - \frac{3712}{729}\right)\Bigg] \tag{E.6}$$

$$\begin{aligned} g_h^{(1)} &= g_h^{(1)}(\lambda) \\ &= \frac{A^{(1)}}{\pi b_0 \lambda}\left[2\lambda + (1-2\lambda)\ln(1-2\lambda)\right], \end{aligned} \tag{E.7}$$

$$\begin{aligned} g_h^{(2)} &= g_h^{(2)}(\lambda, m_h^2/\mu_R^2; m_h^2/\mu_F^2) \\ &= -\frac{A^{(2)}}{\pi^2 b_0^2}\left[2\lambda + \ln(1-2\lambda)\right] - \frac{2A^{(1)}\gamma_E}{\pi b_0}\ln(1-2\lambda) \\ &+ \frac{A^{(1)} b_1}{\pi b_0^3}\left[2\lambda + \ln(1-2\lambda) + \frac{1}{2}\ln^2(1-2\lambda)\right] \\ &+ \frac{A^{(1)}}{\pi b_0}\left[2\lambda + \ln(1-2\lambda)\right]\ln\frac{m_h^2}{\mu_R^2} - \frac{2A^{(1)}}{\pi b_0}\lambda\ln\left(\frac{m_h^2}{\mu_F^2}\right), \end{aligned} \tag{E.8}$$

$$\begin{aligned} g_h^{(3)} &= g_h^{(3)}(\lambda, m_h^2/\mu_R^2; m_h^2/\mu_F^2) \\ &= +\frac{4A^{(1)}}{\pi}(\zeta_2 + \gamma_E^2)\frac{\lambda}{1-2\lambda} - \frac{2A^{(1)}\gamma_E b_1}{\pi b_0^2(1-2\lambda)}\left[2\lambda + \ln(1-2\lambda)\right] \\ &+ \frac{A^{(1)} b_1^2}{\pi b_0^4(1-2\lambda)}\left[2\lambda^2 + 2\lambda\ln(1-2\lambda) + \frac{1}{2}\ln^2(1-2\lambda)\right] \\ &+ \frac{A^{(1)} b_2}{\pi b_0^3}\left[2\lambda + \ln(1-2\lambda) + \frac{2\lambda^2}{1-2\lambda}\right] \\ &+ \frac{2A^{(3)}}{\pi^3 b_0^2}\frac{\lambda^2}{1-2\lambda} - \frac{D^{(2)}}{\pi^2 b_0}\frac{\lambda}{1-2\lambda} + \frac{4\gamma_E A^{(2)}}{\pi^2 b_0}\frac{\lambda}{1-2\lambda} \\ &- \frac{A^{(2)} b_1}{\pi^2 b_0^3}\frac{1}{1-2\lambda}\left[2\lambda + \ln(1-2\lambda) + 2\lambda^2\right] - \frac{2A^{(2)}}{\pi^2 b_0}\lambda\ln\left(\frac{m_h^2}{\mu_F^2}\right) - \frac{A^{(1)}}{\pi}\lambda\ln^2\left(\frac{m_h^2}{\mu_F^2}\right) \\ &+ \frac{2A^{(1)}}{\pi}\lambda\ln\frac{m_h^2}{\mu_R^2}\ln\left(\frac{m_h^2}{\mu_F^2}\right) \\ &+ \frac{1}{1-2\lambda}\Big(\frac{A^{(1)} b_1}{\pi b_0^2}\left[2\lambda + \ln(1-2\lambda)\right] - \frac{4A^{(1)}\gamma_E}{\pi}\lambda - \frac{4A^{(2)}}{\pi^2 b_0}\lambda^2\Big)\ln\frac{m_h^2}{\mu_R^2} \\ &+ \frac{2A^{(1)}}{\pi}\frac{\lambda^2}{1-2\lambda}\ln^2\frac{m_h^2}{\mu_R^2}, \end{aligned} \tag{E.9}$$

$$g_h^{(4)} = g_h^{(4)}(\lambda, m_h^2/\mu_R^2; m_h^2/\mu_F^2)$$

$$
\begin{aligned}
&= -\frac{A^{(1)}\ln^3(1-2l)b_1^3}{6b_0^5(1-2l)^2\pi} - \frac{A^{(1)}\ln(1-2l)b_1^3}{b_0^5(1-2l)\pi} + \frac{A^{(1)}\ln(1-2l)b_1^3}{2b_0^5(1-2l)^2\pi} \\
&+ \frac{A^{(1)}\ln(1-2l)b_1^3}{2b_0^5\pi} + \frac{2A^{(1)}lb_1^3}{3b_0^5\pi} - \frac{A^{(1)}b_1^3}{b_0^5(1-2l)\pi} + \frac{A^{(1)}b_1^3}{3b_0^5(1-2l)^2\pi} + \frac{2A^{(1)}b_1^3}{3b_0^5\pi} \\
&+ \frac{A^{(1)}\gamma_E\ln^2(1-2l)b_1^2}{b_0^3(1-2l)^2\pi} + \frac{A^{(3)}\ln^2(1-2l)b_1^2}{2b_0^4(1-2l)^2\pi^2} + \frac{A^{(3)}\ln(1-2l)b_1^2}{2b_0^4(1-2l)^2\pi^2} \\
&+ \frac{2A^{(1)}\gamma_E b_1^2}{b_0^3(1-2l)\pi} - \frac{A^{(1)}\gamma_E b_1^2}{b_0^3(1-2l)^2\pi} - \frac{A^{(1)}\gamma_E b_1^2}{b_0^3\pi} - \frac{2A^{(3)}lb_1^2}{3b_0^4\pi^2} + \frac{A^{(3)}b_1^2}{b_0^4(1-2l)\pi^2} \\
&- \frac{A^{(3)}b_1^2}{12b_0^4(1-2l)^2\pi^2} - \frac{11A^{(3)}b_1^2}{12b_0^4\pi^2} - \frac{A^{(1)}\pi\ln(1-2l)b_1}{3b_0(1-2l)^2} - \frac{A^{(1)}b_2\ln(1-2l)b_1}{b_0^4\pi} \\
&+ \frac{A^{(1)}b_2\ln(1-2l)b_1}{b_0^4(1-2l)\pi} - \frac{A^{(1)}b_2\ln(1-2l)b_1}{2b_0^4(1-2l)^2\pi} - \frac{2A^{(1)}\gamma_E^2\ln(1-2l)b_1}{b_0(1-2l)^2\pi} \\
&+ \frac{D^{(2)}\ln(1-2l)b_1}{2b_0^2(1-2l)^2\pi^2} - \frac{2A^{(3)}\gamma_E\ln(1-2l)b_1}{b_0^2(1-2l)^2\pi^2} - \frac{A^{(3)}\ln(1-2l)b_1}{2b_0^3(1-2l)^2\pi^3} - \frac{7A^{(1)}b_2b_1}{12b_0^4\pi} \\
&- \frac{4A^{(1)}b_2lb_1}{3b_0^4\pi} + \frac{A^{(1)}b_2b_1}{b_0^4(1-2l)\pi} - \frac{5A^{(1)}b_2b_1}{12b_0^4(1-2l)^2\pi} - \frac{D^{(2)}b_1}{4b_0^2\pi^2} + \frac{D^{(2)}b_1}{4b_0^2(1-2l)^2\pi^2} \\
&- \frac{A^{(3)}\gamma_E b_1}{b_0^2(1-2l)^2\pi^2} + \frac{A^{(3)}\gamma_E b_1}{b_0^2\pi^2} + \frac{2A^{(3)}lb_1}{3b_0^3\pi^3} - \frac{5A^{(3)}b_1}{12b_0^3(1-2l)^2\pi^3} + \frac{5A^{(3)}b_1}{12b_0^3\pi^3} \\
&- \frac{2A^{(1)}b_0l\ln^3\left(\frac{m_h^2}{\mu_F^2}\right)}{3\pi} + \left(\frac{A^{(1)}b_0}{6\pi} + \frac{2A^{(1)}lb_0}{3\pi} - \frac{A^{(1)}b_0}{6(1-2l)^2\pi}\right)\ln^3\left(\frac{m_h^2}{\mu_R^2}\right) \\
&+ \left(-\frac{A^{(1)}b_1l}{b_0\pi} - \frac{2A^{(3)}l}{\pi^2}\right)\ln^2\left(\frac{m_h^2}{\mu_F^2}\right) + \left(-\frac{2lA^{(3)}}{\pi^2} + \frac{A^{(3)}}{2(1-2l)^2\pi^2}\right. \\
&\left.-\frac{A^{(3)}}{2\pi^2} - \frac{A^{(1)}b_1\ln(1-2l)}{2b_0(1-2l)^2\pi} - \frac{2A^{(1)}b_0l\ln\left(\frac{m_h^2}{\mu_F^2}\right)}{\pi} - \frac{A^{(1)}b_1l}{b_0\pi} + \frac{A^{(1)}b_0\gamma_E}{(1-2l)^2\pi}\right. \\
&\left.-\frac{A^{(1)}b_0\gamma_E}{\pi}\right)\ln^2\left(\frac{m_h^2}{\mu_R^2}\right) - \frac{A^{(3)}}{3} + \frac{A^{(1)}b_3\ln(1-2l)}{2b_0^3\pi} - \frac{2A^{(3)}l\ln\left(\frac{m_h^2}{\mu_F^2}\right)}{b_0\pi^3} \\
&+ \left(-\frac{A^{(1)}\ln^2(1-2l)b_1^2}{2b_0^3(1-2l)^2\pi} - \frac{A^{(1)}b_1^2}{b_0^3(1-2l)\pi} + \frac{A^{(1)}b_1^2}{2b_0^3(1-2l)^2\pi} + \frac{A^{(1)}b_1^2}{2b_0^3\pi}\right. \\
&\left.+\frac{2A^{(1)}\gamma_E\ln(1-2l)b_1}{b_0(1-2l)^2\pi} + \frac{A^{(3)}\ln(1-2l)b_1}{b_0^2(1-2l)^2\pi^2} - \frac{A^{(3)}b_1}{2b_0^2\pi^2} + \frac{A^{(3)}b_1}{2b_0^2(1-2l)^2\pi^2}\right. \\
&\left.+\frac{2A^{(1)}b_0l\ln^2\left(\frac{m_h^2}{\mu_F^2}\right)}{\pi} + \left(\frac{2A^{(1)}b_1l}{b_0\pi} + \frac{4A^{(3)}l}{\pi^2}\right)\ln\left(\frac{m_h^2}{\mu\mathrm{f}^2}\right) + \frac{A^{(1)}b_0\pi}{3}\right.
\end{aligned}
$$

$$
\begin{aligned}
&-\frac{A^{(1)}b_0\pi}{3(1-2l)^2}-\frac{A^{(1)}b_2}{2b_0^2\pi}+\frac{A^{(1)}b_2}{b_0^2(1-2l)\pi}-\frac{A^{(1)}b_2}{2b_0^2(1-2l)^2\pi}\\
&-\frac{2A^{(1)}b_0\gamma_E^2}{(1-2l)^2\pi}+\frac{2A^{(1)}b_0\gamma_E^2}{\pi}-\frac{D^{(2)}}{2\pi^2}+\frac{D^{(2)}}{2(1-2l)^2\pi^2}-\frac{2A^{(3)}\gamma_E}{(1-2l)^2\pi^2}+\frac{2A^{(3)}\gamma_E}{\pi^2}\\
&+\frac{2A^{(3)}l}{b_0\pi^3}+\frac{A^{(3)}}{2b_0\pi^3}-\frac{A^{(3)}}{2b_0(1-2l)^2\pi^3}\Bigg)\ln\left(\frac{m_h^2}{\mu_R^2}\right)+\frac{A^{(3)}}{3(1-2l)^2}-\frac{8A^{(1)}b_0\zeta(3)}{3\pi}\\
&+\frac{8A^{(1)}b_0\zeta(3)}{3(1-2l)^2\pi}+\frac{2A^{(1)}b_0\gamma_E\pi}{3(1-2l)^2}-\frac{2}{3}A^{(1)}b_0\gamma_E\pi-\frac{A^{(1)}b_3}{12b_0^3\pi}+\frac{2A^{(1)}b_3l}{3b_0^3\pi}-\frac{2A^{(1)}b_2\gamma_E}{b_0^2(1-2l)\pi}\\
&+\frac{A^{(1)}b_3}{12b_0^3(1-2l)^2\pi}+\frac{4A^{(1)}b_0\gamma_E^3}{3(1-2l)^2\pi}+\frac{A^{(1)}b_2\gamma_E}{b_0^2(1-2l)^2\pi}-\frac{4A^{(1)}b_0\gamma_E^3}{3\pi}+\frac{A^{(1)}b_2\gamma_E}{b_0^2\pi}\\
&+\frac{2A^{(3)}b_2}{3b_0^3\pi^2}+\frac{2A^{(3)}b_2l}{3b_0^3\pi^2}-\frac{A^{(3)}b_2}{b_0^3(1-2l)\pi^2}+\frac{A^{(3)}b_2}{3b_0^3(1-2l)^2\pi^2}+\frac{2A^{(3)}\gamma_E^2}{(1-2l)^2\pi^2}\\
&-\frac{D^{(2)}\gamma_E}{(1-2l)^2\pi^2}-\frac{2A^{(3)}\gamma_E^2}{\pi^2}+\frac{D^{(2)}\gamma_E}{\pi^2}+\frac{D^{(3)}}{4b_0\pi^3}-\frac{D^{(3)}}{4b_0(1-2l)^2\pi^3}+\frac{A^{(3)}\gamma_E}{b_0(1-2l)^2\pi^3}\\
&-\frac{A^{(3)}\gamma_E}{b_0\pi^3}-\frac{2A^{(4)}l}{3b_0^2\pi^4}-\frac{A^{(4)}}{6b_0^2\pi^4}+\frac{A^{(4)}}{6b_0^2(1-2l)^2\pi^4}
\end{aligned}
\tag{E.10}
$$

$$
\begin{aligned}
G_{ggH,N}^{(1)\,\mathrm{SV}-N}&=G_{ggH,N}^{(1)\,\mathrm{SV}-N}(m_h^2/\mu_R^2;m_h^2/\mu_F^2)\\
&=+2A^{(1)}\ln^2N+\ln N\left[4\gamma_EA^{(1)}-2A^{(1)}\ln\left(\frac{m_h^2}{\mu_F^2}\right)\right]+C_{gg}^{(1)},
\end{aligned}
\tag{E.11}
$$

$$
\begin{aligned}
G_{ggH,N}^{(2)\,\mathrm{SV}-N}&=G_{ggH,N}^{(2)\,\mathrm{SV}-N}(m_h^2/\mu_R^2;m_h^2/\mu_F^2)\\
&=+2\left(A^{(1)}\right)^2\ln^4N+\ln^3N\left[-4\left(A^{(1)}\right)^2\ln\left(\frac{m_h^2}{\mu_F^2}\right)+8\gamma_E\left(A^{(1)}\right)^2+\frac{4\pi A^{(1)}b_0}{3}\right]\\
&+\ln^2N\left[2\left(A^{(1)}\right)^2\ln^2\left(\frac{m_h^2}{\mu_F^2}\right)-8\gamma_E\left(A^{(1)}\right)^2\ln\left(\frac{m_h^2}{\mu_F^2}\right)+8\gamma_E^2\left(A^{(1)}\right)^2\right.\\
&\left.-2\pi A^{(1)}b_0\ln\left(\frac{m_h^2}{\mu_R^2}\right)+4\gamma_E\pi A^{(1)}b_0+2A^{(1)}C_{gg}^{(1)}+2A^{(2)}\right]\\
&+\ln N\left[2\pi A^{(1)}b_0\ln\left(\frac{m_h^2}{\mu_F^2}\right)\ln\left(\frac{m_h^2}{\mu_R^2}\right)-\pi(A^{(1)})b_0\ln^2\left(\frac{m_h^2}{\mu_F^2}\right)\right.\\
&-4\gamma_E\pi A^{(1)}b_0\ln\left(\frac{m_h^2}{\mu_R^2}\right)+4\pi A^{(1)}b_0\zeta_2+4\gamma_E^2\pi A^{(1)}b_0-2A^{(1)}C_{gg}^{(1)}\ln\left(\frac{m_h^2}{\mu_F^2}\right)\\
&\left.+4\gamma_EA^{(1)}C_{gg}^{(1)}-2A^{(2)}\ln\left(\frac{m_h^2}{\mu_F^2}\right)+4\gamma_EA^{(2)}-D^{(2)}\right]\\
&+C_{gg}^{(2)},
\end{aligned}
\tag{E.12}
$$

$$
\begin{aligned}
G_{ggH,N}^{(3)\,\mathrm{SV}-N} &= G_{ggH,N}^{(3)\,\mathrm{SV}-N}(m_h^2/\mu_R^2; m_h^2/\mu_F^2) \\
&= + \frac{4\left(A^{(1)}\right)^3}{3} \ln^6 N \\
&\quad + \ln^5 N \left[-4\left(A^{(1)}\right)^3 \ln\left(\frac{m_h^2}{\mu_F^2}\right) + 8\gamma_E \left(A^{(1)}\right)^3 + \frac{8}{3}\pi \left(A^{(1)}\right)^2 b_0 \right] \\
&\quad + \ln^4 N \left[4\left(A^{(1)}\right)^3 \ln^2\left(\frac{m_h^2}{\mu_F^2}\right) - 16\gamma_E \left(A^{(1)}\right)^3 \ln\left(\frac{m_h^2}{\mu \mathrm{f}^2}\right) \right. \\
&\quad + 16\gamma_E^2 \left(A^{(1)}\right)^3 - \frac{8}{3}\pi \left(A^{(1)}\right)^2 b_0 \ln\left(\frac{m_h^2}{\mu_F^2}\right) \\
&\quad - 4\pi \left(A^{(1)}\right)^2 b_0 \ln\left(\frac{m_h^2}{\mu_R^2}\right) + \frac{40}{3}\gamma_E \pi \left(A^{(1)}\right)^2 b_0 + 2\left(A^{(1)}\right)^2 C_{gg}^{(1)} \\
&\quad \left. + 4A^{(1)}A^{(2)} + \frac{4}{3}\pi^2 A^{(1)} b_0^2 \right] \\
&\quad + \ln^3 N \left[-\frac{4}{3}\left(A^{(1)}\right)^3 \ln^3\left(\frac{m_h^2}{\mu_F^2}\right) + 8\gamma_E \left(A^{(1)}\right)^3 \ln^2\left(\frac{m_h^2}{\mu_F^2}\right) \right. \\
&\quad - 16\gamma_E^2 \left(A^{(1)}\right)^3 \ln\left(\frac{m_h^2}{\mu_F^2}\right) + \frac{32\gamma_E^3 \left(A^{(1)}\right)^3}{3} \\
&\quad + 8\pi \left(A^{(1)}\right)^2 b_0 \ln\left(\frac{m_h^2}{\mu_F^2}\right) \ln\left(\frac{m_h^2}{\mu_R^2}\right) \\
&\quad - 2\pi \left(A^{(1)}\right)^2 b_0 \ln^2\left(\frac{m_h^2}{\mu_F^2}\right) - 8\gamma_E \pi \left(A^{(1)}\right)^2 b_0 \ln\left(\frac{m_h^2}{\mu_F^2}\right) \\
&\quad - 16\gamma_E \pi \left(A^{(1)}\right)^2 b_0 \ln\left(\frac{m_h^2}{\mu_R^2}\right) + 8\pi \left(A^{(1)}\right)^2 b_0 \zeta_2 + 24\gamma_E^2 \pi \left(A^{(1)}\right)^2 b_0 \\
&\quad - 4\left(A^{(1)}\right)^2 C_{gg}^{(1)} \ln\left(\frac{m_h^2}{\mu_F^2}\right) + 8\gamma_E \left(A^{(1)}\right)^2 C_{gg}^{(1)} - 8A^{(1)}A^{(2)} \ln\left(\frac{m_h^2}{\mu_F^2}\right) \\
&\quad + 16\gamma_E A^{(1)}A^{(2)} - \frac{8}{3}\pi^2 A^{(1)} b_0^2 \ln\left(\frac{m_h^2}{\mu_R^2}\right) + \frac{16}{3}\gamma_E \pi^2 A^{(1)} b_0^2 \\
&\quad \left. + \frac{4}{3}\pi A^{(1)} b_0 C_{gg}^{(1)} + \frac{4}{3}\pi^2 A^{(1)} b_1 - 2A^{(1)} D^{(2)} + \frac{8\pi A^{(2)} b_0}{3} \right] \\
&\quad + \ln^2 N \left[-4\pi \left(A^{(1)}\right)^2 b_0 \ln^2\left(\frac{m_h^2}{\mu_F^2}\right) \ln\left(\frac{m_h^2}{\mu \mathrm{r}^2}\right) \right. \\
&\quad \left. + 16\gamma_E \pi \left(A^{(1)}\right)^2 b_0 \ln\left(\frac{m_h^2}{\mu_F^2}\right) \ln\left(\frac{m_h^2}{\mu_R^2}\right) \right.
\end{aligned}
$$

$$
\begin{aligned}
&+ 2\pi \left(A^{(1)}\right)^2 b_0 \ln^3\left(\frac{m_h^2}{\mu_F^2}\right) - 4\gamma_E \pi \left(A^{(1)}\right)^2 b_0 \ln^2\left(\frac{m_h^2}{\mu_F^2}\right) \\
&- 8\gamma_E^2 \pi \left(A^{(1)}\right)^2 b_0 \ln\left(\frac{m_h^2}{\mu_F^2}\right) - 16\gamma_E^2 \pi \left(A^{(1)}\right)^2 b_0 \ln\left(\frac{m_h^2}{\mu_R^2}\right) \\
&- 8\pi \left(A^{(1)}\right)^2 b_0 \zeta_2 \ln\left(\frac{m_h^2}{\mu_F^2}\right) + 16\gamma_E \pi \left(A^{(1)}\right)^2 b_0 \zeta_2 + 16\gamma_E^3 \pi \left(A^{(1)}\right)^2 b_0 \\
&+ 2\left(A^{(1)}\right)^2 C_{gg}^{(1)} \ln^2\left(\frac{m_h^2}{\mu_F^2}\right) - 8\gamma_E \left(A^{(1)}\right)^2 C_{gg}^{(1)} \ln\left(\frac{m_h^2}{\mu_F^2}\right) \\
&+ 8\gamma_E^2 \left(A^{(1)}\right)^2 C_{gg}^{(1)} 4A^{(1)} A^{(2)} \ln^2\left(\frac{m_h^2}{\mu_F^2}\right) - 16\gamma_E A^{(1)} A^{(2)} \ln\left(\frac{m_h^2}{\mu_F^2}\right) \\
&+ 16\gamma_E^2 A^{(1)} A^{(2)} + 2\pi^2 A^{(1)} b_0^2 \ln^2\left(\frac{m_h^2}{\mu_R^2}\right) - 8\gamma_E \pi^2 A^{(1)} b_0^2 \ln\left(\frac{m_h^2}{\mu_R^2}\right) \\
&+ 8\pi^2 A^{(1)} b_0^2 \zeta_2 + 8\gamma_E^2 \pi^2 A^{(1)} b_0^2 - 2\pi A^{(1)} b_0 C_{gg}^{(1)} \ln\left(\frac{m_h^2}{\mu_R^2}\right) \\
&+ 4\gamma_E \pi A^{(1)} b_0 C_{gg}^{(1)} - 2\pi^2 A^{(1)} b_1 \ln\left(\frac{m_h^2}{\mu_R^2}\right) + 4\gamma_E \pi^2 A^{(1)} b_1 \\
&+ 2A^{(1)} C_{gg}^{(3)} + 2A^{(1)} D^{(2)} \ln\left(\frac{m_h^2}{\mu_F^2}\right) \\
&- 4\gamma_E A^{(1)} D^{(2)} - 4\pi A^{(2)} b_0 \ln\left(\frac{m_h^2}{\mu_R^2}\right) \\
&+ 8\gamma_E \pi A^{(2)} b_0 + 2A^{(2)} C_{gg}^{(1)} + 2A^{(3)} - 2\pi b_0 D^{(2)}\Big] \\
&+ \ln N \left[2\pi^2 A^{(1)} b_0^2 \ln^2\left(\frac{m_h^2}{\mu_F^2}\right) \ln\left(\frac{m_h^2}{\mu_R^2}\right)\right. \\
&- 2\pi^2 A^{(1)} b_0^2 \ln\left(\frac{m_h^2}{\mu_F^2}\right) \ln^2\left(\frac{m_h^2}{\mu_R^2}\right) \\
&- \frac{2}{3}\pi^2 A^{(1)} b_0^2 \ln^3\left(\frac{m_h^2}{\mu_F^2}\right) + 4\gamma_E \pi^2 A^{(1)} b_0^2 \ln^2\left(\frac{m_h^2}{\mu_R^2}\right) \\
&- \frac{4}{3}\pi^4 A^{(1)} b_0^2 \ln\left(\frac{m_h^2}{\mu_R^2}\right) - 8\gamma_E^2 \pi^2 A^{(1)} b_0^2 \ln\left(\frac{m_h^2}{\mu_R^2}\right) \\
&+ \frac{32}{3}\pi^2 A^{(1)} b_0^2 \zeta(3) + \frac{8}{3}\gamma_E \pi^4 A^{(1)} b_0^2 + \frac{16}{3}\gamma_E^3 \pi^2 A^{(1)} b_0^2 \\
&+ 2\pi A^{(1)} b_0 C_{gg}^{(1)} \ln\left(\frac{m_h^2}{\mu_F^2}\right) \ln\left(\frac{m_h^2}{\mu_R^2}\right) \\
&- \pi A^{(1)} b_0 C_{gg}^{(1)} \ln^2\left(\frac{m_h^2}{\mu_F^2}\right) - 4\gamma_E \pi A^{(1)} b_0 C_{gg}^{(1)} \ln\left(\frac{m_h^2}{\mu_R^2}\right) \\
&+ 4\pi A^{(1)} b_0 C_{gg}^{(1)} \zeta_2 + 4\gamma_E^2 \pi A^{(1)} b_0 C_{gg}^{(1)}
\end{aligned}
$$

$$
\begin{aligned}
&+ 2\pi^2 A^{(1)} b_1 \ln\left(\frac{m_h^2}{\mu_F^2}\right) \ln\left(\frac{m_h^2}{\mu_R^2}\right) \\
&- \pi^2 A^{(1)} b_1 \ln^2\left(\frac{m_h^2}{\mu_F^2}\right) \\
&- 4\gamma_E \pi^2 A^{(1)} b_1 \ln\left(\frac{m_h^2}{\mu_R^2}\right) + \frac{2}{3}\pi^4 A^{(1)} b_1 + 4\gamma_E^2 \pi^2 A^{(1)} b_1 \\
&- 2A^{(1)} C_{gg}^{(3)} \ln\left(\frac{m_h^2}{\mu_F^2}\right) + 4\gamma_E A^{(1)} C_{gg}^{(3)} + \pi A^{(2)} b_0 \ln\left(\frac{m_h^2}{\mu_F^2}\right) \ln\left(\frac{m_h^2}{\mu_R^2}\right) \\
&- 2\pi A^{(2)} b_0 \ln^2\left(\frac{m_h^2}{\mu_F^2}\right) - 8\gamma_E \pi A^{(2)} b_0 \ln\left(\frac{m_h^2}{\mu_R^2}\right) + \frac{4}{3}\pi^3 A^{(2)} b_0 + 8\gamma_E^2 \pi A^{(2)} b_0 \\
&- 2A^{(2)} C_{gg}^{(1)} \ln\left(\frac{m_h^2}{\mu_F^2}\right) + 4\gamma_E A^{(2)} C_{gg}^{(1)} - 2A^{(3)} \ln\left(\frac{m_h^2}{\mu_F^2}\right) \\
&+ 4\gamma_E A^{(3)} + 2\pi b_0 D^{(2)} \ln\left(\frac{m_h^2}{\mu_R^2}\right) \\
&- 4\gamma_E \pi b_0 D^{(2)} - C_{gg}^{(1)} D^{(2)} - D^{(3)}\big] \\
&+ C_{gg}^{(3)}
\end{aligned}
\tag{E.13}
$$

$$
\begin{aligned}
C_{ggH}^{(1)} &= C_{ggH}^{(1)}(m_h^2/\mu_R^2; m_h^2/\mu_F^2) \\
&= \delta G_{gg}^{(1)} + 6\gamma_E^2 + \pi^2 - 6\gamma_E \ln\left(\frac{m_h^2}{\mu_F^2}\right) \ ,
\end{aligned}
\tag{E.14}
$$

$$
\begin{aligned}
C_{ggH}^{(2)} &= C_{ggH}^{(1)}(m_h^2/\mu_R^2; m_h^2/\mu_F^2) \\
&= \delta G_{gg}^{(2)} + \gamma_E \left(\frac{101}{3} - \frac{14}{9} N_f - \frac{63}{2}\zeta_3\right) \\
&+ \gamma_E^2 \left(\frac{133}{2} - \frac{5N_f}{3} + \frac{21\,\pi^2}{2}\right) + \gamma_E^3 \left(11 - \frac{2N_f}{3}\right) + 18\gamma_E^4 \\
&+ \frac{133\,\pi^2}{12} - \frac{5\,N_f\,\pi^2}{18} + \frac{29\,\pi^4}{20} + 22\,\zeta_3 - \frac{4\,N_f\,\zeta_3}{3} \\
&+ \ln^2\left(\frac{m_h^2}{\mu_F^2}\right) \left(-\frac{165}{4}\gamma_E + 18\gamma_E^2 + \frac{5}{2} N_f \gamma_E + 3\pi^2\right) \\
&+ \frac{3}{2}\gamma_E (33 - 2N_f) \ln\left(\frac{m_h^2}{\mu_F^2}\right) \ln\left(\frac{m_h^2}{\mu_R^2}\right) - \frac{1}{4}(33 - 2N_f)(6\gamma_E^2 + \pi^2) \ln\left(\frac{m_h^2}{\mu_R^2}\right) \\
&+ \ln\left(\frac{m_h^2}{\mu_F^2}\right) \Bigg[-36\gamma_E^3 + (33 - 2N_f)\gamma_E^2 + \gamma_E \left(-\frac{133}{2} + \frac{5\,N_f}{3} - \frac{21\,\pi^2}{2}\right) \\
&+ \frac{11\,\pi^2}{2} - \frac{N_f\,\pi^2}{3} - 72\,\zeta(3)\Bigg] \ ,
\end{aligned}
\tag{E.15}
$$

where

$$\delta G^{(1)}_{ggH} = c_H(\tau_t^H) + 6\zeta_2 + \frac{33-2N_f}{6}\ln\frac{\mu_R^2}{\mu_F^2}\ , \tag{E.16}$$

$$\begin{aligned}\delta G^{(2)}_{ggH} = {} & \frac{11399}{144} + \frac{133}{2}\zeta_2 - \frac{9}{20}\zeta_2^2 - \frac{165}{4}\zeta_3 \\ & + \left(\frac{19}{8} + \frac{2}{3}N_f\right)\ln\frac{m_h^2}{M_t^2} + N_f\left(-\frac{1189}{144} - \frac{5}{3}\zeta_2 + \frac{5}{6}\zeta_3\right) \\ & + \frac{(33-2N_f)^2}{48}\ln^2\frac{\mu_F^2}{\mu_R^2} - 18\,\zeta_2\ln^2\left(\frac{m_h^2}{\mu_F^2}\right) \\ & + \left(\frac{169}{4} + \frac{171}{2}\zeta_3 - \frac{19}{6}N_f + (33-2N_f)\,\zeta_2\right)\ln\left(\frac{m_h^2}{\mu_F^2}\right) \\ & + \left(-\frac{465}{8} + \frac{13}{3}N_f - \frac{3}{2}\,(33-2N_f)\,\zeta_2\right)\ln\left(\frac{m_h^2}{\mu_R^2}\right)\ .\end{aligned} \tag{E.17}$$

$$\begin{aligned}C^{(3)}_{ggH} &= C^{(3)}_{ggH}(m_h^2/\mu_R^2; m_h^2/\mu_F^2) \\ &= \left(-\frac{N_f^3}{54} - \frac{13\gamma_E N_f^2}{18} + \frac{11N_f^2}{12} - 9\gamma_E^2 N_f + \frac{143\gamma_E N_f}{6} - \frac{121N_f}{8} - 36\gamma_E^3 + \frac{297\gamma_E^2}{2}\right. \\ &\quad \left. - \frac{1573\gamma_E}{8} + \frac{1331}{16}\right)\ln^3\left(\frac{m_h^2}{\mu_F^2}\right) + \left(\frac{\pi^2 N_f^2}{6} + \frac{\gamma_E^2 N_f^2}{2} - \frac{5\gamma_E N_f^2}{6} + \frac{181N_f^2}{144} - \frac{27\zeta(3)N_f}{4}\right. \\ &\quad + \frac{17}{4}\gamma_E\pi^2 N_f - \frac{11\pi^2 N_f}{2} + 15\gamma_E^3 N_f - \frac{53\gamma_E^2 N_f}{2} + \frac{437\gamma_E N_f}{8} - \frac{3395N_f}{96} \\ &\quad - 81\gamma_E\zeta(3) + \frac{891\zeta(3)}{8} + 27\gamma_E^2\pi^2 - \frac{561\gamma_E\pi^2}{8} + \frac{363\pi^2}{8} + 108\gamma_E^4 - \frac{495\gamma_E^3}{2} \\ &\quad \left. + \frac{3489\gamma_E^2}{8} - \frac{4755\gamma_E}{8} + \frac{3861}{16}\right)\ln^2\left(\frac{m_h^2}{\mu_F^2}\right) + \left(-\frac{2}{9}\ln\left(\frac{m_h^2}{m_t^2}\right)N_f^2\right. \\ &\quad + \frac{\zeta(3)N_f^2}{6} + \frac{5\pi^2 N_f^2}{27} + \frac{2\gamma_E^3 N_f^2}{9} + \frac{5\gamma_E^2 N_f^2}{9} + \frac{31\gamma_E N_f^2}{54} + \frac{5105N_f^2}{1728} \\ &\quad - 4\gamma_E\ln\left(\frac{m_h^2}{m_t^2}\right)N_f + \frac{23}{8}\ln\left(\frac{m_h^2}{m_t^2}\right)N_f + 20\gamma_E\zeta(3)N_f - \frac{23\zeta(3)N_f}{6} \\ &\quad - \frac{47\pi^4 N_f}{96} - \frac{7}{2}\gamma_E^2\pi^2 N_f + \frac{35}{6}\gamma_E\pi^2 N_f - \frac{953\pi^2 N_f}{72} - 2\gamma_E^4 N_f + \frac{38\gamma_E^3 N_f}{3} \\ &\quad - 30\gamma_E^2 N_f + \frac{470\gamma_E N_f}{9} - \frac{145829N_f}{1728} - \frac{57}{4}\gamma_E\ln\left(\frac{m_h^2}{m_t^2}\right) + \frac{209}{16}\ln\left(\frac{m_h^2}{m_t^2}\right) \\ &\quad - \frac{135\zeta(5)}{2} + \frac{99\pi^2\zeta(3)}{4} + 270\gamma_E^2\zeta(3) - \frac{165\gamma_E\zeta(3)}{2} + \frac{953\zeta(3)}{8} - \frac{129\gamma_E\pi^4}{20} \\ &\quad \left. + \frac{517\pi^4}{64} - 54\gamma_E^3\pi^2 + \frac{231\gamma_E^2\pi^2}{4} - 175\gamma_E\pi^2 + \frac{3511\pi^2}{24} - 108\gamma_E^5 + 33\gamma_E^4\right)\end{aligned}$$

$$
-\frac{1079\gamma_E^3}{2}+\frac{943\gamma_E^2}{4}-\frac{29369\gamma_E}{48}+\frac{307991}{576}\Bigg)\ln\left(\frac{m_h^2}{\mu_F^2}\right)
$$
$$
+\left(\frac{N_f^3}{54}-\frac{11N_f^2}{12}+\frac{121N_f}{8}-\frac{1331}{16}\right)\ln^3\left(\frac{m_h^2}{\mu_R^2}\right)
$$
$$
+\frac{\gamma_E^4N_f^2}{9}+\frac{10\gamma_E^3N_f^2}{27}+\frac{25\gamma_E^2N_f^2}{54}+\frac{58\gamma_EN_f^2}{243}+\frac{4037N_f^2}{648}
$$
$$
-\frac{1}{9}N_f^2\ln^2\left(\frac{m_h^2}{m_t^2}\right)+\frac{23}{16}N_f\ln^2\left(\frac{m_h^2}{m_t^2}\right)+\frac{209}{32}\ln^2\left(\frac{m_h^2}{m_t^2}\right)
$$
$$
+\Bigg(\frac{\pi^2N_f^2}{3}+\gamma_E^2N_f^2+\frac{265N_f^2}{144}-11\pi^2N_f-33\gamma_E^2N_f-\frac{5081N_f}{96}
$$
$$
+\left(-\frac{N_f^3}{18}-\gamma_EN_f^2+\frac{11N_f^2}{4}+33\gamma_EN_f-\frac{363N_f}{8}-\frac{1089\gamma_E}{4}+\frac{3993}{16}\right)\ln\left(\frac{m_h^2}{\mu_F^2}\right)
$$
$$
+\frac{363\pi^2}{4}+\frac{1089\gamma_E^2}{4}+\frac{11913}{32}\Bigg)\ln^2\left(\frac{m_h^2}{\mu_R^2}\right)-4\gamma_E^5N_f-\frac{41\gamma_E^4N_f}{3}
$$
$$
-\frac{535\gamma_E^3N_f}{18}-\frac{826\gamma_E^2N_f}{9}-\frac{52667\gamma_EN_f}{1296}-\frac{882763N_f}{3456}+\frac{77}{864}N_f^2\ln\left(\frac{m_h^2}{m_t^2}\right)
$$
$$
+4\gamma_E^2N_f\ln\left(\frac{m_h^2}{m_t^2}\right)+\frac{209}{54}N_f\ln\left(\frac{m_h^2}{m_t^2}\right)+\frac{4}{3}N_f\pi^2\ln\left(\frac{m_h^2}{m_t^2}\right)
$$
$$
+\frac{19}{4}\pi^2\ln\left(\frac{m_h^2}{m_t^2}\right)+\frac{57}{4}\gamma_E^2\ln\left(\frac{m_h^2}{m_t^2}\right)+\frac{5347}{288}\ln\left(\frac{m_h^2}{m_t^2}\right)
$$
$$
+\ln\left(\frac{m_h^2}{\mu_R^2}\right)\left(\frac{4}{9}\ln\left(\frac{m_h^2}{m_t^2}\right)N_f^2-\frac{\zeta(3)N_f^2}{3}-\frac{10\pi^2N_f^2}{27}-\frac{4\gamma_E^3N_f^2}{9}\right.
$$
$$
-\frac{10\gamma_E^2N_f^2}{9}-\frac{28\gamma_EN_f^2}{27}-\frac{1093N_f^2}{192}-\frac{23}{4}\ln\left(\frac{m_h^2}{m_t^2}\right)N_f-21\gamma_E\zeta(3)N_f
$$
$$
-\frac{22\zeta(3)N_f}{3}+\frac{23\pi^4N_f}{24}+7\gamma_E^2\pi^2N_f+\frac{923\pi^2N_f}{36}+12\gamma_E^4N_f+\frac{44\gamma_E^3N_f}{3}
$$
$$
+\frac{923\gamma_E^2N_f}{12}+\frac{356\gamma_EN_f}{9}+\frac{285811N_f}{1728}+\left(\frac{N_f^3}{18}+\frac{5\gamma_EN_f^2}{3}-\frac{11N_f^2}{4}\right.
$$
$$
\left.+12\gamma_E^2N_f-55\gamma_EN_f+\frac{363N_f}{8}-198\gamma_E^2+\frac{1815\gamma_E}{4}-\frac{3993}{16}\right)\ln^2\left(\frac{m_h^2}{\mu_F^2}\right)
$$
$$
-\frac{209}{8}\ln\left(\frac{m_h^2}{m_t^2}\right)+\ln\left(\frac{m_h^2}{\mu_F^2}\right)\left(-\frac{4}{9}\pi^2N_f^2-\frac{4\gamma_E^2N_f^2}{3}+\frac{10\gamma_EN_f^2}{9}\right.
$$
$$
-\frac{209N_f^2}{72}+9\zeta(3)N_f-7\gamma_E\pi^2N_f+\frac{44\pi^2N_f}{3}-24\gamma_E^3N_f
$$
$$
\left.+44\gamma_E^2N_f-\frac{923\gamma_EN_f}{12}+\frac{1319N_f}{16}-\frac{297\zeta(3)}{2}+\frac{231\gamma_E\pi^2}{2}-121\pi^2\right.
$$

$$
\begin{aligned}
&+396\gamma_E^3 - 363\gamma_E^2 + \frac{3385\gamma_E}{4} - \frac{9119}{16}\Bigg) + \frac{693\gamma_E\zeta(3)}{2} + \frac{847\zeta(3)}{4} \\
&-\frac{253\pi^4}{16} - \frac{231\gamma_E^2\pi^2}{2} - \frac{3385\pi^2}{12} - 198\gamma_E^4 - 121\gamma_E^3 - \frac{3385\gamma_E^2}{4} - \frac{1111\gamma_E}{3} \\
&-\frac{587857}{576}\Bigg) + \frac{989N_f\zeta(5)}{72} + 162\gamma_E\zeta(5) + \frac{2607\zeta(5)}{16} + \frac{81\zeta(3)^2}{2} + \frac{1}{3}\gamma_E N_f^2\zeta(3) \\
&+ \frac{41N_f^2\zeta(3)}{108} + \gamma_E^2 N_f\zeta(3) + \frac{491\gamma_E N_f\zeta(3)}{36} + \frac{27383N_f\zeta(3)}{2304} \\
&- \frac{17}{8}N_f\pi^2\zeta(3) - \frac{219}{4}\gamma_E\pi^2\zeta(3) - \frac{759\pi^2\zeta(3)}{16} - 189\gamma_E^3\zeta(3) \\
&- 264\gamma_E^2\zeta(3) - \frac{1117\gamma_E\zeta(3)}{2} - \frac{2729801\zeta(3)}{4608} + \frac{121\pi^6}{240} - \frac{193N_f^2\pi^4}{9720} \\
&- \frac{1}{360}\gamma_E N_f\pi^4 - \frac{1673N_f\pi^4}{12960} + \frac{129\gamma_E^2\pi^4}{20} - \frac{33\gamma_E\pi^4}{80} + \frac{52693\pi^4}{2880} \\
&- \frac{43N_f^2\pi^2}{216} - \gamma_E^3 N_f\pi^2 - \frac{35}{6}\gamma_E^2 N_f\pi^2 - \frac{569}{216}\gamma_E N_f\pi^2 - \frac{8999N_f\pi^2}{432} \\
&+ 27\gamma_E^4\pi^2 + \frac{33\gamma_E^3\pi^2}{2} + 175\gamma_E^2\pi^2 + \frac{4049\gamma_E\pi^2}{72} + \frac{832\pi^2}{3} + 36\gamma_E^6 \\
&+ 66\gamma_E^5 + \frac{1321\gamma_E^4}{4} + \frac{2465\gamma_E^3}{6} + \frac{15715\gamma_E^2}{16} + \frac{457013\gamma_E}{864} + \frac{27407317}{20736}
\end{aligned} \tag{E.18}
$$

$$
\begin{aligned}
C_{ggA-H}^{(1)\mathrm{SV}} =& C_{ggA-H}^{(2)\mathrm{SV}}\left(\frac{M_A^2}{\mu_F^2}, \frac{M_A^2}{\mu_F^2}, \frac{M_A^2}{M_t^2}\right) \\
=& c^A(\tau_t) - c^H(\tau_t)
\end{aligned} \tag{E.19}
$$

$$
\begin{aligned}
C_{ggA-H}^{(2)\mathrm{SV}} =& C_{ggA-H}^{(2)\mathrm{SV}}\left(\frac{M_A^2}{\mu_F^2}, \frac{M_A^2}{\mu_F^2}\right) \\
=& \frac{1939}{144} + 3\gamma_E^2 - \frac{19}{8}\ln\frac{M_A^2}{M_t^2} + 6\zeta_2 \\
&+ N_f\left(\frac{21}{16} + \frac{1}{3}\ln\frac{M_A^2}{M_t^2}\right) \\
&\left(+\frac{11}{4} - \frac{1}{6}N_f - 3\gamma_E\right)\ln\frac{M_A^2}{\mu_F^2} + \left(-\frac{33}{8} + \frac{1}{4}N_f\right)\ln\frac{M_A^2}{\mu_R^2}
\end{aligned} \tag{E.20}
$$

Bibliography

[1] S.L. Glashow. Partial Symmetries of Weak Interactions. *Nucl.Phys.*, 22:579–588, 1961.

[2] Steven Weinberg. A Model of Leptons. *Phys.Rev.Lett.*, 19:1264–1266, 1967.

[3] Abdus Salam. Weak and Electromagnetic Interactions. *Conf.Proc.*, C680519:367–377, 1968.

[4] F. Englert and R. Brout. Broken symmetry and the mass of gauge vector mesons. *Phys. Rev. Lett.*, 13:321–323, Aug 1964.

[5] Peter W. Higgs. Broken symmetries and the masses of gauge bosons. *Phys. Rev. Lett.*, 13:508–509, Oct 1964.

[6] G. S. Guralnik, C. R. Hagen, and T. W. B. Kibble. Global conservation laws and massless particles. *Phys. Rev. Lett.*, 13:585–587, Nov 1964.

[7] Peter W. Higgs. Spontaneous symmetry breakdown without massless bosons. *Phys. Rev.*, 145:1156–1163, 1966.

[8] T. W. B. Kibble. Symmetry breaking in non-abelian gauge theories. *Phys. Rev.*, 155:1554–1561, 1967.

[9] Georges Aad et al. Observation of a new particle in the search for the Standard Model Higgs boson with the ATLAS detector at the LHC. *Phys.Lett.*, B716:1–29, 2012.

[10] Serguei Chatrchyan et al. Observation of a new boson at a mass of 125 GeV with the CMS experiment at the LHC. *Phys.Lett.*, B716:30–61, 2012.

[11] Benjamin W. Lee, C. Quigg, and H.B. Thacker. The Strength of Weak Interactions at Very High-Energies and the Higgs Boson Mass. *Phys.Rev.Lett.*, 38:883–885, 1977.

[12] William J. Marciano, G. Valencia, and S. Willenbrock. Renormalization Group Improved Unitarity Bounds on the Higgs Boson and Top Quark Masses. *Phys.Rev.*, D40:1725, 1989.

[13] S. Dawson and S. Willenbrock. Unitarity constraints of heavy Higgs bosons. *Phys.Rev.Lett.*, 62:1232, 1989.

[14] T.P. Cheng, E. Eichten, and Ling-Fong Li. Higgs Phenomena in Asymptotically Free Gauge Theories. *Phys.Rev.*, D9:2259, 1974.

[15] B. Pendleton and Graham G. Ross. Mass and Mixing Angle Predictions from Infrared Fixed Points. *Phys.Lett.*, B98:291, 1981.

[16] Christopher T. Hill. Quark and Lepton Masses from Renormalization Group Fixed Points. *Phys.Rev.*, D24:691, 1981.

[17] Jonathan Bagger, Savas Dimopoulos, and Eduard Masso. Heavy Families: Masses and Mixings. *Nucl.Phys.*, B253:397, 1985.

[18] M.A.B. Beg, C. Panagiotakopoulos, and A. Sirlin. Mass of the Higgs Boson in the Canonical Realization of the Weinberg-Salam Theory. *Phys.Rev.Lett.*, 52:883, 1984.

[19] Malcolm J. Duncan, R. Philippe, and Marc Sher. Theoretical Ceiling on Quark Masses in the Standard Model. *Phys.Lett.*, B153:165, 1985.

[20] K.S. Babu and Ernest Ma. Probing the Desert With Boson and Fermion Masses. *Phys.Rev.Lett.*, 55:3005, 1985.

[21] S. Dittmaier et al. Handbook of LHC Higgs Cross Sections: 1. Inclusive Observables. 2011.

[22] S. Dawson. Radiative corrections to Higgs boson production. *Nucl.Phys.*, B359:283–300, 1991.

[23] A. Djouadi, M. Spira, and P.M. Zerwas. Production of Higgs bosons in proton colliders: QCD corrections. *Phys.Lett.*, B264:440–446, 1991.

[24] M. Spira, A. Djouadi, D. Graudenz, and P.M. Zerwas. Higgs boson production at the LHC. *Nucl.Phys.*, B453:17–82, 1995.

[25] Michael Spira. QCD effects in Higgs physics. *Fortsch.Phys.*, 46:203–284, 1998.

[26] Tao Han, G. Valencia, and S. Willenbrock. Structure function approach to vector boson scattering in p p collisions. *Phys.Rev.Lett.*, 69:3274–3277, 1992.

[27] T. Figy, C. Oleari, and D. Zeppenfeld. Next-to-leading order jet distributions for Higgs boson production via weak boson fusion. *Phys.Rev.*, D68:073005, 2003.

[28] Terrance Figy and Dieter Zeppenfeld. QCD corrections to jet correlations in weak boson fusion. *Phys.Lett.*, B591:297–303, 2004.

[29] Edmond L. Berger and John M. Campbell. Higgs boson production in weak boson fusion at next-to-leading order. *Phys.Rev.*, D70:073011, 2004.

[30] Mariano Ciccolini, Ansgar Denner, and Stefan Dittmaier. Electroweak and QCD corrections to Higgs production via vector-boson fusion at the LHC. *Phys.Rev.*, D77:013002, 2008.

[31] Tao Han and S. Willenbrock. QCD correction to the p p —¿ W H and Z H total cross-sections. *Phys.Lett.*, B273:167–172, 1991.

[32] H. Baer, B. Bailey, and J.F. Owens. O (alpha-s) Monte Carlo approach to W + Higgs associated production at hadron supercolliders. *Phys.Rev.*, D47:2730–2734, 1993.

[33] J. Ohnemus and W. James Stirling. Order alpha-s corrections to the differential cross-section for the W H intermediate mass Higgs signal. *Phys.Rev.*, D47:2722–2729, 1993.

[34] Oliver Brein, Abdelhak Djouadi, and Robert Harlander. NNLO QCD corrections to the Higgs-strahlung processes at hadron colliders. *Phys.Lett.*, B579:149–156, 2004.

[35] M.L. Ciccolini, S. Dittmaier, and M. Kramer. Electroweak radiative corrections to associated WH and ZH production at hadron colliders. *Phys.Rev.*, D68:073003, 2003.

[36] W. Beenakker, S. Dittmaier, M. Kramer, B. Plumper, M. Spira, et al. Higgs radiation off top quarks at the Tevatron and the LHC. *Phys.Rev.Lett.*, 87:201805, 2001.

[37] W. Beenakker, S. Dittmaier, M. Kramer, B. Plumper, M. Spira, et al. NLO QCD corrections to t anti-t H production in hadron collisions. *Nucl.Phys.*, B653:151–203, 2003.

[38] S. Dawson, L.H. Orr, L. Reina, and D. Wackeroth. Associated top quark Higgs boson production at the LHC. *Phys.Rev.*, D67:071503, 2003.

[39] Rudolf Haag, Jan T. Lopuszanski, and Martin Sohnius. All Possible Generators of Supersymmetries of the s Matrix. *Nucl.Phys.*, B88:257, 1975.

[40] Russel P. Kauffman and Wendy Schaffer. QCD corrections to production of Higgs pseudoscalars. *Phys.Rev.*, D49:551–554, 1994.

[41] S. Dawson and R. Kauffman. QCD corrections to Higgs boson production: nonleading terms in the heavy quark limit. *Phys.Rev.*, D49:2298–2309, 1994.

[42] Robert V. Harlander and William B. Kilgore. Production of a pseudoscalar Higgs boson at hadron colliders at next-to-next-to leading order. *JHEP*, 0210:017, 2002.

[43] V. Ravindran, J. Smith, and W. L. van Neerven. NNLO corrections to the total cross-section for Higgs boson production in hadron hadron collisions. *Nucl.Phys.*, B665:325–366, 2003.

[44] Charalampos Anastasiou and Kirill Melnikov. Pseudoscalar Higgs boson production at hadron colliders in NNLO QCD. *Phys.Rev.*, D67:037501, 2003.

[45] Daniel de Florian and Jose Zurita. Soft-gluon resummation for pseudoscalar Higgs boson production at hadron colliders. *Phys.Lett.*, B659:813–820, 2008.

[46] S. Dawson, C.B. Jackson, L. Reina, and D. Wackeroth. Exclusive Higgs boson production with bottom quarks at hadron colliders. *Phys.Rev.*, D69:074027, 2004.

[47] Stefan Dittmaier, 1 Kramer, Michael, and Michael Spira. Higgs radiation off bottom quarks at the Tevatron and the CERN LHC. *Phys.Rev.*, D70:074010, 2004.

[48] D. Dicus, T. Stelzer, Z. Sullivan, and S. Willenbrock. Higgs boson production in association with bottom quarks at next-to-leading order. *Phys.Rev.*, D59:094016, 1999.

[49] Csaba Balazs, Hong-Jian He, and C.P. Yuan. QCD corrections to scalar production via heavy quark fusion at hadron colliders. *Phys.Rev.*, D60:114001, 1999.

[50] Robert V. Harlander and William B. Kilgore. Higgs boson production in bottom quark fusion at next-to-next-to leading order. *Phys.Rev.*, D68:013001, 2003.

[51] Marcela Carena, S. Heinemeyer, C.E.M. Wagner, and G. Weiglein. Suggestions for benchmark scenarios for MSSM Higgs boson searches at hadron colliders. *Eur.Phys.J.*, C26:601–607, 2003.

[52] William A. Bardeen, A.J. Buras, D.W. Duke, and T. Muta. Deep Inelastic Scattering Beyond the Leading Order in Asymptotically Free Gauge Theories. *Phys.Rev.*, D18:3998, 1978.

[53] K. Hikasa et al. Review of particle properties. Particle Data Group. *Phys.Rev.*, D45:S1, 1992.

[54] T. Kinoshita. Mass singularities of Feynman amplitudes. *J.Math.Phys.*, 3:650–677, 1962.

[55] T.D. Lee and M. Nauenberg. Degenerate Systems and Mass Singularities. *Phys.Rev.*, 133:B1549–B1562, 1964.

[56] Guido Altarelli, R. Keith Ellis, and G. Martinelli. Large Perturbative Corrections to the Drell-Yan Process in QCD. *Nucl.Phys.*, B157:461, 1979.

[57] John C. Collins and Davison E. Soper. Parton Distribution and Decay Functions. *Nucl.Phys.*, B194:445, 1982.

[58] G. Curci, W. Furmanski, and R. Petronzio. Evolution of Parton Densities Beyond Leading Order: The Nonsinglet Case. *Nucl.Phys.*, B175:27, 1980.

[59] L. Baulieu, E.G. Floratos, and C. Kounnas. Parton Model Interpretation of the Cut Vertex Formalism. *Nucl.Phys.*, B166:321, 1980.

[60] John C. Collins, Davison E. Soper, and George F. Sterman. Factorization of Hard Processes in QCD. *Adv.Ser.Direct.High Energy Phys.*, 5:1–91, 1988.

[61] V.N. Gribov and L.N. Lipatov. Deep inelastic e p scattering in perturbation theory. *Sov.J.Nucl.Phys.*, 15:438–450, 1972.

[62] Guido Altarelli and G. Parisi. Asymptotic Freedom in Parton Language. *Nucl.Phys.*, B126:298, 1977.

[63] Yuri L. Dokshitzer. Calculation of the Structure Functions for Deep Inelastic Scattering and e+ e- Annihilation by Perturbation Theory in Quantum Chromodynamics. *Sov.Phys.JETP*, 46:641–653, 1977.

[64] S.D. Drell and Tung-Mow Yan. Massive Lepton Pair Production in Hadron-Hadron Collisions at High-Energies. *Phys.Rev.Lett.*, 25:316–320, 1970.

[65] D. Amati, R. Petronzio, and G. Veneziano. Relating Hard QCD Processes Through Universality of Mass Singularities. *Nucl.Phys.*, B140:54, 1978.

[66] Stephen B. Libby and George F. Sterman. Jet and Lepton Pair Production in High-Energy Lepton-Hadron and Hadron-Hadron Scattering. *Phys.Rev.*, D18:3252, 1978.

[67] Alfred H. Mueller. Cut Vertices and their Renormalization: A Generalization of the Wilson Expansion. *Phys.Rev.*, D18:3705, 1978.

[68] R. Keith Ellis, Howard Georgi, Marie Machacek, H. David Politzer, and Graham G. Ross. Perturbation Theory and the Parton Model in QCD. *Nucl.Phys.*, B152:285, 1979.

[69] Geoffrey T. Bodwin. Factorization of the Drell-Yan Cross-Section in Perturbation Theory. *Phys.Rev.*, D31:2616, 1985.

[70] John C. Collins, Davison E. Soper, and George F. Sterman. Factorization for Short Distance Hadron - Hadron Scattering. *Nucl.Phys.*, B261:104, 1985.

[71] G. Parisi. Summing Large Perturbative Corrections in QCD. *Phys.Lett.*, B90:295, 1980.

[72] George F. Sterman. Summation of Large Corrections to Short Distance Hadronic Cross-Sections. *Nucl.Phys.*, B281:310, 1987.

[73] S. Catani and L. Trentadue. Resummation of the QCD Perturbative Series for Hard Processes. *Nucl.Phys.*, B327:323, 1989.

[74] Nikolaos Kidonakis and George F. Sterman. Resummation for QCD hard scattering. *Nucl.Phys.*, B505:321–348, 1997.

[75] Harry Contopanagos, Eric Laenen, and George F. Sterman. Sudakov factorization and resummation. *Nucl.Phys.*, B484:303–330, 1997.

[76] Jiro Kodaira and Luca Trentadue. Summing Soft Emission in QCD. *Phys.Lett.*, B112:66, 1982.

[77] S. Catani and L. Trentadue. Comment on QCD exponentiation at large x. *Nucl.Phys.*, B353:183–186, 1991.

[78] John R. Ellis, Mary K. Gaillard, and Dimitri V. Nanopoulos. A Phenomenological Profile of the Higgs Boson. *Nucl.Phys.*, B106:292, 1976.

[79] Frank Wilczek. Decays of Heavy Vector Mesons Into Higgs Particles. *Phys.Rev.Lett.*, 39:1304, 1977.

[80] H.M. Georgi, S.L. Glashow, M.E. Machacek, and Dimitri V. Nanopoulos. Higgs Bosons from Two Gluon Annihilation in Proton Proton Collisions. *Phys.Rev.Lett.*, 40:692, 1978.

[81] Mikhail A. Shifman, A.I. Vainshtein, M.B. Voloshin, and Valentin I. Zakharov. Low-Energy Theorems for Higgs Boson Couplings to Photons. *Sov.J.Nucl.Phys.*, 30:711–716, 1979.

[82] K.G. Chetyrkin, V.P. Spiridonov, and S.G. Gorishnii. Wilson Expansion for correlators of vector currents at the two loop level: Dimension four operators. *Phys.Lett.*, B160:149–153, 1985.

[83] Bernd A. Kniehl and Michael Spira. Low-energy theorems in Higgs physics. *Z.Phys.*, C69:77–88, 1995.

[84] Michael Kramer, Eric Laenen, and Michael Spira. Soft gluon radiation in Higgs boson production at the LHC. *Nucl.Phys.*, B511:523–549, 1998.

[85] K.G. Chetyrkin, Bernd A. Kniehl, and M. Steinhauser. Decoupling relations to O (alpha-s**3) and their connection to low-energy theorems. *Nucl.Phys.*, B510:61–87, 1998.

[86] Y. Schroder and M. Steinhauser. Four-loop decoupling relations for the strong coupling. *JHEP*, 0601:051, 2006.

[87] K.G. Chetyrkin, Bernd A. Kniehl, M. Steinhauser, and William A. Bardeen. Effective QCD interactions of CP odd Higgs bosons at three loops. *Nucl.Phys.*, B535:3–18, 1998.

[88] M. Spira, A. Djouadi, D. Graudenz, and P.M. Zerwas. SUSY Higgs production at proton colliders. *Phys.Lett.*, B318:347–353, 1993.

[89] D. Graudenz, M. Spira, and P.M. Zerwas. QCD corrections to Higgs boson production at proton proton colliders. *Phys.Rev.Lett.*, 70:1372–1375, 1993.

[90] U. Aglietti, R. Bonciani, G. Degrassi, and A. Vicini. Analytic Results for Virtual QCD Corrections to Higgs Production and Decay. *JHEP*, 0701:021, 2007.

[91] Charalampos Anastasiou, Stefan Beerli, Stefan Bucherer, Alejandro Daleo, and Zoltan Kunszt. Two-loop amplitudes and master integrals for the production of a Higgs boson via a massive quark and a scalar-quark loop. *JHEP*, 0701:082, 2007.

[92] Michael Spira. HIGLU: A program for the calculation of the total Higgs production cross-section at hadron colliders via gluon fusion including QCD corrections. 1995.

[93] A.D. Martin, W.J. Stirling, R.S. Thorne, and G. Watt. Parton distributions for the LHC. *Eur.Phys.J.*, C63:189–285, 2009.

[94] Robert V. Harlander and William B. Kilgore. Soft and virtual corrections to proton proton → H + x at NNLO. *Phys.Rev.*, D64:013015, 2001.

[95] Stefano Catani, Daniel de Florian, and Massimiliano Grazzini. Higgs production in hadron collisions: Soft and virtual QCD corrections at NNLO. *JHEP*, 0105:025, 2001.

[96] Robert V. Harlander and William B. Kilgore. Next-to-next-to-leading order Higgs production at hadron colliders. *Phys.Rev.Lett.*, 88:201801, 2002.

[97] Charalampos Anastasiou and Kirill Melnikov. Higgs boson production at hadron colliders in NNLO QCD. *Nucl.Phys.*, B646:220–256, 2002.

[98] Charalampos Anastasiou, Claude Duhr, Falko Dulat, Elisabetta Furlan, Thomas Gehrmann, et al. Higgs boson gluon?fusion production at threshold in N^3LO QCD. *Phys.Lett.*, B737:325–328, 2014.

[99] Charalampos Anastasiou, Claude Duhr, Falko Dulat, Elisabetta Furlan, Thomas Gehrmann, et al. Higgs boson gluon–fusion production beyond threshold in N^3LO QCD. *JHEP*, 1503:091, 2015.

[100] Charalampos Anastasiou, Claude Duhr, Falko Dulat, Franz Herzog, and Bernhard Mistlberger. Higgs boson gluon-fusion production in N3LO QCD. 2015.

[101] A. Djouadi and P. Gambino. Leading electroweak correction to Higgs boson production at proton colliders. *Phys.Rev.Lett.*, 73:2528–2531, 1994.

[102] K.G. Chetyrkin, Bernd A. Kniehl, and M. Steinhauser. Virtual top quark effects on the H —¿ b anti-b decay at next-to-leading order in QCD. *Phys.Rev.Lett.*, 78:594–597, 1997.

[103] U. Aglietti, R. Bonciani, G. Degrassi, and A. Vicini. Two loop light fermion contribution to Higgs production and decays. *Phys.Lett.*, B595:432–441, 2004.

[104] Giuseppe Degrassi and Fabio Maltoni. Two-loop electroweak corrections to Higgs production at hadron colliders. *Phys.Lett.*, B600:255–260, 2004.

[105] Stefano Actis, Giampiero Passarino, Christian Sturm, and Sandro Uccirati. NLO Electroweak Corrections to Higgs Boson Production at Hadron Colliders. *Phys.Lett.*, B670:12–17, 2008.

[106] Stefano Actis, Giampiero Passarino, Christian Sturm, and Sandro Uccirati. NNLO Computational Techniques: The Cases H $\rightarrow$ gamma gamma and H $\rightarrow$ g g. *Nucl.Phys.*, B811:182–273, 2009.

[107] Charalampos Anastasiou, Radja Boughezal, and Frank Petriello. Mixed QCD-electroweak corrections to Higgs boson production in gluon fusion. *JHEP*, 0904:003, 2009.

[108] Stefano Catani, Daniel de Florian, Massimiliano Grazzini, and Paolo Nason. Soft gluon resummation for Higgs boson production at hadron colliders. *JHEP*, 0307:028, 2003.

[109] S. Moch and A. Vogt. Higher-order soft corrections to lepton pair and Higgs boson production. *Phys.Lett.*, B631:48–57, 2005.

[110] V. Ravindran. On Sudakov and soft resummations in QCD. *Nucl.Phys.*, B746:58–76, 2006.

[111] V. Ravindran. Higher-order threshold effects to inclusive processes in QCD. *Nucl.Phys.*, B752:173–196, 2006.

[112] Ahmad Idilbi, Xiang-dong Ji, Jian-Ping Ma, and Feng Yuan. Threshold resummation for Higgs production in effective field theory. *Phys.Rev.*, D73:077501, 2006.

[113] Daniel de Florian and Massimiliano Grazzini. Higgs production through gluon fusion: Updated cross sections at the Tevatron and the LHC. *Phys.Lett.*, B674:291–294, 2009.

[114] Daniel de Florian and Massimiliano Grazzini. Higgs production at the LHC: updated cross sections at $\sqrt{s} = 8$ TeV. *Phys.Lett.*, B718:117–120, 2012.

[115] Marco Bonvini, Richard D. Ball, Stefano Forte, Simone Marzani, and Giovanni Ridolfi. Updated Higgs cross section at approximate N^3LO. *J.Phys.*, G41:095002, 2014.

[116] Marco Bonvini and Simone Marzani. Resummed Higgs cross section at N^3LL. *JHEP*, 1409:007, 2014.

[117] Stefano Catani, Leandro Cieri, Daniel de Florian, Giancarlo Ferrera, and Massimiliano Grazzini. Threshold resummation at N^3LL accuracy and soft-virtual cross sections at N^3LO. *Nucl.Phys.*, B888:75–91, 2014.

[118] D. de Florian, J. Mazzitelli, S. Moch, and A. Vogt. Approximate N^3LO Higgs-boson production cross section using physical-kernel constraints. *JHEP*, 1410:176, 2014.

[119] M.I. Kotsky and Oleg I. Yakovlev. On the resummation of double logarithms in the process Higgs → gamma gamma. *Phys.Lett.*, B418:335–344, 1998.

[120] R. Akhoury, H. Wang, and Oleg I. Yakovlev. On the Resummation of large QCD logarithms in Higgs → gamma gamma decay. *Phys.Rev.*, D64:113008, 2001.

[121] V.V. Sudakov. Vertex parts at very high-energies in quantum electrodynamics. *Sov.Phys.JETP*, 3:65–71, 1956.

[122] James Carazzone, Enrico C. Poggio, and Helen R. Quinn. Asymptotic Behavior of Form-Factor in Nonabelian Gauge Theories. *Phys.Lett.*, B57:161, 1975.

[123] Andrei V. Smilga. Next-to-leading logarithms in the High-energy asymptotics of the quark form factor and the jet cross-section. *Nucl.Phys.*, B161:449–468, 1979.

[124] Stefano Catani, Michelangelo L. Mangano, Paolo Nason, and Luca Trentadue. The Resummation of soft gluons in hadronic collisions. *Nucl.Phys.*, B478:273–310, 1996.

[125] G. Peter Lepage. A New Algorithm for Adaptive Multidimensional Integration. *J.Comput.Phys.*, 27:192, 1978.

[126] A. Vogt. Efficient evolution of unpolarized and polarized parton distributions with QCD-PEGASUS. *Comput.Phys.Commun.*, 170:65–92, 2005.

[127] Anna Kulesza, George F. Sterman, and Werner Vogelsang. Joint resummation in electroweak boson production. *Phys.Rev.*, D66:014011, 2002.

[128] Stefano Forte, Andrea Isgro, and Gherardo Vita. Do we need N^3LO Parton Distributions? *Phys.Lett.*, B731:136–140, 2014.

[129] David J. Gross and Frank Wilczek. Ultraviolet behavior of non-abelian gauge theories. *Phys. Rev. Lett.*, 30:1343–1346, Jun 1973.

[130] H. David Politzer. Reliable perturbative results for strong interactions? *Phys. Rev. Lett.*, 30:1346–1349, Jun 1973.

[131] William E. Caswell. Asymptotic behavior of non-abelian gauge theories to two-loop order. *Phys. Rev. Lett.*, 33:244–246, Jul 1974.

[132] D.R.T. Jones. Two-loop diagrams in yang-mills theory. *Nuclear Physics B*, 75(3):531 – 538, 1974.

[133] E. Egorian and O.V. Tarasov. Two Loop Renormalization of the QCD in an Arbitrary Gauge. *Teor.Mat.Fiz.*, 41:26–32, 1979.

[134] O.V. Tarasov, A.A. Vladimirov, and A. Yu. Zharkov. The Gell-Mann-Low Function of QCD in the Three Loop Approximation. *Phys.Lett.*, B93:429–432, 1980.

[135] S.A. Larin and J.A.M. Vermaseren. The Three loop QCD Beta function and anomalous dimensions. *Phys.Lett.*, B303:334–336, 1993.

[136] T. van Ritbergen, J.A.M. Vermaseren, and S.A. Larin. The Four loop beta function in quantum chromodynamics. *Phys.Lett.*, B400:379–384, 1997.

[137] M. Czakon. The Four-loop QCD beta-function and anomalous dimensions. *Nucl.Phys.*, B710:485–498, 2005.

[138] William J. Marciano. Flavor Thresholds and Lambda in the Modified Minimal Subtraction Prescription. *Phys.Rev.*, D29:580, 1984.

[139] G.P. Korchemsky. Asymptotics of the Altarelli-Parisi-Lipatov Evolution Kernels of Parton Distributions. *Mod.Phys.Lett.*, A4:1257–1276, 1989.

[140] S. Moch, J.A.M. Vermaseren, and A. Vogt. The Three loop splitting functions in QCD: The Nonsinglet case. *Nucl.Phys.*, B688:101–134, 2004.

[141] A. Vogt, S. Moch, and J.A.M. Vermaseren. The Three-loop splitting functions in QCD: The Singlet case. *Nucl.Phys.*, B691:129–181, 2004.

[142] S. Catani, E. D'Emilio, and L. Trentadue. The Gluon Form-factor to Higher Orders: Gluon Gluon Annihilation at Small Q^-transverse. *Phys.Lett.*, B211:335–342, 1988.

[143] S. Moch, J.A.M. Vermaseren, and A. Vogt. Nonsinglet structure functions at three loops: Fermionic contributions. *Nucl.Phys.*, B646:181–200, 2002.

[144] Carola F. Berger. Higher orders in A(alpha(s))/[1-x]+ of nonsinglet partonic splitting functions. *Phys.Rev.*, D66:116002, 2002.

[145] S. Moch, J.A.M. Vermaseren, and A. Vogt. Higher-order corrections in threshold resummation. *Nucl.Phys.*, B726:317–335, 2005.